University of Udine

PhD course in Cellular and Molecular Medicine (XXIX cycle)

Department of Medical and Biological Sciences

Analysis of the biological mechanisms de-regulated after pharmacological BET inhibition in a model of anaplastic thyroid cancer

Supervisor:

Prof. Carla di Loreto

PhD student:

Catia Mio

Assistant supervisor:

Prof. Giuseppe Damante

Year Of The Final Exam: 2017

“Nothing in life is to be feared, it is only to be understood. Now is the time to understand more, so that we may fear less.”

-Marie Curie

Summary

Abstract

In the portrait of epigenetic anti-cancer drugs, BET inhibitors (BETi) represent an appealing innovative class of compounds. They target the Bromodomain and Extra-Terminal (BET) proteins that act as regulators of gene transcription due to the interaction with histone acetyl groups. BETi are known to affect multiple biological pathways. The aim of this study is to outline which are the chief pathways underlying the biological effects derived from BET inhibition, in order to better understand their anti-neoplastic potential. To pursue this aim, anaplastic thyroid carcinoma (ATC)-derived cell lines were used as a model of highly aggressive cancer subtype. The effects of BET inhibition were evaluated in terms of different biological outputs, in diverse ATC cell lines (FRO, SW1736 and 8505c). The treatment with different BETi (JQ1, I-BET762 and I-BET151) decreased cell viability, increased the proportion of cells stacked in G0-G1 cell cycle phases and determined an increase in cell death phenomena. In order to find BETi effectors, a global transcriptome analysis was performed after JQ1 treatment. RNA-seq data highlighted a significant deregulation of cell cycle regulators. Among them, MCM5 was down-regulated at both mRNA and protein levels in all tested cell lines. Furthermore, ChIP experiments indicated that *MCM5* is a direct target of BRD4. *MCM5* silencing reduced ATC cell proliferation in an analogous way as JQ1 treatment, thus underlining its connection in the block of proliferation induced by BETi. Moreover, JQ1 treatment reduced *Mcm*5 mRNA expression in two murine ATC-derived cell lines. Thus, these data proved that, through MCM5, BET inhibition directly affects cell cycle progression. Nowadays, many reports showed that miRNAs are key elements in the regulation of several biological processes and that, if deregulated, could contribute to several diseases, including cancer. Hitherto, data concerning the relationship between BET inhibition and miRNA expression are very scanty. Therefore, a second goal of this study was to delineate if BET inhibitors could regulate miRNA expression in ATC cells. JQ1 treatment altered the expression of several miRNAs, 7 of which turned out to be commonly deregulated in ATC cells after both 48h and 72h treatments in two cell lines. An algorithm was

applied to enlist the putative miRNA-associated target genes of this pool. These targets have been, then, subjected to gene ontology analysis, in order to outline the biological pathways in which these miRNAs are involved. It has been assessed a strong enrichment in the STAT3 and PTEN signal transduction pathways, which was confirmed by detecting an up-regulation of *PTEN*, p21 and p27 levels. A subgroup of miRNAs (hsa-miR-4516, hsa-miR-1234, hsa-miR-4488) turned out to be down-regulated in ATC cell lines, when compared to the non-tumorigenic ones (NThy ori 3.1), and interestingly JQ1 treatment in ATC cells induced the up-regulation of these miRNAs, restoring, in some way, their expression levels. Thus, these data hypothesized that modulation of miRNA expression is one of the multiple mechanisms of BETi action in thyroid cancer cells.

Taken together, these data highlighted the multi-target output due to BET inhibition. Moreover, they suggest a possible usage of BET inhibitors in the management of anaplastic thyroid cancer. However, further investigations are needed to have a better insight on the multiple targets of these pharmacological inhibitors.

Introduction

1. *Epige*netics

While the term 'epigenetics' is often used loosely, the current definition name it as 'the study of heritable changes in gene expression that occur independent of changes in the primary DNA sequence' (Khan et al., 2015). Epigenetic mechanisms include DNA methylation, noncoding RNA signaling, nucleosome positioning and histone post-transcriptional modifications (PTMs) code. All these mechanisms alter the local structure of the chromatin in order to control gene expression, mostly regulating chromatin accessibility and compactness (Fig. 1). All together, these mechanisms oversee the chromatin architecture and gene expression in various cell types, developmental stages and diseases (Bernstein et al., 2007).

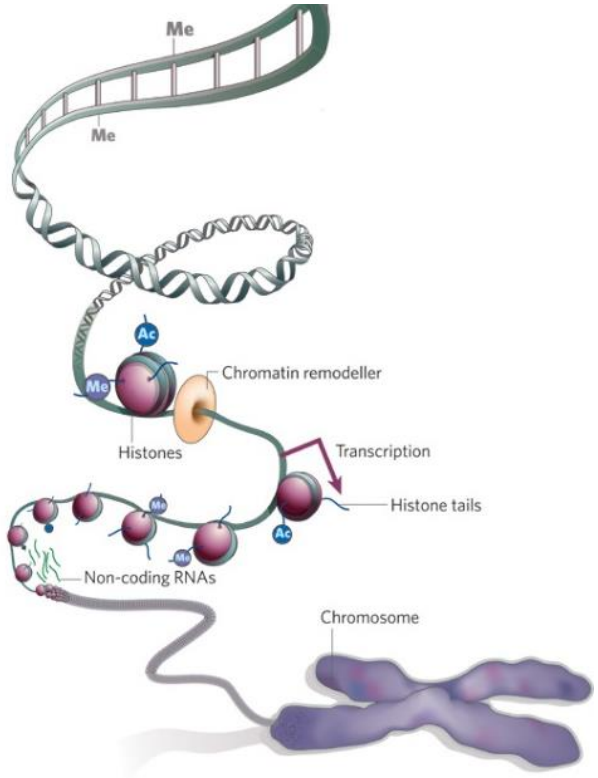

***Figure 1**. The coding and structural information in the base sequence of DNA is organized in chromatin to form multiple epigenomes. Epigenetic regulation is mediated by DNA methylation, histone modifications, and RNA-mediated gene silencing (adapted from Jones et al., 2008).*

1.1. Chromatin structure

Eukaryotic DNA is packaged and regulated by a histone protein core. Nucleosomes are the functional units composing the chromatin: a 146 base pairs DNA stretch is wrapped around a histone octamer formed by a $(H3\text{-}H4)_2$ tetramer and by two H2A-H2B dimers (Fig. 2).

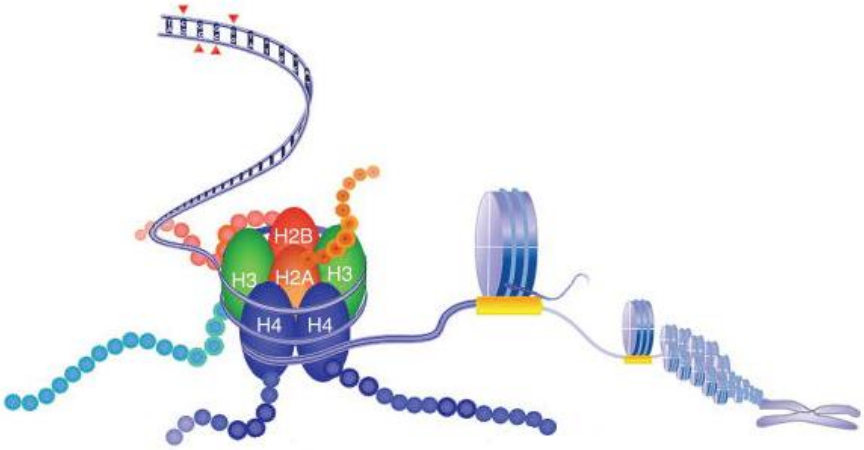

***Figure 2**. The functional unit of chromatin is the nucleosome, a histone octamer around which DNA is wrapped (adapted from James and Frye, 2013).*

Chromatin can be condensed or 'closed' (and called heterochromatin), a phenomenon associated to transcriptional repression. Conversely, chromatin can be 'open' (the so-called euchromatin), a state which allows transcription factors complexes to access the DNA and regulate RNA synthesis (Fig. 3). Therefore, the organization of eukaryotic DNA into chromatin regulates whether proteins mediating essential cellular processes can gain access to specific genomic regions (Cosgrove et al., 2004).

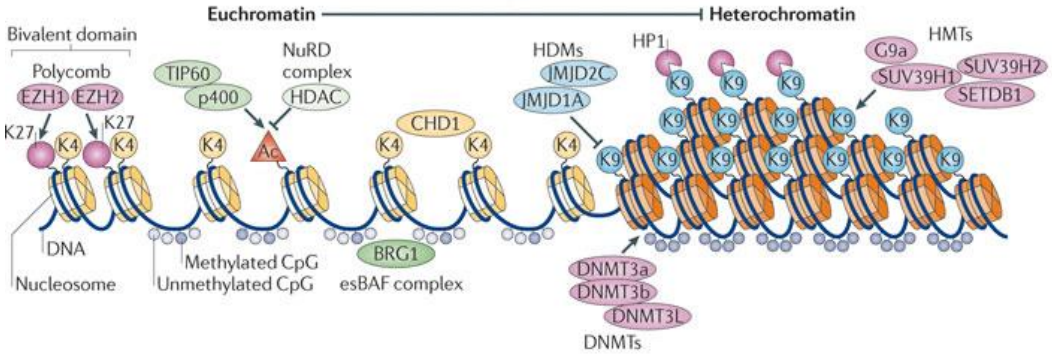

***Figure 3**. Modifications and complexes regulating the open chromatin state, possibly by contributing to boundary determination between euchromatin and heterochromatin (adapted from Gaspar-Maia et al., 2011).*

1.1.1. DNA methylation

DNA methylation plays a key role in embryonic development, cell-type lineage specification, X-chromosome inactivation, and genomic imprinting (Gillette and Hill, 2015). This process is limited to cytosine residues: it occurs on di-nucleotide CpGs by means of DNMTs (DNA methyltransferases), enzymes committed to direct and preserve this kind of modification (Fig. 4). DNA methylation is closely related to heterochromatin formation and, thus, levels of gene transcription.

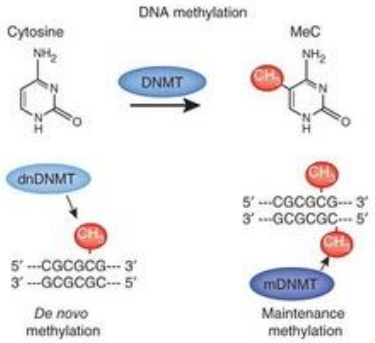

***Figure 4**. DNA methylation arises at cytosines when a methyl group is added at the 5' position by a DNMT. Two types of DNMTs exist: de novo DNMTs (dnDNMTs) methylate previously nonmethylated cytosines, whereas maintenance DNMTs (mDNMTs) methylate hemi-methylated DNA at the complementary strand (adapted from Day and Sweatt, 2010).*

Three DNA methytransferases (DNMT1, DNMT3A, and DNMT3B) have been identified (Fuks et al., 2003). DNMT3A and 3B usually establish embryonic methylation patterns, while DNMT1 operates at the replication forks to maintain the methylation patterns in a semi-conservative way. However, being DNMT1 inefficient in maintaining the methylation of many CpG dense regions, the *de-novo* activities of DNMT3A and DNMT3B are required in order to re-establish the methylation patterns (Seo et al., 2013). DNA methylation is a straightforward mechanism meant to regulate stable epigenetic marks. However, the discovery of *de-novo* DNMTs suggests that a certain amount of flexibility may also be possible.

1.1.2. Nucleosome positioning

The positioning of nucleosomes can directly influence gene regulation. Remodelers are needed to fully package the genome, i.e. to move, eject, or re-structure nucleosomes composition. Certain remodelers promote genome-wide dense nucleosome packaging; others instead move and eject nucleosomes to help transcription factors access DNA sequences in a regulated manner (Clapier and Cairns, 2009). Four different families of chromatin remodelers exist, which utilize adenosine triphosphate (ATP) hydrolysis in order to alter histone-DNA contacts (Fig. 5). These remodelers can change the position of nucleosomes on DNA or the histone variants embedded in nucleosomes, or else they may entirely disassemble them (Bartholomew, 2014).

Additionally, chromatin remodelers harbor some non-catalytic subunits that are required for targeting and regulating distinct nucleosome positioning activities; this way, they determine gene expression programs and cell fate (Längst and Manelyte, 2015). On the other hand, perturbation of this balanced phenomenon results in sustained chromatin and gene expression changes that can lead to disease development.

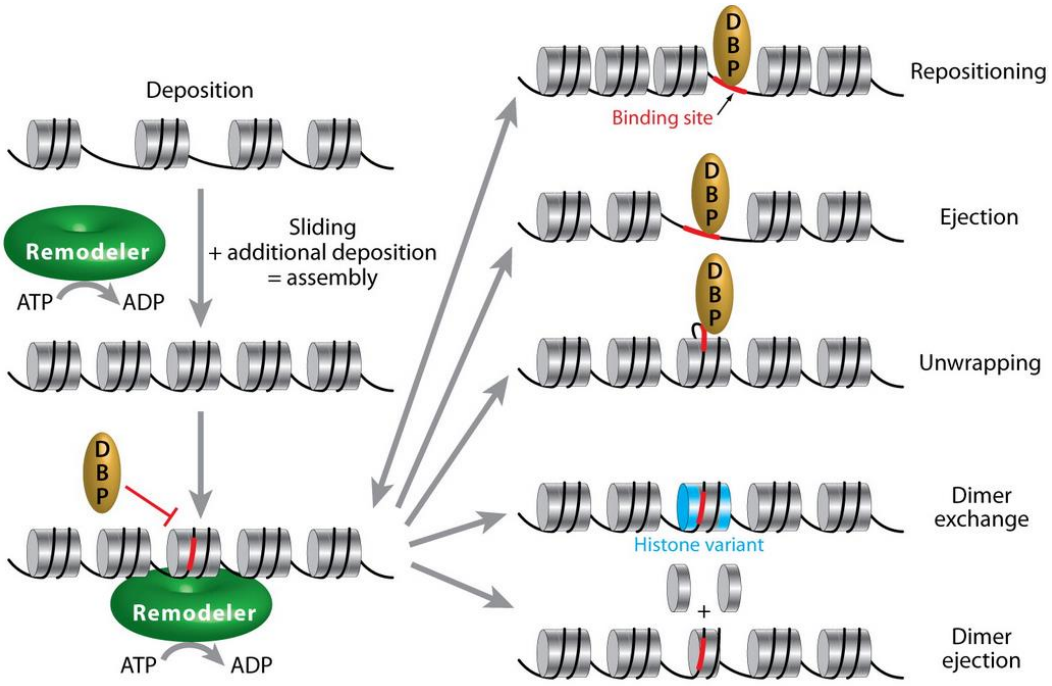

***Figure 5**. Chromatin remodeling. Remodelers (green) can move already deposited histone octamers, generating space for additional deposition. They could create a site exposure, in which a site (red) for a DNA-binding protein (DBP), initially occluded, becomes accessible by nucleosomal sliding (repositioning) or nucleosomal eviction (ejection). They could managed localized unwrapping, and modified composition by dimer replacement [exchange of H2A-H2B dimer with an alternative dimer containing a histone variant (blue)] or through dimer ejection (adapted from Bartholomew, 2014).*

Several multi-system developmental disorders arise when a mutation affects functions and targets of chromatin remodelers, i.e. COFS (cerebro-oculo-facio-skeletal syndrome), ATRX-syndrome (α-thalassemia X-linked mental retardation), Williams-Beuren syndrome (Citterio et al., 2000; Baumann et al., 2008; Poot et al., 2004). Moreover, mutations in chromatin remodelers are linked to specific types of cancers, suggesting that specific transcriptional programs that regulate growth and/or differentiation are connected to defined subunits (Wang et al., 2007).

1.1.3. Noncoding RNAs

Nowadays, many evidences indicate the existence of an extensive regulatory network involving RNA signaling. Noncoding RNAs (ncRNAs) are a heterogeneous class of transcripts with no protein coding potential involved in diverse cellular

processes. They are divided into lncRNA (long noncoding RNA), miRNA (microRNA), siRNA (small interfering RNA), piRNA (Piwi-interacting RNA) snRNA (small nuclear RNA), and circRNA (circular RNA) (Fig. 6). ncRNAs control chromosome dynamics, chromatin modification and epigenetic memory, i.e. imprinting, DNA methylation and gene silencing (Tollervey and Lunyac, 2012).

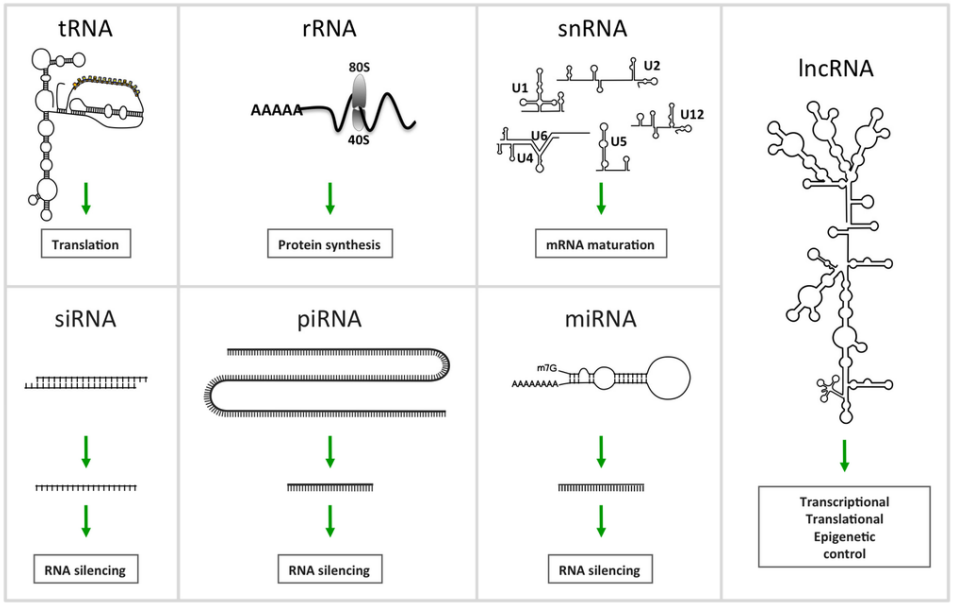

***Figure 6**. Schematic representation of the different noncoding RNAs (adapted from Morceau et al., 2013).*

Among all, lncRNAs constitute the most recent and least characterized family of ncRNAs. This sub-type gather all ncRNA larger than 200 nucleotides that are transcribed from diverse regions of eukaryotic genomes. As for mRNA, lncRNAs are transcribed by RNA polymerase II (RNApol II) and undergo 3'-poly(A) tailing and 5'-end capping as well as splicing (Fig. 7). lncRNAs are tissue specific and differently expressed under both normal and pathological conditions. They play important roles in cell differentiation, chromosome dosage compensation, organ development, and disease progression processes (Morceau et al., 2013). lncRNAs can modulate gene expression through different mechanisms. Of those, many seem to direct gene expression through recruitment of chromatin modifiers. This is consistent with several observations that chromatin modifiers, such as Polycomb Repressive Complex 2 (PCR2), can associate with multiple noncoding transcripts. Interestingly, lncRNAs

can act as scaffolds to recruit histone modifiers (Hu et al., 2012; Zhang and Pradhan, 2014).

miRNAs are small ncRNAs of 19-22 nucleotides (nt) which possess a seed region (2-8 nt) that binds to complementary mRNAs sequence in order to repress their translation or reduce their stability. As each miRNA can recognize hundreds of targets, and multiple miRNAs may target individual mRNAs, these gene regulatory networks can become further complex. miRNAs influence numerous cellular processes including cell cycle regulation, differentiation, and apoptosis. Therefore, they can act as tumor suppressors or oncogenes (Diederichs et al., 2016). miRNAs are generally produced either from the coding sequence of their corresponding target genes or from the splicing product of their introns. Clusters of miRNA-encoding genes are typically transcribed by RNApol II yielding the pri-miRNA sequence, which may contain multiple tandem miRNAs. Drosha processes pri-miRNAs by cleaving them about eleven nucleotides from the hairpin base to produce the “so-called” pre-miRNAs. The resulting product has a two-nucleotide overhang at its 3’ end that enables it to be recognized and exported to the cytoplasm by exportin-5. Dicer, then, is able to produce the mature miRNA from the pre-miRNA sequence (Fig. 7) and usually load it into the RNA-induced silencing complex (RISC). The Argonaute (Ago) protein in the RISC complex will then cut mRNAs that are complementary to the loaded miRNA. This cutting of targeted mRNAs is needed to enforce transcriptional gene silencing (Zhang and Pradhan, 2014). Indeed, a large number of miRNA participate in both normal physiological processes and diseases, including cancer. This has led researchers to look into miRNAs as diagnostic or prognostic markers in cancer. For example, miR-21 overexpression in breast cancer is associated with advanced clinical stage, lymph node metastasis, and poor patient prognosis (Takamizawa et al., 2004).

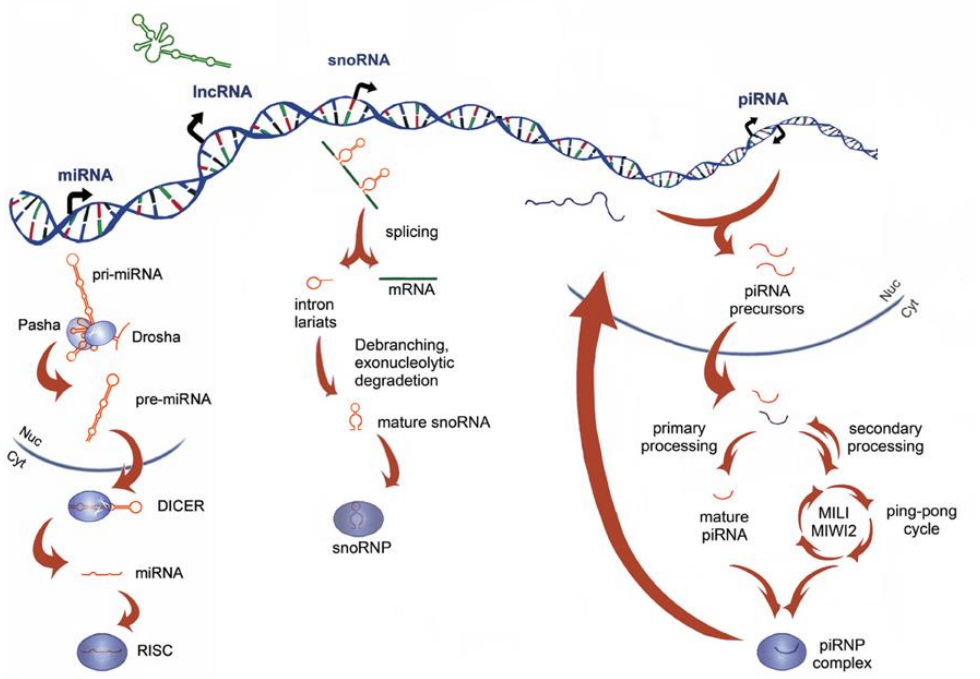

***Figure 7**. Non-coding RNAs biogenesis. MicroRNAs originate as pri-miRNAs that are processed by the Drosha/Pasha complex in the nucleus. The resulting pre-miRNAs are exported into the cytoplasm, where they are processed by Dicer to form mature miRNAs, which interact with the RISC complex, acquiring a post-transcriptional silencing activity. Long noncoding RNA are transcribed from intra- and inter-genic regions by RNApol II. Small nucleolar RNAs (snoRNAs) are codified primarily from introns. After the pre-mRNA generation, the transcript is spliced and the intron lariat is debranched and trimmed. The mature snoRNA interacts with ribonuclear proteins (RNPs), before being exported into the cytoplasm having a role in ribosomal RNA (rRNA) modification and processing, or being retained into the nucleus, where it plays a role in alternative splicing. piRNAs originate as precursors from transposons and large piRNA clusters. Then, they are processed and exported into cytoplasm, where they undergo a primary or cyclic secondary processing (ping pong cycle, mediated by PIWI, MIWI, and MIWI2 proteins in mouse) and the assembly in piRNP complexes that modulate transposon activity and gene expression (adapted from Della Ragione et al., 2014).*

P-element-induced wimpy testis (PIWI)-interacting RNAs (piRNAs) have originally been identified in *Drosophila Melanogaster* and are mainly involved in the silencing of transposable elements (TEs) (Fig. 7), especially in germ cells (Girard et al., 2006). siRNAs are double-stranded small RNAs that can suppress the post-transcriptional gene expression via the RNA interference (RNAi) pathway. It must

be pointed out that the production of these siRNAs is Dicer-dependent but not Drosha-dependent (Song et al., 2011).

Small nuclear RNAs (snRNAs), form a class of RNA molecules with an average length of 150 nt, localized within the nucleus of eukaryotic cells. Their primary function is pre-mRNA processing; for this reason they are always associated with a set of specific proteins forming complexes that are named small nuclear ribonucleoproteins (snRNP) (Fig. 7).

1.1.4. Histones post-translational modifications (PTMs)

Since the position of nucleosomes on DNA and the organization of chromatin into higher-order structures can affect the DNA-proteins binding, eukaryotes have evolved a complex array of enzymes that modify chromatin. Therefore, histones are not mere packaging proteins but represent chief regulators in chromatin dynamics. They undergo a wide range of post-translational modifications, essentially on their N-terminal tails, which emerge from the nucleosome surface (Fig. 8). Histone-modifying enzymes introduce a composite range of PTMs that can either trigger or suppress transcription, relying on the type of modification and its location in the histone octamer. A wide range of PTMs have been enlisted, including acetylation, methylation, phosphorylation, ubiquitination, glycosylation, SUMOylation, poli-ADP-ribosylation and carbonylation (Khorasanizadeh, 2004).

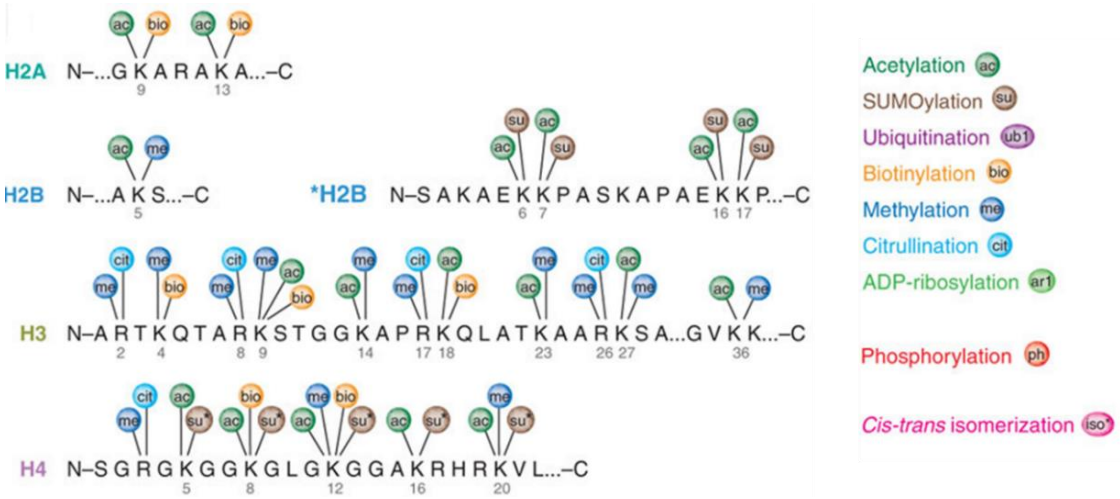

***Figure 8**. Known post-translational modifications. Residues that can undergo several different forms of post-translational modification. Each modification inhibits subsequent modifications (adapted from Latham and Dent, 2007).*

The mechanisms by which histone PTMs affect chromatin structure and dynamics could be divided into two categories. Histone PTMs can directly either influence histone-DNA and histone-histone interactions or they can be targeted by protein effectors (also referred to as histone-binding domains, HBDs). The specific recognition of PTMs by HBDs recruits various components of the nuclear signaling network, mediating fundamental processes such as gene transcription, DNA replication and recombination, DNA damage response and chromatin remodeling (Musselman et al., 2012).

1.2. Writers, Erasers and Readers

Management of chromatin structure through histone PTMs has emerged as a fundamental driver of transcriptional responses in numerous cell types. Three major functional classes of proteins are involved in the regulation and turnover of these modifications, namely writers, erasers and readers. They belong to the protein machinery that adds, removes, or recognizes these PTMs (Janzen et al., 2010). Writers, erasers and readers are usually divided into PTM-specific classes (Fig. 9).

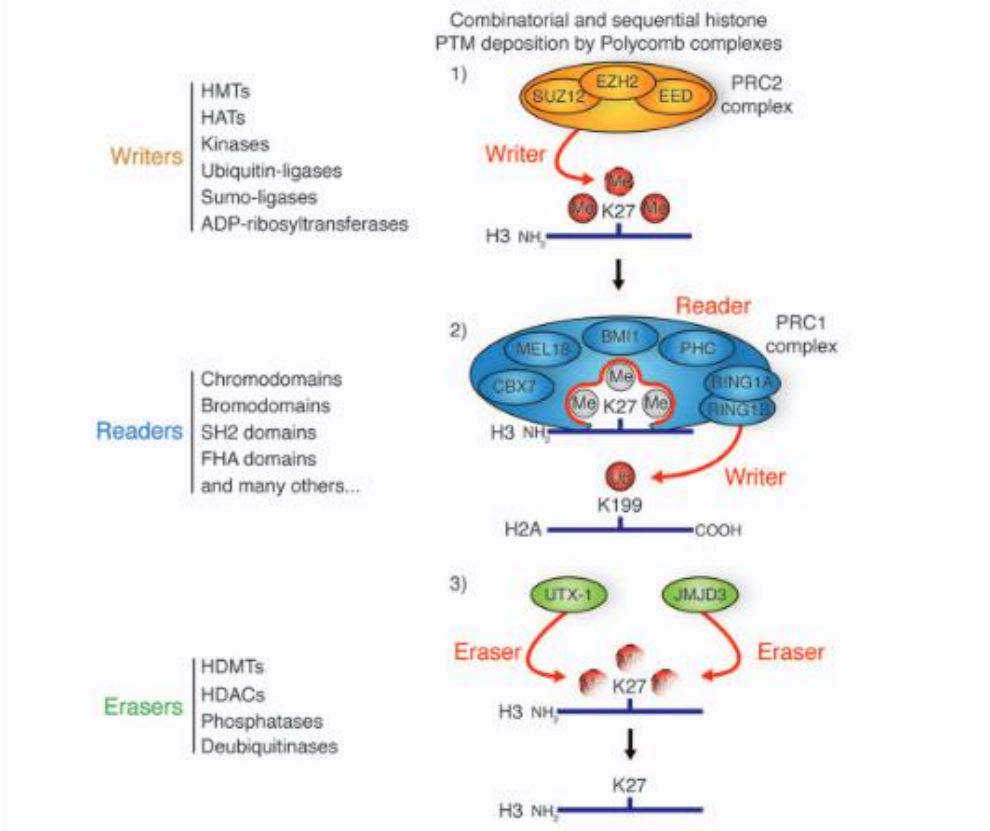

***Figure 9**. Representation of histone writers, which add covalent PTMs to histone tails, readers, which recognize and bind histone PTMs, and erasers, which remove histone PTMs. Associated protein families are enumerated on the left. In this example, the PRC2 complex adds tri-methylation on lysine 27 of histone H3 (top right image). This modification is then recognized by the reader complex PRC1 (lower right image). The RING1A and RING1B subunits of PRC1 subsequently ubiquitinate lysine 199 of histone H2A. UTX-1 and JMJD3 can act to remove histone H3 K27 tri-methylation (bottom right image) (adapted from Tollervey and Lunyac, 2012).*

Writers comprise histone acetyltransferases (HATs) and histone methyltransferases (HMTs), whose effects are reversed by the corresponding erasers, named histone deacetylases (HDACs) and histone lysine/arginine demethylases (KDMs or RDMs), respectively (Ferri et al., 2016). These have been intensively studied and targeted for drug discovery in cancer, inflammation and various other diseases.

Readers are often found in association with other epigenetic regulators, e.g. writers and erasers, to form large multi-protein complexes (Dawson et al., 2012). Over the past decades, many conserved domains that recognize modified histones have been discovered, including Chromo (Chromodomain), Tudor, MBT (Malignant Brain Tumor)

and BRD (Bromodomain) (Taverna et al., 2007). The specificity of a reader for a certain PTM derives from a direct interaction between the modified histone residue and the readers' binding pocket, as well as by secondary contacts involving the flanking histone sequence (Ferri et al., 2015).

1.2.1. Bromodomains

Histone acetylation is usually linked to enhanced DNA accessibility and transcriptional activation. Acetylation, indeed, weakens histone-DNA interactions neutralizing the positive charge on lysine residues and inducing histones structural changes. This way, acetylation loosens chromatin packing, increasing accessibility (Ferri et al., 2015). One of the most important reader domain is the bromodomain, which specifically recognizes N-acetylated lysine residues (Kac). There are eight human BRD-containing protein families including 46 proteins with various structures and functions (Tab. 2). BRDs are evolutionarily conserved and are found in different proteins including chromatin-modifying enzymes (i.e. HAT and HAT-associated proteins), methyltransferases, helicases, chromatin remodelers, transcriptional co-activators and mediators, and the BET family (Chaidos et al., 2015). All these elements are enlisted in Table 1.

Table 1. Bromodomain-containing proteins and their functions (Muller et al., 2011).

Protein	Name	Function	BRDs
ASH1L	Absent, small or homeotic-like	Methyltransferase	1
ATAD2A/B	AAA domain-containing protein 2	ATPase, coactivator	1
BAZ1A/B	BRD adjacent to zinc finger domain protein 1A	Chromatin assembly and remodelling	1
BAZ2A/B	BRD adjacent to zinc finger domain protein 2A/B	Unknown	1
BRD1	BRD-containing 1	Transcription factor	1
BRD2	BRD-containing 2	Transcription factor	2
BRD3	BRD-containing 3	Transcription factor	2
BRD4	BRD-containing 4	Transcription factor	2
BRDT	BRD-containing protein testis specific	Transcription factor	2
BRD7	BRD-containing 7	Transcriptional repressor	1
BRD8A/B	BRD-containing 8A/B	TRRAP/TIP60 complex	2
BRD9	BRD-containing 9	Unknown	1
BRPF1A/B	Peregrin	MOZ complex subunit	1
BRPF3A	BRD and PHD-finger-containing protein 3	Unknown	1
BRWD3	BRD and WD-repeat-containing protein 3	JAK/STAT signalling	2
CECR2	Cat eye syndrome critical region 2	Chromatin remodelling	1
CREBBP	CREB-binding protein	HAT	1
EP300	HAT p300	HAT	1
FALZ	Fetal Alzheimer antigene	Chromatin remodelling	1
GCN5L2	General control of amino acid synthesis protein 5-like 2	HAT	1
MLL	Mixed lineage leukaemia	Histone methyltransferase	1
PB1	Polybromo	SWI/SNF PBAF subunit	6
PCAF	P300/CBP-associated factor	HAT	1
PHIP	PH-interacting protein	Insulin signalling	2
PRKCBP1	Protein kinase C-binding protein 1	Transcriptional regulator	1
SMARCA2A/B	SWI/SNF-related, matrix-associated, actin-dependent regulator of chromatin	SWI/SNF ATPase	1
SMARCA4	SWI/SNF-related, matrix-associated, actin-dependent regulator of chromatin	SWI/SNF ATPase	1
SP100/SP110/ SP140	Nuclear body protein	Transcriptional regulator	
TAF1/TAF1L	Transcription initiation TFIID-associated factor	Transcription initiation	2
TRIM24/TRIM28/ TRIM33/TRIM66	Transcription intermediary factor	Transcriptional silencer	1
WDR9	BRD and WD-repeat-containing protein 1	Chromatin remodelling	2
ZMYND11	Zinc finger MYND-domain-containing protein 11	Corepressor	1

All BRDs share an evolutionary conserved structure that is a left-handed four-helix bundle (α_Z, α_A, α_B and α_C), termed the 'BRD fold'. The inter-helical α_Z-α_A (ZA) and α_B-α_C (BC) loops constitute a pocket that recognizes the acetyl-lysine modification (Dhalluin et al., 1999) (Fig. 10).

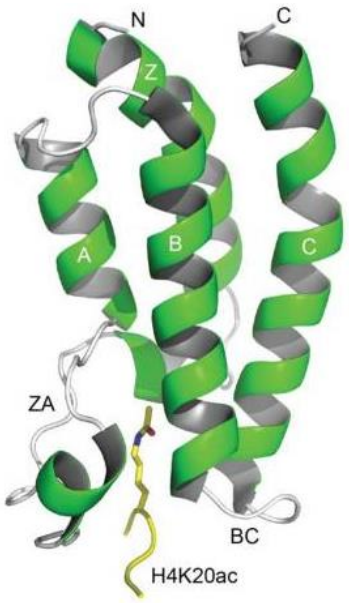

***Figure 10**. The BRD fold. Structure of the CREBBP-BRD in complex with H4K20ac peptide (adapted from Sanchez et al., 2014)*

BRDs are often associated with other PTM-related proteins and this way they generate high target selectivity and an increased binding affinity by the simultaneous binding of several interaction domains. This property leads to the idea that epigenetic regulation recognizes patterns of PTMs (words) rather than single modifications (letters) (Wu et al., 2009). BRD-containing proteins rule a large variety of biological processes, including cell growth, genomic stability, development, neuronal plasticity and memory.

1.2.2. BET proteins

The most BRD-containing protein family studied is the Bromodomain and Extra-Terminal (BET) one (Nicodeme et al. 2010). This family includes four members: BRD2, BRD3, and BRD4, which are ubiquitously expressed, and BRDT, whose expression is confined to germ cells (Fig. 11). They possess a tandem bromodomain at the N-terminal tail, by which they interact with histone acetyl-lysines, to control gene transcription and cell growth (Mio et al., 2016). Firstly detected as protein scaffolds, BET proteins recruit a variety of effectors on chromatin and transcription sites in order to control gene expression.

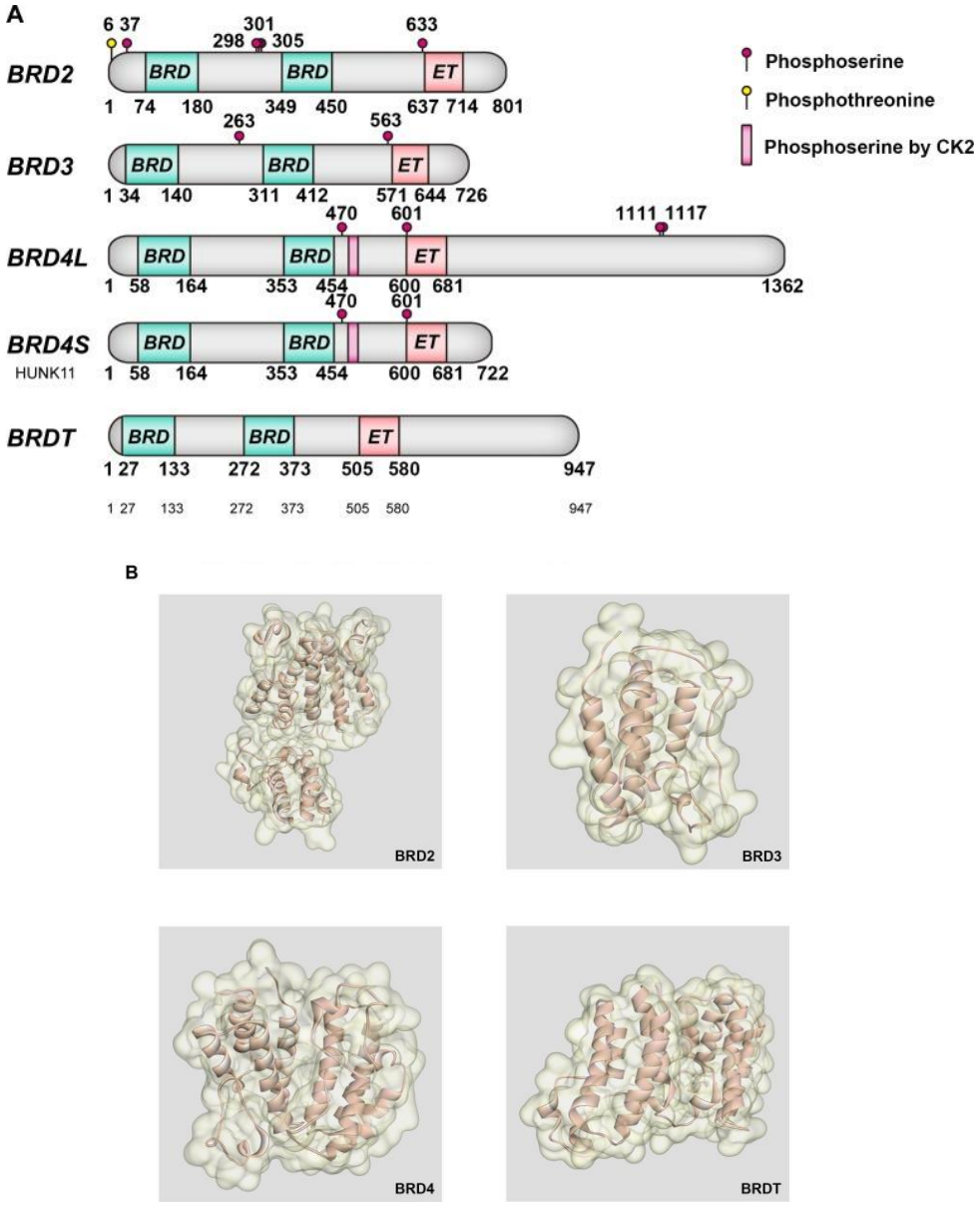

***Figure 11**. Molecular structures of BET bromodomains. Crucial post-translational modification sites and main features of BET proteins. (B) Structure of BET proteins (adapted from Fu et al., 2015).*

The bromodomains of BRD2 and BRD4 shared about 80% amino-acid identity in both humans and mice. It has been reported a substantial functional discrepancy between BRD2- and BRD4-derived phenotypes that probably does not lie in the relative specificity of the dual BRDs for their targets, but perhaps on the enzymes recruited through the interaction with the ET domain and C-terminal domain (CTD) (Belkina and Denis, 2012). The ET domain, indeed, independently recruits transcription-modifying factors, i.e. glioma tumor suppressor candidate region gene 1 (GLTSCR1),

a SET domain-containing histone methyltransferase (NSD3), a histone arginine demethylase (JMJD6) and a catalytic component of the NuRD nucleosome remodeling complex (CHD4) (Florence and Faller, 2001). BRD4 and BRD2 play a crucial part in cell cycle control of normal cells (Kanno et al., 2004). It has been shown that E2 transcription factor 1 (E2F1) and 2 (E2F2), which are key transcriptional regulators of S phase-associated genes, are associated with BRD2-containing complexes (Denis et al., 2006), while BRD4 inhibition leads to cell cycle arrest in G1-S phase through MCM5 down-regulation and significantly reduces cell growth (Mio et al., 2016). Recent evidence shows that BRD2 and BRD4 persist bound to mitotic chromatin in order to trigger the maintenance of epigenetic memory (Zhang et al., 2008). These properties of BET proteins are highly conserved through phylogeny, including yeast, thale cress (*Arabidopsis Thaliana*), zebrafish (*Danio Rerio*), murine and human cells (Belkina and Denis, 2012) (Fig. 12).

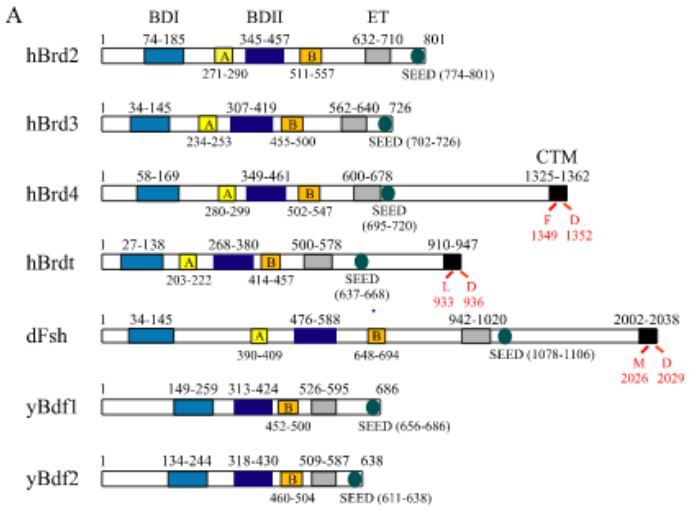

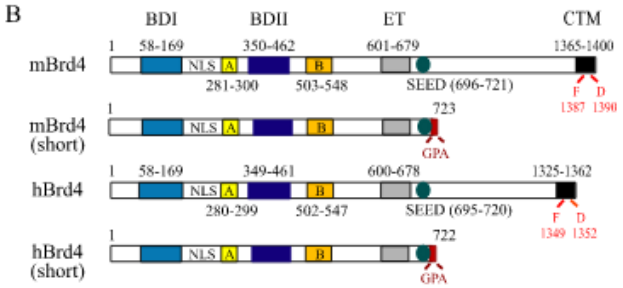

***Figure 12**. BET proteins domain organization. A, human (h), Drosophila (d) and yeast (y) BET proteins. Numbers indicate the amino-acid boundaries of each domain. B, protein isoforms of mouse and human Brd4 proteins. The short forms of mouse and human Brd4 have the same N-terminal amino acid residues (720 for mouse and 719 for human) as found in their long forms but differ in the last three amino acids (GPA), which are encoded by a different exon (adapted from Wu and Chiang, 2007).*

Among BET proteins, BRD4 is the most intensively studied due to its direct role in transcriptional control. It possesses a marked preference for acetylated lysine 14 on histone H3 (H3K14) and lysine 5/12 on H4 (H4K5-12) (Wu and Chiang, 2007). Two BRD4 isoforms exist. The long one is the isoform accounted for almost all the biological functions attributed to BRD4. Indeed, it is involved in a wide range of cellular processes, e.g. cell cycle regulation, transcription, bookmarking of active genes during mitosis and transcription factors scaffolding (Fig.13). Intriguingly, BRD4 is found to be associated with most active enhancer (super-enhancers, SEs) and promoter regions (Loven et al., 2013). Super-enhancers are described as a class of regulatory regions with unusually strong enrichment for the binding of transcriptional co-activators, occupancy, high levels of H3K27ac together with low levels of H3K4me3 (Lin et al., 2012).

Although the two BDs and the ET domains are characteristic features of all the BET family proteins, BRD4 possesses a unique C-terminal domain (CTD) through which recruits the positive transcription elongation factor complex (P-TEFb). The latter is composed of cyclin-dependent kinase-9 (CDK9) and its activator cyclin T (Muller et al., 2011). BRD4 displaces negative regulators from P-TEFb, thereby transforming it into an active form where CDK9 can phosphorylate RNApol II C-terminal domain. This

recruitment of P-TEFb by BRD4 is thought to stimulate the transcription of primary responsive genes (Rahman et al., 2011).

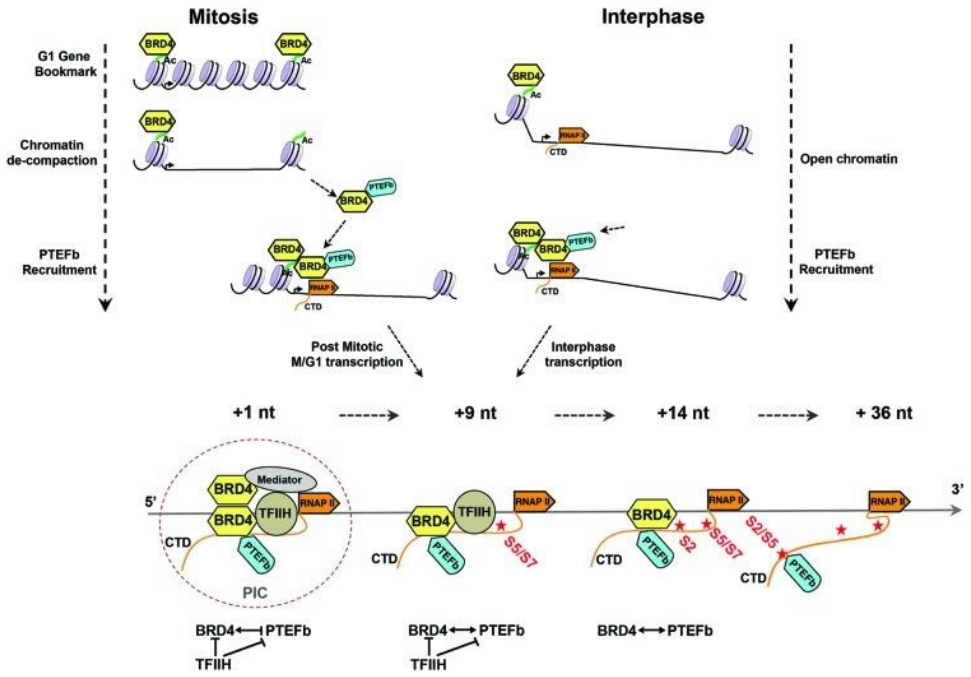

***Figure 13**. BRD4 function during cell cycle and gene transcription. The upper left panel shows, BRD4 as a G1 gene bookmarker during mitosis by binding to acetylated chromatin, as a P-TEFb recruiter and chromatin de-compacter. During interphase (upper right), it recruits P-TEFb to RNA Pol II, either directly binding chromatin or dimerizing with chromatin-bound BRD4. The lower panel shows the transcription initiation in which direct and indirect interactions among the CTD kinases, including BRD4, initially maintain their activity, with the release of their activities as the transcription complexes proceeds (adapted from Devaiah and Singer, 2012).*

Since BET proteins have a crucial role in regulating gene transcription through the recruitment of chromatin modifiers complexes, any mutation or alteration in their expression could lead to a different spectrum of diseases.

1.3. Epigenetics and diseases

It is well known that either genetic or epigenetic changes could contribute to the development of human diseases. Although precise underlying mechanisms are not yet clear, in recent years, scientific interest in epigenetics has increased insofar as it represents an important tool to improve our knowledge on pathogenesis, in particular tumorigenesis, and to help in the development of strategies for cancer treatment and prevention (Nebbioso et al., 2012).

Each cell possesses its own epigenetic pattern that must be carefully maintained to regulate proper gene expression. Any perturbation in this carefully arranged phenomenon can lead to congenital disorders or predispose subjects to acquired disease states such as sporadic cancers and neurodegenerative disorders (Fig. 14). Epigenetic proteins can contribute to diseases mostly in two ways. Mutations altering the activity or the expression levels of an epigenetic protein may directly cause or maintain the disease state. In this scenario, they could represent good candidates for direct drug targeting (Ferri et al., 2016). Alternatively, disruption in the proper maintenance of these heritable epigenetic mechanisms can lead to activation or inhibition of various critical cell signaling pathways thus leading to pathological conditions such as cancer (Egger et al., 2004). The misreading of epigenetic marks has been shown to underlie a multitude of human diseases, including autoimmune and developmental abnormalities (Portela and Esteller, 2010), schizophrenia and other mental disorders (Tsankova et al., 2007), cardiovascular and neurological diseases, metabolic disorders (Heerboth at al., 2014) and cancer development.

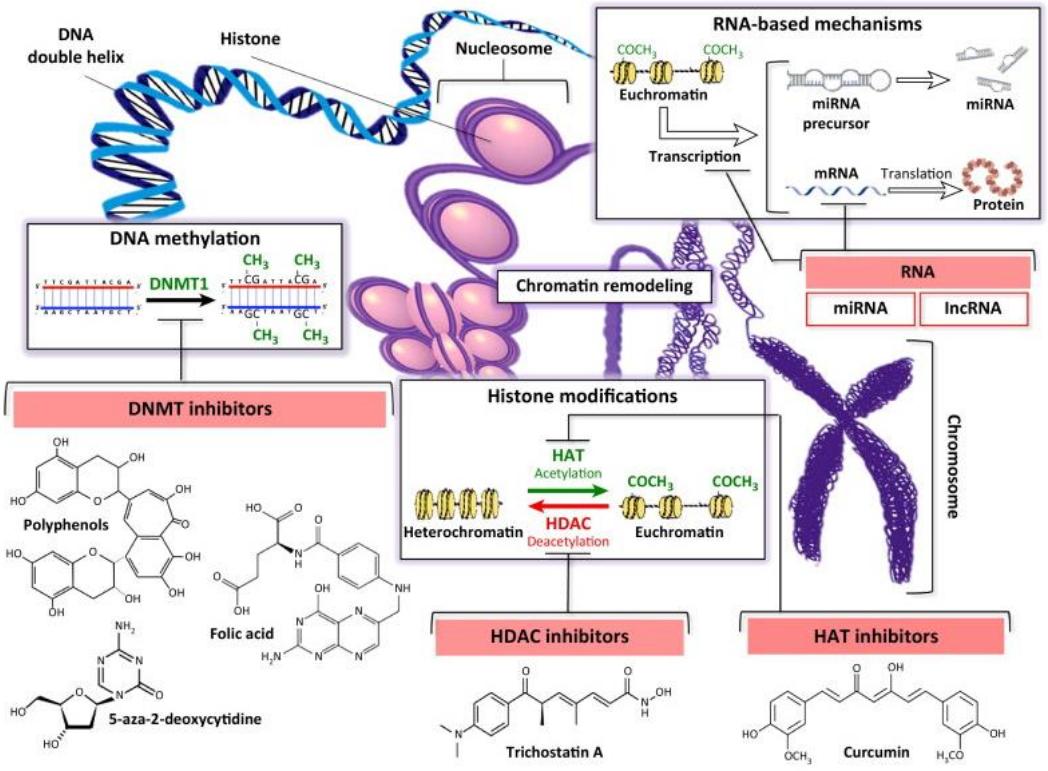

***Figure 14**. Some examples of epigenetic mechanisms and compounds. This schematic representation illustrates the potential epigenetic mechanisms, including DNA methylation, histone alterations, and RNA-based transcriptional control, which can alter the cellular gene expression profile. Chemical structures of selected compounds targeting epigenetic modifications are also reported. (adapted from Schiano et al., 2015).*

Unlike genetic alterations, epigenetic changes are reversible in nature and can be potentially restored to their original state by epigenetic therapy. Therefore, identifying drugs that can inhibit these epigenetic changes are of great clinical interest. So far, four epigenetic drugs have been approved for clinical use:

- the DNMT inhibitors (DNMTi) azacitidine and decitibine, used to treat myelodysplastic syndrome, a hematological disease;
- the HDAC inhibitors (HDACi) vorinostat and romidepsin, used to treat relapsed cutaneous T cell lymphoma (De Woskin and Million, 2013).

Nowadays, preclinical research is focusing on different epigenetic pathways in order to create new valuable epigenetic drugs, such as DNA methylation inhibiting drugs, BRD inhibitors, poly-(ADP-ribose)-polymerases (PARP) inhibitors (PARPi), HAT inhibitors (HATi), HDAC inhibitors (HDACi) and HMT inhibitors (HMTi).

1.3.1. Epigenetics and cancer

All findings presented so far have inspired many studies aimed to understand the role of epigenetics in tumorigenesis and further explore its utility in cancer diagnosis, prognosis and therapy (Yoo and Jones, 2006). First clues for the underlying mechanisms leading to global epigenetic reprograming in cancer come from the next-generation sequencing (NGS)-based profiling projects that catalog mutations, structural variations, epigenomic patterns as well as transcriptome data (Weichenhan and Plass, 2013). For example:

- in acute myeloid leukemia, there have been uncovered mutations in isocitrate dehydrogenase 1 (*IDH1*) or *DNMT3A*, enzymes involved in establishing and maintaining DNA methylation (Ley et al., 2010);
- there are mutations in AT-rich interactive domain-containing protein 1A (*ARID1A*) in non-small-cell lung cancer, a protein involved in transcriptional activation and repression of selected genes by chromatin remodeling (Imielinski et al., 2012);
- CREB binding protein (*CREBBP*), E1A binding protein p300 (*EP300*) and lysine methyltransferase 2A (*KMT2A*) are found mutated in small-cell lung cancer (Peifer et al., 2012);
- the histone variant H3.3 (H3F3A) is found in pediatric glioblastoma (Schwartzentruber et al., 2012).

Most of these mutations are associated with altered global DNA or histone modification patterns; however, the underlying cause of these patterns is mostly still elusive.

Not only mutations but also deregulation of epigenetic control has been frequently associated with several human diseases, such as cancer. Tumor cells suffer global epigenetic reorganization resulting in the CpG-specific hypermethylation of tumor-suppressor gene promoters and a generalized loss of DNA methylation at microsatellite regions, repetitive sequences and oncogene promoters (Simó-Riudalbas and Esteller, 2015). Depending on the protein involved and the pathway

affected, these alterations could lead to changes in gene transcription or to global changes in chromatin structure, leading ultimately to cancer development. Cancer-specific DNA methylation can serve as a marker for early detection of a disease or as a prognostic marker that helps classifying tumor subgroups with different biological or clinical features. This has been shown for glutathione S-transferase P (*GSTP1*) promoter methylation as a marker for early detection of prostate cancer (Lee et al., 1994) or O^6-methylguanine DNA methyltransferase (*MGMT*) methylation as a marker for treatment response in glioblastoma (Esteller et al., 2012).

Histone acetylation and deacetylation possess a huge influence on gene expression regulation, thus, any dysregulation in this fine balance can have substantial impact, for example, on cell proliferation. For these reason, HDAC and/or HAT gene expression levels have been proposed as potential prognostic markers for several tumor types or to predict the aggressiveness of various cancers (Russo et al., 2011). The effects of HDACi on various hematologic malignancies and solid tumors have already been assessed (Tan et al., 2010; Baldan et al, 2015).

MicroRNAs (miRs), a recent target of intense investigation for their diagnostic and therapeutic potential, have also been implicated in normal development as well as in solid and hematological tumors. For example, several miRs including miR-125, miR-23 and miR-181 have been associated to various steps of hematopoiesis and leukemogenesis (Zaidi et al., 2013).

All these considerations sustain the hypothesis that appropriate patterns of DNA methylation, histone modifications and ncRNAs modulation are required to maintain cell identity and its disturbance can contribute to cancer insurgence.

1.3.2. BET inhibitors

It has been shown that, in cancer, aberrant lysine acetylation often leads to gene expression changes that result in inactivation of tumor-suppressors and activation of pro-survival and proliferation-promoting pathways. Bromodomains, then, have attracted great interest as promising new epigenetic targets for several human diseases, including inflammation, cancer and cardiovascular disease. In 2010, the BET

BRD inhibitors (BETi) JQ1 and I-BET762 (Fig. 15 and Tab. 3) have been synthetized, inaugurating a new chapter in the history of epigenetic drug discovery (Filippakopoulos et al., 2012; Nicodeme et al., 2010).

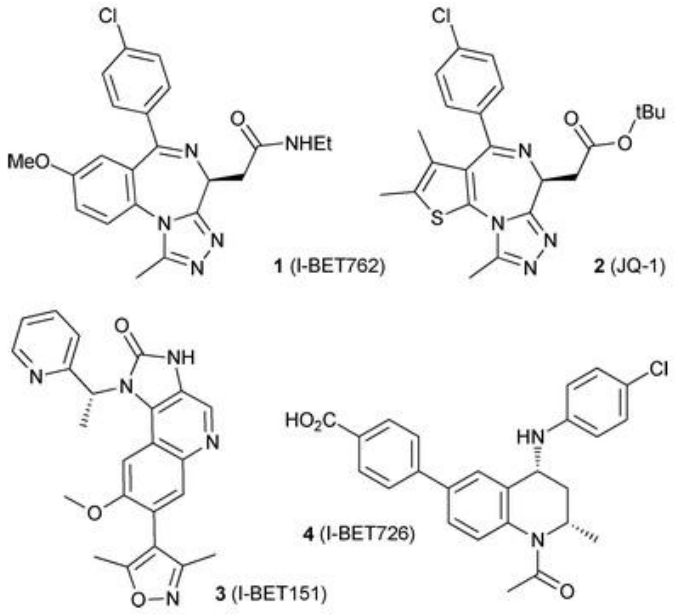

***Figure 15**. BET inhibitors discovered directly or indirectly through cell-based screening (adapted from Bamborough and Chung, 2015).*

JQ1 and IBET762 interact with the BRD pocket competitively with acetylated peptides, resulting in the displacement of BET proteins from acetylated chromatin. JQ1 is chiefly selective for the BET family, with a dissociation constant (KD) of 50 nM for BRD4 and of 60–190 nM for the other family members. It has been shown, using a crystallographic approach, that JQ1 triazole moiety mimics a Kac (Filippakopoulos et al., 2010) (Fig. 16). In contrast, the (-)-JQ1 enantiomer has no BET BRDs binding properties, providing a useful negative control for validating the biological effects of (+)-JQ1.

Table 2. Representative BRD inhibitors (Ferri et al., 2016)

Inhibitor	Affiliation	Scaffold	Target BRD	Potency	Discovery method
JQ1	Dana-Farber Cancer Institute	Triazolodiazepine	BET	K_D = 50–190 nM (BRD2-4,BRDT)	Phenotypic screen (ApoA1)
I-BET762	GSK	Triazolodiazepine	BET	K_D = 50–61 nM (BRD2-4)	Phenotypic screen (ApoA1)
RVX-208	Resverlogix	Quinazolone	BET (2nd BRD)	K_D = 140 nM (BRD4(2))	Phenotypic screen (ApoA1)
I-BET151	GSK	Dimethylisoxazole	BET	20–100 nM (BRD2-4)	Fragment-based screen
Ischemin	Mount Sinai Hospital	Azobenzene	CBP/p300	K_D = 19 μM (CBP)	NMR-based screen
PFI-1	Pfizer	Dihydroquinazolinone	BET	IC_{50} = 220 nM (BRD4(1))	Fragment-based screen
CBP30	SGC	Dimethylisoxazole	CBP/p300	K_D = 21 nM (CBP)	Fragment-based screen
OTX015	Oncoethix (Merck)	Triazolodiazepine	BET	IC_{50} = 92–112 nM (BRD2-4)	Phenotypic screen (cell adhesion)
BAZ2-ICR	SGC	Pyrazole	BAZ2A/BAZ2B	K_D = 109 nM (BAZ2A)	Virtual screen
IACS-9571	MD Anderson Cancer Center	Benzimidazolone	TRIM24/BRPF1	K_D = 14 nM (BRPF1)	Virtual screen/focused HTS
LP99	SGC	1-Methyl-quinolone	BRD9/BRD7	K_D = 99 nM (BRD9)	Fragment-based screen

Abbreviations: ApoA1, Apolipoprotein A; BET, Bromodomain and Extra-Terminal; GSK, GlaxoSmithKline; SGC, Structural Genomics Consortium.

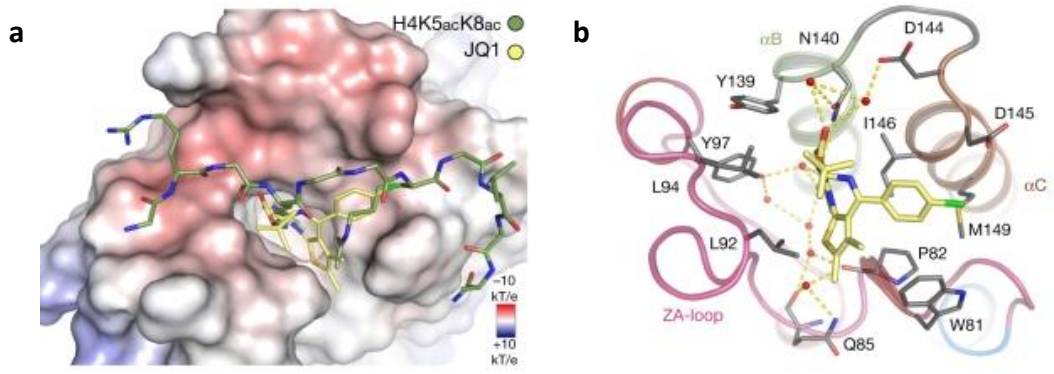

***Figure 16**. Structural overview of a BET-BRD and its binding to an inhibitor. (a) Superimposition of a diacetylated BET substrate and JQ1. Inhibitor and peptide molecules are shown in stick representation and are colored according to atom types. (b) Binding of JQ1 to the BRD4-BRD. Conserved water molecules in the active site are highlighted and hydrogen bonds are shown as dashed lines. (Adapted from Muller et al., 2011).*

JQ1 showed preclinical efficacy in NUT midline carcinoma (NMC), an aggressive type of human squamous cancer, corroborating BET inhibition as a useful therapeutic strategy in oncology. The nuclear protein in testis (NUT) locus (15q14) and the BRD4 locus (19p13.1) translocate to create a BRD4–NUT fusion gene whose product is driven by the BRD4 promoter, an oncogenic rearrangements that lead to a highly tumorigenic fusion protein (Filippakopoulos et al., 2010; Dawson et al., 2011). I-BET762 (also called I-BET or GSK525762) is a triazolodiazepine that present binding affinities, selectivity profile, and interaction patterns with BET BRDs analogous to JQ1 (Dawson et al., 2011). It binds to the tandem bromodomains of BRD2–4 with a KD (BRD4) of 55 nM. Additionally, I-BET762 down-regulates several inflammatory genes in cell studies and reduces inflammation in vivo (Ferri et al., 2016). I-BET151 has been identified by phenotypic screening and developed simultaneously to I-BET762. It possesses a KD of 36 nM that improves its pharmacokinetic properties compared to triazolobenzodiazepine scaffolds (Mirguet et al., 2012).

The majority of BRDi reported so far target BET proteins, including all ten inhibitors currently in clinical trials (Tab 4). Most inhibitors mimic Kac by hydrogen bonding with the conserved asparagine (Asn) residue.

Table 3. BET inhibitors in clinical trials (Ferri et al., 2016)

Inhibitor	Sponsor	Phase	Condition	Start date	Status	Clinical trial
RVX-208	Resverlogix	I,II	Atherosclerosis, Dyslipidemia, CAD	October 2008	Completed	NCT00768274
		II	Atherosclerosis, CAD	December 2009	"	NCT01058018
		IIb	CAD	September 2011	"	NCT01067820
		IIb	Dyslipidemia, CAD	August 2011	"	NCT01423188
		II	Diabetes	November 2012	"	NCT01728467
		II	Dyslipidemia, CAD	May 2013	Terminated	NCT01863225
		III	T2DM, CAD	October 2015	Recruiting	NCT02586155
I-BET762	GSK	I	NMC & other solid tumors	March 2012	Recruiting	NCT01587703
		I	Hematological Malignancies	May 2014	"	NCT01943851
OTX-015	Oncoethix (Merck)	I	AML, DLCBL	December 2012	Recruiting	NCT01713582
		Ib	NMC, CRPC & other solid tumors	October 2014	"	NCT02259114
		IIa	Glioblastoma Multiforme	October 2014	Active	NCT02296476
CPI-0610	Constellation	I	Lymphoma	September 2013	Recruiting	NCT01949883
	Pharmaceuticals	I	Multiple myeloma	July 2014	"	NCT02157636
		I	AML, MDS, MDS/MPN	June 2014	"	NCT02158858
TEN-010	Tensha	I	NMC & other solid tumors	October 2013	Recruiting	NCT01987362
	Therapeutics	I	AML, MDS	October 2014	"	NCT02308761
BAY 1238097	Bayer	I	Advanced malignancies	March 2015	Recruiting	NCT02369029
ABBV-075	AbbVie	I	Breast cancer, multiple myeloma, NSCLC, AML	April 2015	Recruiting	NCT02391480
INCB 054329	Incyte	I/II	Advanced malignancies	May 2015	Recruiting	NCT02431260
BMS-986158	Bristol-Myers Squibb	I/IIA	TNBC, ovarian cancer, small-cell lung cancer	June 2015	Recruiting	NCT02419417
FT-1101	Forma Therapeutics	I	AML, MDS	September 2015	Recruiting	NCT02543879

Abbreviations: AML, Adult Myeloid Leukemia; BET, Bromodomain and Extra-Terminal; CAD, coronary artery disease; CRPC, castrate-resistant prostate cancer; DLCBL, Diffuse Large B-Cell Lymphoma; GSK, GlaxoSmithKline; MDS, Myelodysplastic syndrome; MDS/MPN, Myelodysplastic/Myeloproliferative Neoplasms; MF, myelofibrosis; MLL, Mixed-Lineage Leukemia; NSCLC, non-small cell lung cancer; NMC, Nut-Midline Carcinoma; TNBC, triple negative breast cancer; T2DM, Type 2 Diabetes Mellitus.

Translational studies have mostly focused on JQ1 and I-BET762 because of the numerous cellular pathways affected by these drugs. BETi repress v-myc avian myelocytomatosis viral oncogene homolog (*MYC*) transcription, an effect that was first described in multiple myeloma and more recently in medulloblastoma and other solid tumors. They also suppress tumor growth in several mouse models such as Burkitt's lymphoma, acute myeloid leukaemia (AML) and acute lymphoblastic leukaemia (ALL), glioblastoma, melanoma, non-small-cell lung cancer, breast and prostate cancer (Brand et al., 2015). Given that BRD4 is enriched at enhancer regions (Fig. 17), it has been postulated that super enhancer-mediated expression of key oncogenic drivers (as *MYC*) results in oncogene addiction in tumors and a high sensitivity to BRD4 loss by BET inhibitors (Loven et al., 2013).

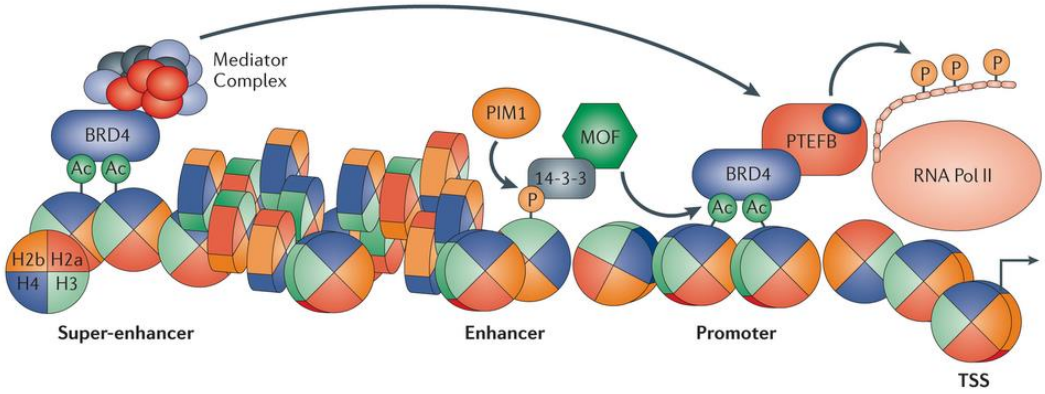

***Figure 17**. BRD4 transcriptional regulation. BRD4 can recruit the Mediator complex by docking to acetylated chromatin regions. The kinase PIM1 phosphorylates histone H3 and this modification recruit a 14-3-3 protein, which enables docking of the acetyltransferase MOF. The latter acetylates histone H4, resulting in new docking sites for BRD4, which further acts to recruit P-TEFb to acetylated promoter regions, leading to phosphorylation of the C-ter of RNA Pol II. BRD4 is particularly enriched at enhancer and super-enhancer regions, which strongly stimulates the expression of some oncogenes in cancer. Abbreviations: TSS, transcription start site (adapted from Filippakopoulos and Knapp, 2014).*

I-BET762 is currently undergoing two phase 1 clinical trials for NUT midline carcinoma (NCT01587703) and for relapsed refractory hematological malignancies (NCT01943851) (Filippakopoulos and Knapp, 2014). Inhibition of BRD4 bromodomains by I-BET762 and JQ1 strongly attenuate the expression of pro-inflammatory genes, i.e.protecting septic mice from lipopolysaccharides (LPS)-induced death (Belkina et al., 2013). Moreover, I-BET151 shows profound efficacy against human and murine MLL-fusion leukemic cell lines, via induction of early cell cycle arrest and apoptosis (Chaidos et al., 2015).

The availability of pan-BET inhibitors has enabled research into the involvement of BET proteins in transcriptional regulation and their perturbation in several diseases (Liu et al., 2012). Current available BET inhibitors have a high selectivity for BET proteins. They are not able, instead, to discriminate between the two bromodomains (BD1 and BD2): the two BRD pockets of a given BET protein are indeed more divergent with each other than with the corresponding pockets of a different BET protein (Vidler et al., 2012). Thus, more selective drugs might be needed to fulfill the challenge of 'single-member inhibition'. On the other hand, pan-BRD inhibitors might be useful for

poly-pharmacological applications in which multiple targets are inhibited by a single drug, thereby bypassing problems related with drug cocktails. Given the promising effects of bromodomain inhibitors observed in preclinical studies on oncology and inflammation, BETi have become a powerful molecular tool to disentangle epigenetic processes in physiopathological conditions.

2. Thyroid

The thyroid gland is a butterfly-shaped organ, composed by two lobes connected by an isthmus that lies on the trachea approximately at the level of the second tracheal ring. Each lobe is located between the trachea and larynx medially and the carotid sheath and sternocleidomastoid muscles laterally (Fig. 18). Both lobes are anteriorly connected to the strap muscles. The normal thyroid varies in size in different parts of the world, depending on the dietary iodine content (about 20-25 grams).

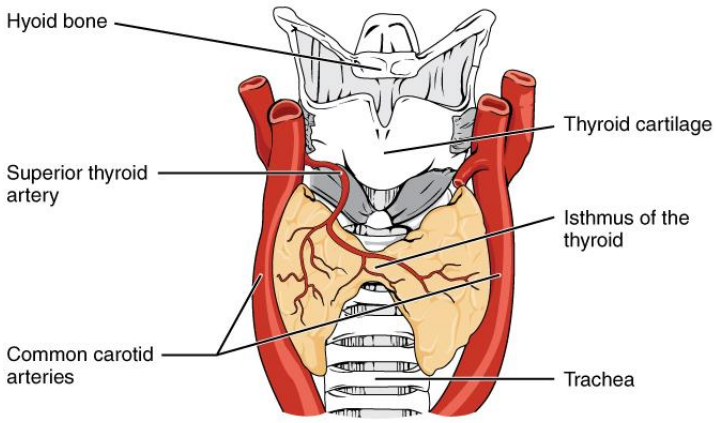

a) Anterior view

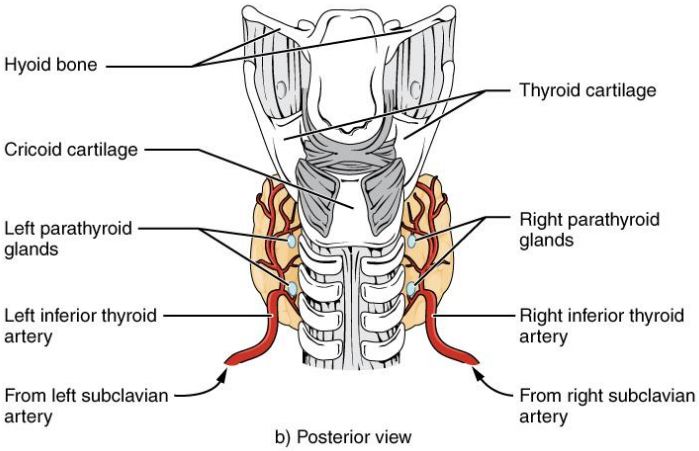

***Figure 18**. (a) Anterior view of the thyroid gland. (b) Posterior view of the thyroid gland. (Micrograph provided by the Regents of University of Michigan Medical School © 2012)*

The thyroid has an abundant blood supply provided by both the superior and the inferior thyroid arteries. A venous plexus forms under the thyroid capsule. Each lobe is drained by the superior, the middle and the inferior thyroid veins, which flow into the internal jugular vein, the internal -jugular and the innominate vein, respectively (Kaplan et al., 2015). Each of the thyroid lobes is surrounded with parathyroid glands. The thyroid gland is composed mostly of thyroid follicles, structures characterized by a central cavity filled with a sticky fluid called colloid and bounded by a wall of epithelial cells (Fig. 19).

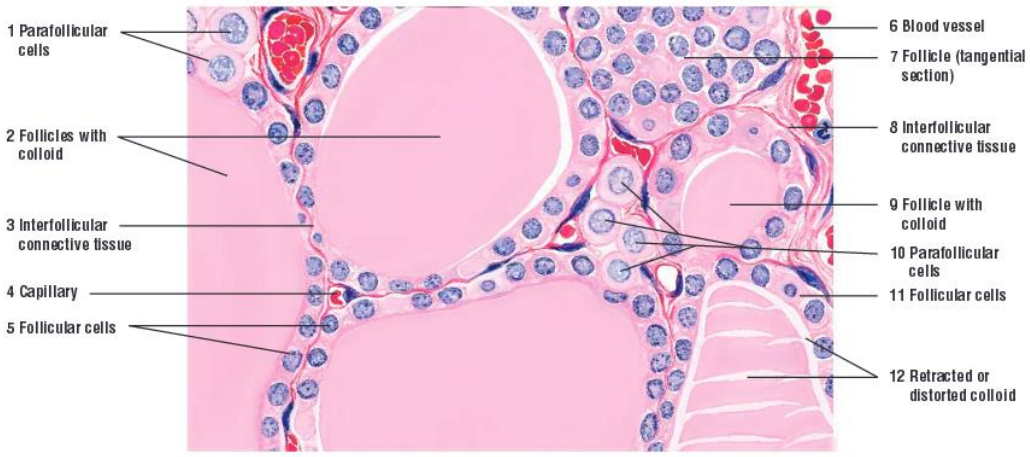

***Figure 19**. Immunohystochemical section of thyroid gland follicles (adapted from Eroschenko, 2008).*

Hormones are produced in the colloid when crystals of mineral iodine attach to a glycoprotein, called thyroglobulin (TG), which is secreted into the colloid by the follicle cells. The following steps outline the hormones' assembly:

- Binding of thyroid-stimulating hormone (TSH) to its receptors in the follicle cells of the thyroid gland causes cells to actively transport iodide ions (I^-) across their cell membrane, from the bloodstream into the cytosol.
- Iodide ions then move to the follicle cells lumen where they undergo oxidation. The oxidation of two iodide ions ($2\ I^-$) results in iodine (I_2), which passes through the follicle cell membrane into the colloid.
- In the colloid, peroxidase enzymes link the iodine to the tyrosine amino acids in TG to produce two intermediaries: a tyrosine attached to one iodine and a tyrosine attached to two iodines. When one of each of these intermediaries is linked by covalent bonds, the resulting compound is triiodothyronine (T3), a thyroid hormone with three iodines. Much more commonly, two copies of the second intermediary bond, forming tetraiodothyronine, also known as thyroxine (T4), a thyroid hormone with four iodines.

These hormones remain in the colloid center of the thyroid follicles until TSH stimulates endocytosis of colloid back into the follicle cells. There, lysosomal enzymes break apart the thyroglobulin colloid, releasing free T3 and T4, which diffuse across the cell membrane and enter the bloodstream. In the bloodstream, less than one percent of the circulating T3 and T4 remains unbound. This free T3 and T4 can cross the lipid bilayer of cell membranes and be uptaken by cells. The remaining 99% of circulating T3 and T4 is bound to specialized transport proteins called thyroxine-binding globulins (TBGs), to albumin, or to other plasma proteins. This "packaging" prevents their free diffusion into cells. When blood levels of T3 and T4 begin to decline, bound T3 and T4 are released from these plasma proteins and readily cross the membrane of target cells.

Low blood levels of T3 and T4 stimulate the release of thyrotropin-releasing hormone (TRH) from the hypothalamus, which triggers secretion of TSH from the anterior

pituitary. In turn, TSH stimulates the thyroid gland to secrete T3 and T4. The levels of TRH, TSH, T3, and T4 are regulated by a negative feedback system, in which increasing levels of T3 and T4 decrease the production and secretion of TSH. All these mechanisms are summarized in Figure 20.

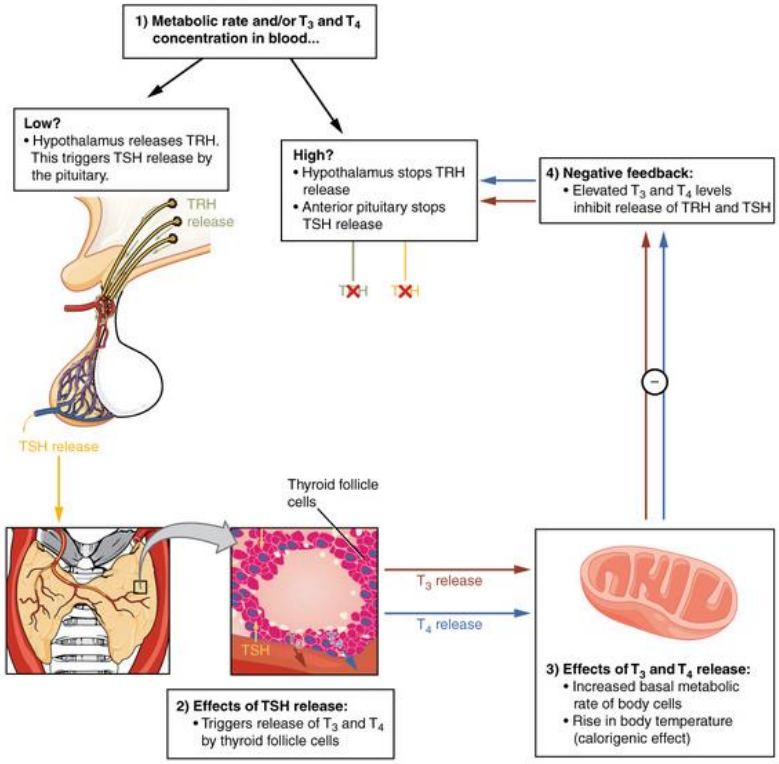

***Figure 20**. Thyroid hormones regulation (adapted from Mescher, 2013).*

The thyroid hormones are often referred as metabolic hormones because their levels influence the body's basal metabolic rate, the amount of energy used by the body at rest. When T3 and T4 bind to intracellular receptors located on the mitochondria, they cause an increase in nutrient breakdown and the use of oxygen to produce ATP. In addition, T3 and T4 initiate the transcription of genes involved in glucose oxidation. Adequate levels of thyroid hormones are also required for protein synthesis and for tissue development and growth. They are especially critical for nervous system development both in utero and in early childhood, and they continue to support neurological function in adults. Because thyroid hormones regulate many body functions, thyroid disorders can have severe and widespread consequences.

The thyroid gland also secretes calcitonin, a hormone produced by the parafollicular cells (also called C cells) that stud the tissue between distinct follicles. The release of this hormone depends on blood calcium levels. Calcium is a second messenger in many signaling pathways, and is essential for muscle contraction, nerve impulse transmission, and blood coagulation. Moreover, C cells produce and secrete the parathyroid hormone (PTH), the major hormone involved in the regulation of blood calcium levels. PTH secretion causes the release of calcium from the bones by stimulating osteoclasts. PTH also inhibits osteoblasts, the cells involved in bone deposition, thereby sparing blood calcium. A negative feedback loop regulates the levels of PTH and is summarized in Figure 21.

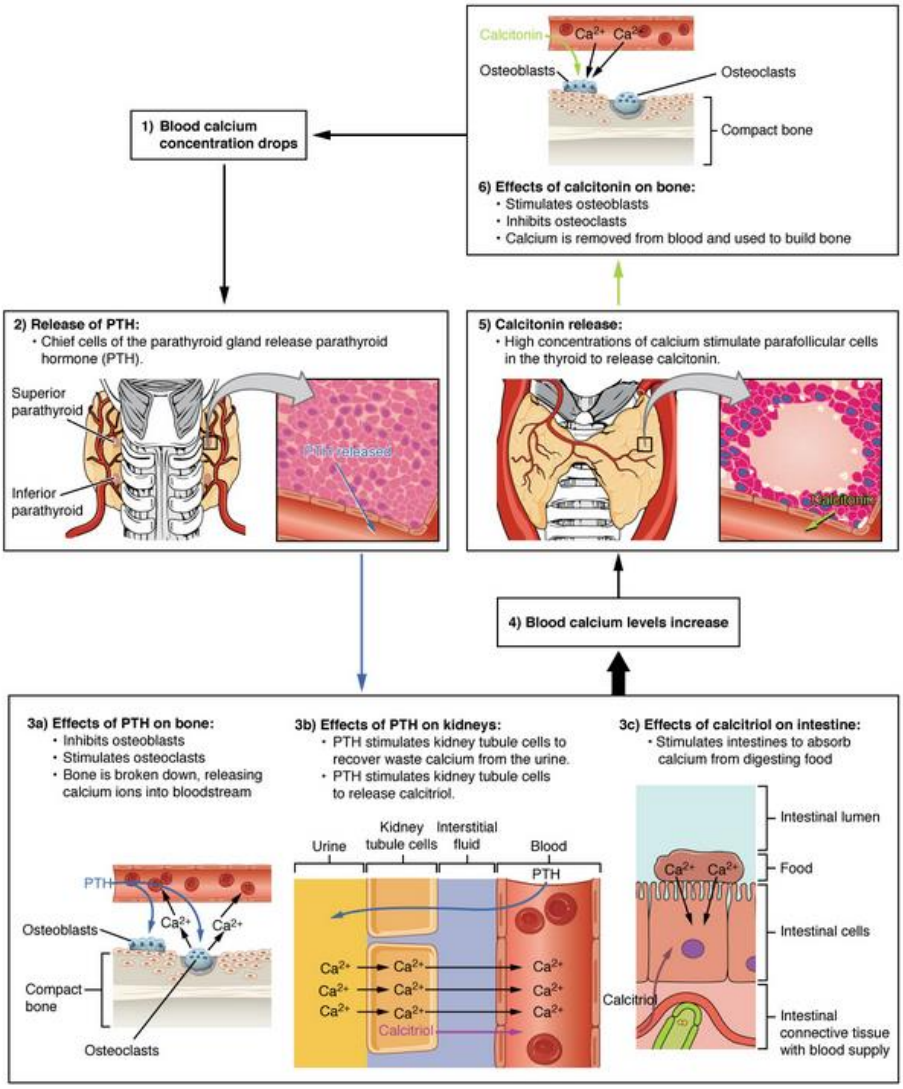

***Figure 21**. Parathyroid hormone regulation (Mescher, 2013).*

An abnormal activity of C cells can cause either hyperparathyroidism or hypoparathyroidism, disorders caused by an overproduction of PTH or by PTH deficiency, respectively.

Diseases associated with the thyroid gland are one of the most frequently endocrine conditions across the globe, with an incidence ratio of 3:1 of females and males respectively (Padur et al., 2016). Thyroid diseases can be grouped into benign and malignant types. The common benign diseases encountered are thyroiditis (mostly Hashimoto thyroiditis), goiter and thyroid adenoma. These are quite common, with at least 10-15% of elderly patients affected by hypothyroidism (Shaw et al., 2005). Total thyroidectomy is currently the preferred treatment consisting in a surgical procedure wherein the thyroid gland is removed (Bellantone et al., 2002).

2.1. Thyroid cancer

Thyroid cancers are the most widespread malignancies of the endocrine system and represent approximately 1-1.5% of all tumor-related diseases (Mio et al., 2016). For still unclear reasons, thyroid cancer is two to three folds more common in females than males. Although the incidence peak of thyroid cancer diagnosis is 45 to 49 years in women and 65 to 69 years in men, it also affects young people (Brown et al., 2011). Thyroid carcinoma can arise from either follicular or non-follicular thyroid cells. Follicular cancers include papillary thyroid cancer (PTC, 80%), follicular thyroid cancer (FTC, up to 15%), and anaplastic thyroid cancer (ATC, 2%). PTC and FTC, which together account for the vast majority of cancers, are commonly referred as differentiated thyroid cancers (DTCs). In contrast to DTC, ATC are acknowledged as undifferentiated thyroid cancers (UCs). Medullary thyroid cancer (MTC) arises from non-follicular calcitonin-producing cells and accounts for about 4% of thyroid cancers. FTC has a peak incidence in the fifth decade of life. It is a slow growing tumor and frequently it is recognized as a nodule in the thyroid gland (Fig. 22). Follicular carcinomas tend to invade locally and metastasize distantly and are especially prone to metastasize to bone or lung. The tumor and metastases often retain the ability to

accumulate and hold iodide, and are therefore sometimes susceptible to treatment with adjuvant radioactive iodine ^{131}-I (RAI).

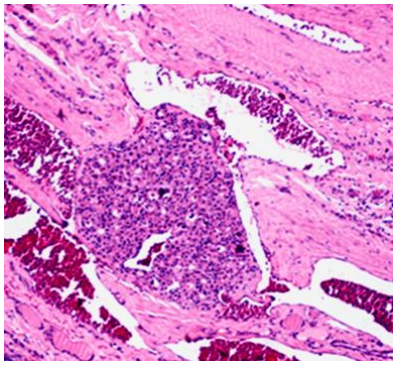

***Figure 22**. Histological appearance of follicular thyroid carcinoma displaying vascular invasion. Stained with hematoxylin and eosin; Magnification × 100 (adapted from Sobrinho-Simões et al., 2011).*

PTC is the most common subtype within thyroid cancers and has a peak of incidence in the third and fourth decades. It tends to remain localized in the thyroid gland and metastasizes locally to the cervical or upper mediastinal nodes. This tumor is usually indolent and may exist for decades. It has an epithelial origin and it typically shows tumor cells around a fibrovascular core with areas of follicular differentiation (Fig.23). Papillary lesions tend to be infiltrative, and encapsulation is rare. Lymphocytic "reactions" are prominent.

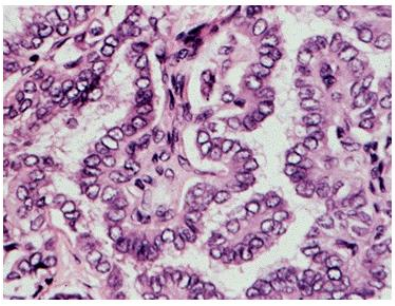

Figure 23. Papillary thyroid carcinoma. The structure is composed by complex fibrovascular core structures covered by crowded, overlapping, vesicular nuclei (artifact of fixation). Little colloid is visible (adapted from Pacini and DeGroot, 2013).

A consistent proportion of PTC shares some features of follicular cancers and for this reason are known as the "follicular variant" of papillary cancer (FVPTC). Tumor progression and clinical features resemble the ones of the classic PTC (Fig. 24).

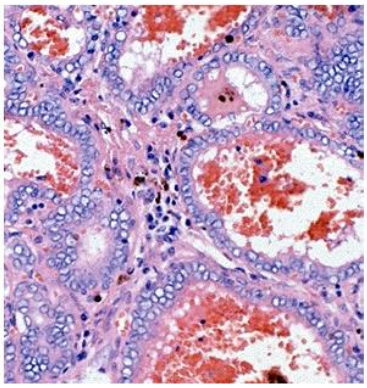

***Figure 24**. Follicular variant of papillary carcinoma with more typical vesicular nuclei, and hemorrhage in follicular lumens* (adapted from Pacini and DeGroot, 2013).

UCs occur predominantly in people over 50 years of age. By the time of diagnosis, the disease has spread beyond the area that can be attacked surgically, and patients usually die within 6 months to 1 year. Spindle cells and giant-cells grow rapidly and are very invasive (Fig. 25). These tumors metastasize to lymph nodes both locally and widely, but not characteristically to bone; pulmonary metastases are frequent.

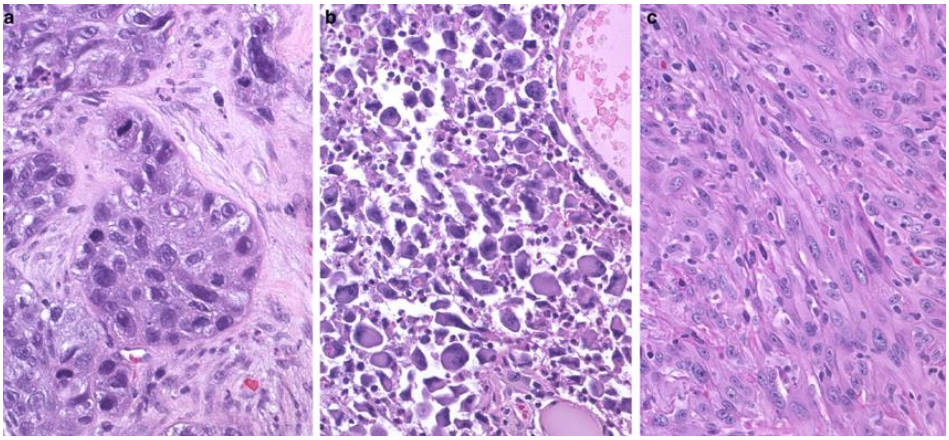

***Figure 25**. Microscopic appearance of anaplastic thyroid carcinoma is highly variable. Frequently encountered patterns include squamoid (a), giant cell (b), and spindle cell (c) (adapted from Begum et al., 2004).*

MTCs arise from parafollicular cells. They have a histologic pattern made of solid masses of cells with large vesicular nuclei (Fig. 26). There may be considerable associated fibrosis and deposits of amyloid. Over 50% of tumors may have local or distant metastases at diagnosis. These tumors may metastasize locally, or to bones and soft tissues. Primary tumors and metastases may show dense calcification on x-

ray film. The course tends to be progressive, and the 10-year survival ratio varies from 50 to 70%.

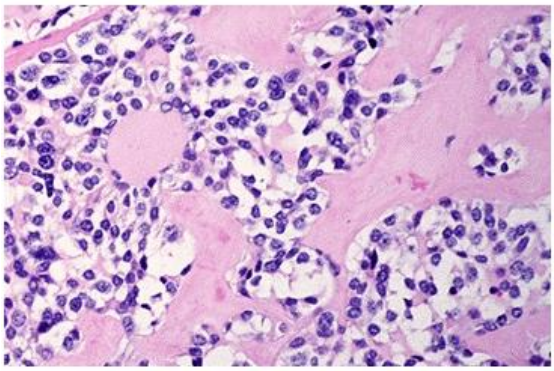

***Figure 26**. Medullary thyroid carcinoma with amyloid stroma (adapted from Pacini and DeGroot, 2013).*

MTC may occur sporadically (about 70%) or as part of multiple endocrine neoplasia (MEN)-II syndromes, which constitute about 10-20% of the cases, and are transmitted in families as dominant traits due to activating germline point mutations of the rearranged during transfection (*RET*) proto-oncogene. MEN-II (or IIA) includes patients with medullary thyroid cancers, pheochromocytomas, and parathyroid hyperplasia or adenomas. MEN-III (or MEN-IIB) includes medullary thyroid carcinoma, mucosal neuromas, pheochromocytomas, which are usually bilateral and often malignant, occasionally cafe-au-lait spots, and possibly Gardner's syndrome (mucocutaneous pigmented nevi and small intestinal polyps).

Nowadays, alterations of several oncogenes (i.e. *RET/PTC*, paired-box gene 8/peroxisome proliferator-activated receptor gamma -*PAX8/PPARγ*-, v-ras oncogene homologue –*RAS*-, *TP53*, and tyrosine kinase receptor -*TKR*-) involved in the pathogenesis of thyroid tumors have been identified (Tab 5). Commercially available tests for panels of mutations are increasingly used in combination with fine-needle aspiration (FNA) cytopathology to obtain additional information regarding the risk of malignancy (Lebastchi and Callender, 2014).

The B-raf proto-oncogene serine/threonine kinase V600E ($BRAF^{V600E}$) mutation shows a high specificity for PTC, especially the classic variant, whereas it has never been

found in follicular and medullary thyroid carcinomas or in benign thyroid neoplasms (Xing, 2005). It is also present in 20–25% of anaplastic thyroid carcinomas, most likely originating from the dedifferentiation of PTC. It has been demonstrated a relationship between the presence of the *BRAF*^{V600E} mutation and more aggressive clinical and pathological features of PTC (Xing, 2005), together with a worse outcome and thyroid cancer-related death (Elisei et al., 2012).

***Table 4**. Genetic alterations associated to sporadic thyroid cancer (Lebastchi and Callender, 2014).*

Genetic alterations	Associated thyroid malignancy	Frequency
BRAF mutation	Papillary thyroid carcinoma	29%-69%
	Anaplastic thyroid carcinoma	0%-12%
RET/PTC rearrangements*	Papillary thyroid carcinoma	13%-25%
TRK rearrangements	Papillary thyroid carcinoma	5%-13%
Ras mutation	Papillary thyroid carcinoma	0%-21%
	Follicular thyroid carcinoma	40%-53%
	Anaplastic thyroid carcinoma	20%-60%
PAX8-PPAR-γ	Follicular thyroid carcinoma	35%-45%
CTNNB1 mutation	Anaplastic thyroid carcinoma	66%
p53 mutation	Papillary thyroid carcinoma	0%-5%
	Follicular thyroid carcinoma	0%-9%
	Anaplastic thyroid carcinoma	67%-88%

CTNNB1, β-catenin; PPAR-γ, peroxisome proliferator-activated receptor-γ; TRK, tyrosine kinase receptor.
* Papillary thyroid carcinoma specific.

RET/PTC rearrangements are quite frequent in PTC, whereas *PAX8/PPARγ* rearrangement is often detected in follicular patterned lesions (FVPTC and FTC). *RET/PTC* is a chimeric gene generated by the fusion of the RET tyrosine kinase (TK) domain with the 5' terminal region of genes that are constitutively expressed in thyroid follicular cells, allowing dimerization of the RET TK domain and its constitutive activation. *PAX8/PPARγ* rearrangement has been associated with some adverse prognostic features (multifocality and vascular invasion) of FTC but it has been detected in about 14% of benign follicular adenoma (FA).

RAS are small GTPase-proteins that act as a molecular switch propagating signals from TK and non-TK receptors and activating the mitogen-activated protein kinases (MAPK) and other signalling pathways. All of the three *RAS* genes (*H*, *K* and *N-RAS*) were shown to be mutated in both benign and malignant thyroid tumors but the

frequency of mutations is higher in FTC (36%), poorly differentiated thyroid cancers (PDTC) (55%) and ATC (52%) (Tavares et al., 2016).

About two-thirds of thyroid carcinomas display telomerase activation that is more frequent in ATC than in DTC. Melo et al., found telomerase reverse transcriptase (*TERT*) promoter mutations in 7.5% of PTC, 17.1% of FTC, 29.0% of PDTC and 33.0% of ATC, within a cohort of 469 carcinomas. No TERT promoter mutations were found in normal tissues, benign lesions or medullary thyroid carcinomas (Melo et al., 2014). Furthermore, in DTC the $BRAF^{V600E}$ mutation is found to be associated with hypermethylation of several tumor suppressor genes, including the tissue inhibitor of metalloproteinases 3 (*TIMP3*), solute carrier family 5 member 8 (*SLC5A8*), death-associated protein kinase 1 (*DAPK1*), and retinoic acid receptor-β (*RAR*β) (Zolotov, 2016).

By now, it is an indisputable fact that miRNA and lncRNA could be pointed out as major players in tumor development and progression due to their action in modulating known cancer genes and/or their products (oncogenes, tumor-suppressor genes and apoptotic proteins). Tumor cells have been shown to release miRNAs into the circulation, and miRNA profiles in plasma and serum have been found to be altered in some cancers and in other diseases. Some miRNA have been repeatedly found dysregulated in thyroid cancer (Tab. 6), in particular in PTC (miR-146b, miR-181b, miR-187, miR-221 and miR-222) and the same set of molecules has been associated with tumor aggressiveness in diverse studies (Mazeh, 2012). Unfortunately, the relevant set of miRNAs varies from one report to the other, making difficult or even impossible to draw any meaningful conclusion (Tavares et al., 2015). The same situation is concerning lncRNAs studies. lncRNAs NAMA (non-protein coding RNA, associated with MAPK pathway and growth arrest) and PTCSC1/2/3 (PTC susceptibility candidate 1/2/3) are the only lncRNAs that have been associated with PTC (Kentwell et al., 2014). Until now, it has not been possible to ascertain any role to lncRNA in the prognosis of thyroid cancer patients.

Table 5. microRNAs in thyroid malignancies (Kentwell et al., 2014).

miRNA	Expression	Cancer association	Associated genes
miR-221, -222, -181b, -220, -213	Upregulated	PTCs compared with normal thyroid tissue	*c-KIT*
miR-21, -31, -221, -222	Upregulated	PTCs compared with MNGs	
miR-146b	Upregulated	Consistently upregulated in classical PTC	*NF-κB, IRAK1, TRAF6*
miR-165b-5p	Upregulated	PTCs; PCCL3 cell line	*SMAD4*
miR-146b, -221, -222	Upregulated	PTCs compared with normal thyroid tissue	
miR-187, -221, -222, -146b, -155, -122a, -31, -205, -224	Upregulated	PTCs	
miR-187, -224, -155, -222, -221, -146b	Upregulated	FTCs (conventional type)	
miR-187, -221, -339, -183, -222, -197	Upregulated	FTCs (oncocytic type)	
miR-302c, -205, -137, -187, -214, -155, -224, -222, -221	Upregulated	ATCs	
miR-192, -197, -328, -346	Upregulated	FTCs (oncocytic type)	
miR-30d, -125b, -26a, -30a	Downregulated	ATCs	
miR-21, -146b, -221, -222	Upregulated	ATCs	
miR-26a, -138, -219, -345	Downregulated	ATCs	
miR-17-5p, -17-3p, -18a, -19a, -19b, -20a, -92, -106a, -106b	Upregulated	ATCs	
miR-30, -200	Downregulated	ATCs compared with PTCs and FTCs	*TGF-β, SMAD2*
Let-7a	Downregulated	FTCs compared with adenomas and normal thyroid tissue	*FXYD5*
miR-191	Downregulated	FTCs, follicular adenomas and follicular variant of PTC compared with ATCs and normal thyroid tissue	*CDK6*
miR-146b, -221, -222, -155, -31	Upregulated	Aggressive compared with nonaggressive PTC	Increased *MET* expression; miR-146b increased *MET* expression in *BRAF*-positive tumors
miR-1, -34b, -130b, -138	Downregulated	Aggressive compared with nonaggressive PTC	*MET* identified as potential target gene for miR-34b and miR-1
miR-222, -146b	Upregulated	In plasma of patients with recurrent PTC	
miR-375, -10a	Upregulated	MTCs	*YAP1*
miR-445	Downregulated		
miR-125a-5p, -143, -23b, -425, -623, -654-3p	Upregulated	FTCs	
miR-1225-3p, -1238, -135a, -150, -494, -663, -801, -923	Downregulated		
miR-21, -203	Upregulated	BRAF-positive PTC tissues compared with BRAF-negative PTCs	
miR-146b, -221, -222, -135b	Upregulated	PTCs with high levels of extrathyroidal invasion compared with PTCs with no extrathyroidal invasion	
miR-146b	Upregulated	Overexpression increased cell migration, cell invasiveness and resistance to chemotherapy-induced apoptosis in PTCs	
miR-146b-5p	Upregulated	PTC specimens of stage I, II and III and paired normal tissue	34 target genes predicted
miR-335	Downregulated		36 target genes predicted

2.1.1. Thyroid cancer management

Patients with clinical tumor of any size, sporadic or familial, are usually treated by near-total or total thyroidectomy. Invasive carcinomas are resected only if possible (Scollo et al., 2003). DTC is considered the least aggressive type of thyroid cancer and has, in general, an excellent prognosis. Most cases of DTC are slowly progressive when identified at an early stage and patients can frequently be cured with adequate surgical care and RAI ablation therapy (Lebastchi and Callender, 2014). TSH suppression plays an important role in the management of thyroid cancer post-surgery. Inducing a mild hyperthyroid state, the therapy suppresses TSH and its potential to stimulate tumor cell growth. The overall 10-year survival of these tumors is greater than 90%. However, a small percentage of patients with DTC (about 5%) exhibit a more aggressive disease (Durante et al., 2006). They are usually defined as thyroid cancers that became metastatic, or are inoperable, or are refractory to RAI therapy; they are usually associated with a poor prognosis. Cytotoxic chemotherapy (doxorubicin) and radiotherapy are of limited benefit, with poor response rates and low durability of response for most of these patients.

Over the last decade, a better understanding of the genetic, epigenetic and biologic basis of aggressive thyroid cancers has generated a struggle for innovative therapeutic modalities (Safavi et al., 2012). In the last few years, the advent of targeted therapies fostered an exceptional development in the therapy of several solid tumors, including non-small-cell lung cancer, breast cancer, melanoma, and gastrointestinal stromal tumors (Balsea et al., 2012; Larkin et al., 2014; Blanke et al., 2008). A comprehensive genetic analysis of 496 samples of PTC as part of the cancer genome atlas (TCGA) project showed that driver genomic alterations were found in 97% of cases (Cancer Genome Atlas Research Network, 2014). The vascular endothelial growth factor receptor (VEGFR) was one of the first signaling pathways to be associated with the aggressiveness of thyroid cancer (Yu et al., 2008). Despite its key role in the pathophysiology of thyroid malignancies, other signaling pathways drive the thyroid cancer cells behavior. Fibroblast growth factor receptor (FGFR),

platelet-derived growth factor receptor (PDGFR), RAS, BRAF, and RET/PTC rearrangement receptor, among others, have been recognized as important signaling pathways that are implicated in the physiopathology of thyroid tumors (Costa et al., 2016). Recently, the oncogene pathway-driven approach to the understanding of the pathophysiology of thyroid cancer led to the development of clinical trials that assess the antitumor activity of tyrosine kinase inhibitors (TKi). This ws ultimately supported by the US food and drug administration's (FDA) approval of vandetanib and cabozantinib for the treatment of MTC and, more recently, sorafenib and lenvatinib for progressive radioiodine-refractory PTC and FTC (Costa et al., 2016). Some of the current available molecular therapies are enlisted in Table 6.

Another class of drugs currently under evaluation for the treatment of thyroid cancer is the one targeting epigenetic dysregulation. Treatment with DNA methylation inhibitors as well as HDAC inhibitors has been associated with enhanced radioiodine uptake, along with other markers that suggest improved tumor cell differentiation, prompting clinical trials (Sherman, 2010). The suberoylanide hyroxamic acid (SAHA or Vorinostat), already FDA approved for the treatment of cutaneous T-cell lymphoma, it is able to stop the thyroid cancer cells growth, inducing apoptosis in vitro (Luong et al., 2006). PARPs exhibit various functions ranging from chromatin remodeling, DNA repair and maintenance of genomic stability to regulation of cell death, thus making these enzymes interesting targets in cancer treatment. Several PARP inhibitors are currently under evaluation as anti-cancer drugs. Recently, PJ34 proved to reduce cell viability in different thyroid cancer cell lines (Lavarone et al., 2013). Moreover, the combined administration of SAHA and PJ34 shows to have strong synergic effects on cell viability and apoptosis of anaplastic thyroid cancer cells (Baldan et al., 2015).

The overall goal of developing new treatments is to extend the duration of life without harming its quality. Currently, no novel treatment has yet demonstrated an improved survival for thyroid cancer patients (Sherman, 2010). Moreover, the low rate of partial response, the absence of complete responses, and emergence of resistance uncovers the necessity to develop single agents that are more efficient or

to identify rational drugs combinations (including cytotoxic chemotherapies) that have synergic value without enhanced cross-toxicities.

Table 6. Principal involved pathways and relative targeted therapies in thyroid cancer (Ferrari et al., 2015).

Involved pathways	Drugs	Thyroid cancer	Responses			
			PR	SD	PD	PFS (months)
Raf	Sorafenib	30 DeTC	23.3%	53.3%	7%	21
	Sorafenib	41 DeTC	15%	56%		15
	Sorafenib	207 DeTC				10.8
VEGF	Vandetanib	30 MTC	20%	53%	3%	27.9
	Vandetanib	231 MTC	45%	42%		
	Vandetanib	145 DeTC	8%	57%		11.1
	Motesanib	93 DeTC	14%	35%	8%	40 weeks
	Motesanib	93 DeTC		48% MTC		40 weeks DeTC
		91 MTC				48 weeks MTC
	Axitinib	49 DeTC	30%	38%	7%	18.1
		11 MTC				
	Axitinib	52 MTC	35%	35%		16
	Sunitinib	7 MTC	28% PR + 3% CR	46%	17%	12.8
		28 DeTC				
	Sunitinib	11 DeTC	18% PR + 9% CR	45%	27%	11.5
	Cabozantinib	37 MTC	29%			
	Cabozantinib	15 DeTC	53%	40%		
	Pazopanib	37 DeTC	49%		73%	11.7
	Lenvatinib	58 DeTC	50%	28%	5%	12.6
	Lenvatinib	261 DeTC	63 PR% + 2%			18.3
Vascular disrupting	Combretastatin	18 ATC		33%		7.4 weeks
EGFR	Gefitinib	27 DeTC		12%		3.7
Histone deacetylase	Vorinostat	16 DTC	0%	0%	36%	
		3 MTC				

ATC, anaplastic thyroid cancer; DeTC, dedifferentiated thyroid cancer; MTC, medullary thyroid cancer; PR, partial response; PD, progressive disease; PFS, progression-free survival; SD, stable disease.

2.2. Anaplastic thyroid cancer

ATC is the least common but the most aggressive of all thyroid cancers, with a median survival rate of 3–5 months (Mio et al., 2016). It is thought to develop from existing PTC or FTC (Champa and Di Cristofano, 2015); once ATC is established, it has an extremely high proliferative rate, can quickly invade the neck structures and metastasize to other organs, and, more importantly, it shows resistance to

radioiodine treatment (Elisei, 2012). Patients report ATC mostly in their sixties to seventies with a rapidly enlarging, often painful, thyroid mass. Symptoms related to mechanical compression such as hoarseness (77%), dysphagia (56%), vocal cord paralysis (49%), neck pain (29%) and dyspnea (19%) are always present (Lebastchi and Callender, 2014). The lungs are the most common site of distant metastases (up to 90% of cases), followed by spread to bone (5%-15% of cases) and brain (5% of cases).

There has been a multitude of genetic alterations associated with ATC, most often causing dysfunction in the MAPK (ERK1/2-MEK1/2) and phosphoinositide 3-kinase/ V-Akt Murine Thymoma Viral Oncogene Homolog (PI3K-AKT) signaling pathways. The $BRAF^{V600E}$ mutation occurs in about 38% of ATC and leaves BRAF constitutively able to activate the ERK1/2-MEK1/2 signaling; furthermore, it is thought to be involved with the progression of PTC to ATC and angio-invasion (Smith and Nucera, 2015). Many other mutations lead to an increased PI3K-AKT signaling activation. Phosphatidylinositol-4,5-bisphosphate 3-kinase (*PIK3CA*), which encodes the p110α catalytic subunit of PI3K, has been found to be mutated in 12–23% of ATC (Xing, 2013). Importantly, the over-activation of the PI3K-AKT pathway can be induced by phosphatase and tensin homolog (*PTEN)* inactivation, including its promoter methylation, deletion, or point mutations, which occur in 10–20% of ATC (Xing, 2013). Furthermore, *RAS* mutations seem to preferentially activate the PI3K-AKT pathway and are associated to 17% (*NRAS* mutations) and 6% (*HRAS*) of ATCs (Ricarte-Filho et al., 2009). The *TP53* gene is another gene commonly mutated/inactivated in a variety of advanced human cancers and strongly involved in the ATC pathogenesis. It is mutated in 12–83% ATCs and rarely in DTCs, but the protein could be also aberrantly overexpressed in ATC, causing inactivation of apoptosis and cell cycle progression (Smith and Nucera, 2015). Mutations in *TERT* promoter have been reported in ATCs. This gene encodes for the catalytic domain of telomerase, and, if mutated, leads to an increased telomerase activity, suggesting it can play a role in the aggressiveness of thyroid carcinomas (Melo et al., 2014).

It is a matter of fact that multiple epigenetic factors could foster ATC tumor progression. Enhancer of Zeste homolog 2 (EZH2) is a histone lysine-methyltransferase and is found to be overexpressed in ATC (Catalano et al., 2012). EZH2 is a member of the polycomb family of proteins, which are essential for the regulation of cell proliferation and differentiation. EZH2 overexpression leads to an alteration in global histone methylation, which in turn causes the silencing of the *PAX8* gene: this cascade leads to an aggressive phenotype and poor clinical outcome (Catalano et al., 2012). Increased histone methylation has been found to alter the expression of other genes in ATC cell lines, including *CDKN2A* (or $p16^{INK4A}$), *DAPK1*, ubiquitin carboxy-terminal hydrolase L1 (*UCHL1*), *MGMT*, *TSHR*, *PTEN*, and melanoma-associated antigen 4 (*MAGEA4*) (Smith and Nucera, 2015). All these are known to play a role in tumor suppression, apoptosis, cell cycle regulation and DNA repair. Hyper-methylation of the *TSHR* gene leaves the cell unable to concentrate iodine, enhancing radioiodine therapy resistance and challenging the treatment (Russo et al., 2011). Additionally, histone deacetylation plays a role in ATC pathogenesis. Most ATC tumors show overexpression of HDACs, and a lower acetylation of histones leads to an altered expression of proteins controlling cell cycle and proliferation (Smith and Nucera, 2015).

Similar to histone modifications, miRNA molecules also have the capability to alter the gene expression of ATC cells. They function as negative regulators of the expression of protein-encoding genes involved in major processes such as development, apoptosis, cell proliferation, immune response, and hematopoiesis (Catalano et al., 2012). With such a biological role, improper regulation of miRNAs can contribute to tumor progression, and this has been observed in ATC. Specifically, there are two families of miRNAs that contribute to a tumor's invasiveness via down-regulation (miR-200 and miR-30) or up-regulation (miR-20a) (Fuziwara and Kimura, 2014).

Overall, understanding genetic and epigenetic alterations of ATC is important when looking for targeted therapies that will be effective in patients who harbor this

aggressive malignancy. Insights to this subject will enable to accurately target dysfunctional signaling pathways, leading to improved clinical prognoses for patients.

2.2.1. Anaplastic thyroid cancer therapies

Multimodali therapy including chemotherapy, External Beam Radiation Therapy (EBRT), and (rarely) surgery are the main treatment options for ATC. All approaches have a high failure rate, and in many cases, palliative treatments are the only therapeutic options (Lebastchi and Callender, 2014). Chemotherapy plays a fundamental role in the management of ATC. Unfortunately, as of now, results are very discouraging. The role of surgery in the management of ATC depends on the extent of the disease at the time of insurgence. Surgery can play a role in localized disease, but its benefit in the management of other cases of ATC remains controversial (McIver et al., 2001). A wide range of conventional therapeutic approaches including thyroidectomy, radiotherapy, chemotherapy, or varying combinations of these modalities have been proposed over the years, but they turned out to be largely ineffective (Elisei, 2012). This overall failure is the main reason for the constant search for novel treatment strategies.

Aim of this thesis

Each cell has its own epigenetic pattern that must be carefully maintained to regulate proper gene expression. Perturbations in these carefully arranged patterns could contribute to the development of human diseases, including cancer. Although precise underlying mechanisms are not yet understood, nowadays, scientific interest in epigenetics has increased insofar as it represents an important tool to promote our understanding of tumorigenesis and to help in the development of strategies for cancer treatment and prevention. Among various epigenetic anticancer drugs, BET inhibitors are considered a very appealing novel class of compounds as they target a specific family of proteins that act as regulators of gene transcription.

The goal of this study is to delineate which are the pathways underlying the leading biological effects derived from BET inhibition in anaplastic thyroid cancer cells. ATC has been chosen as a model of aggressive carcinoma sub-type with no successful therapeutic options. BET inhibition deregulate cell cycle progression, mostly inhibiting key element of the G1-S checkpoint, and signaling pathways, modulating diverse microRNAs and restoring the expression of a pool of them, compared to the non-tumorigenic cell line. All these data highlight an intricate pathway deregulation due to BET inhibition and suggests that a better knowledge on how BETi perform their anti-neoplastic activity could enroll them as possible new therapeutic agents in ATC.

Materials and Methods

Human and murine cell lines

FRO (purchased from the European Collection of Cell Cultures, Salisbury, UK), SW1736 (obtained from Cell Lines Service GmbH, Eppelheim, Germany) and 8505c (purchased from Sigma Aldrich, Saint Louis, MO, USA) are *BRAF*^{V600E}-mutated human ATC cell lines (Pilli et al. 2009; Schweppe et al. 2008). NThy ori 3.1 (purchased from Sigma Aldrich) is a human thyroid follicular epithelial cell line immortalized by the SV40 large T gene. All cell lines resulted mycoplasma-free and were authenticated through STR analysis. FRO were grown in DMEM medium (EuroClone, Milan, Italy) while SW1736, 8505c and NThy ori 3.1 were grown in RPMI 1640 medium (EuroClone). Both media were supplemented with 10% fetal bovine serum (FBS, Gibco Invitrogen, Milan, Italy) and 50 mg/ml gentamicin (Gibco Invitrogen). Cells were kept in a humidified incubator (5% CO_2 in air at 37°C). Cultured cells were treated with vehicle (DMSO, Sigma Aldrich) or the following agents: JQ1 (50 nM-10 μM in DMSO) (Cayman Chemical, Ann Arbor, MI, USA), I-BET762 (50 nM -10 μM in DMSO) (Merck Millipore, Darmstadt, Germany) and I-BET151 (50 nM-10 μM in DMSO) (Cayman Chemical).

T4888M and T3531L are ATC cell lines derived from tumors developed by [*Pten, Tp53*]$^{thyr-/-}$ mice (Antico Arciuch et al. 2011). Cells were grown in DMEM supplemented with 10% FBS.

Animals

[*Pten, Tp53*]$^{thyr-/-}$ and *Pten*$^{thyr-/-}$ mice have been previously described (Antico Arciuch et al. 2011; Yeager et al. 2007; Antico Arciuch et al. 2010) and were housed in the Albert Einstein College of Medicine animal facility under specific-pathogen-free conditions.

Human tissues and immunohistochemistry

A series of 12 normal thyroid glands (NTs), 25 follicular adenomas (FAs), 23 follicular thyroid carcinomas (FTCs), 36 papillary thyroid carcinomas (PTCs) and 8 anaplastic thyroid carcinomas (ATCs) were retrieved and representative tumor-bearing areas were selected to constitute a tissue microarray. Briefly, 5 µM formalin-fixed paraffin tissue sections mounted on SuperFrost Plus slides (Menzel-Gläser, Braunschweig, Germany) were placed in the PT Link pre-treatment module (DAKO A/S, Glostrup, Denmark). This module automatically performs the entire pre-treatment process of de-paraffinization, rehydration, and epitope retrieval using the Low pH Target Retrieval Solution (0.001 M citrate buffer pH 6.0) at 98 °C for 40 min from DAKO. Endogenous peroxidase activity was blocked by incubating in peroxidase block solution (DAKO) for 5 minutes. Primary rabbit polyclonal antiserum to MCM5 (Sigma Aldrich) diluted 1:1000 was applied and incubated for 60 minutes at room temperature. After washings, slides were incubated with the DAKO EnVision FLEX System (DAKO) according to manufacturer's guidelines. For reaction visualization, 3-3 diaminobenzidine tetrahydrochloride was used as chromogen. The sections were counterstained with Mayer’s hematoxylin. Using light microscopy, the entire section was scanned at high-power magnification (400×) and nuclear immunostaining was evaluated semi-quantitatively as percentage of positive cells. Staining intensity was scored as light, moderate and strong. A final score was then calculated by multiplying the percent staining by the intensity level.

Cell viability assay

To test cell viability, an MTT assay was performed. Briefly, 5000 cells were seeded onto 96-well plates. On the next day, the growth medium was replaced with vehicle-treated medium (NT, untreated cultures) or with medium containing JQ1, I-BET762 or I-BET151; plates were incubated for 0, 24, 48 and 72 h. All experiments were run in quadruplicate and cell viability was expressed as a percentage relative to baseline samples (T0). The percentage of cell viability assessed by MTT assay was used to determine EC50 concentrations from dose–response curves after 72h treatment.

Caspases-induced apoptosis evaluation

Caspase 3/7 activity was measured as a marker of apoptosis using the Apo-ONE Homogeneous Caspase-3/7 Assay kit (Promega, Milan, Italy) according to the manufacturer's protocol. 5000 cells were seeded onto 96-well plates. On the next day, the growth medium was replaced with vehicle-treated medium (NT, untreated cultures) or medium containing JQ1 5 µM, I-BET762 5 µM or I-BET151 5 µM; plates were incubated for 72h. All experimental points were run in triplicate and apoptosis levels were expressed as a percentage relative to baseline samples (NT).

Cell cycle analysis

Cell cycle was determined by fluorescence-activated cell-sorting (FACS) analysis of DNA content. Briefly, cells were collected after a 24, 48 and 72 h treatment with either JQ1 or vehicle (NT); cells were fixed in cold ethanol 70% and stained with a propidium iodide (PI) solution containing RNase and Triton-X100. Flow cytometric analysis was performed on a FACSCalibur (Becton Dickinson) using Modfit LT analysis software (Verity Software House, Inc., Topsham, ME, USA). A minimum of 20,000 cells was analyzed for each sample. All experiments were run in triplicate.

Hematoxylin/eosin staining

20000 cells were seeded on a Nunc® Lab-Tek® Chamber Slide™ system with 8 chambers (0.8 cm2/well) (Sigma Aldrich). On the next day, the growth medium was replaced with vehicle-treated medium (NT, untreated cultures) or with medium containing JQ1. After 72 hours treatment, cells were fixed in 1mL Carnoy solution (5% acetic acid, 95% ethanol). Slides were stained in Hematoxylin/Eosin solution and images were taken on a Leica DMI-6000B microscope.

Wound healing assay

40000 cells were seeded onto 24-well plates. On the next day, the growth medium was replaced with vehicle-treated medium (NT, untreated cultures) or medium containing JQ1 5 µM. After a 72 hours treatment, a linear wound was carefully generated with a 200-µL sterile pipette tip across the cell monolayer. After changing the medium, images of the wounded monolayers were captured 0, 5, 10, 24 and 30h after wounding. Images were acquired with a Leica DMI-6000B microscope (Leica Microsystems Srl, Milano, Italy). Experiments were run in quadruplicates.

Soft agar assay

A bottom layer of hard-agar (0.8%) with DMEM or RPMI media (10% FBS) was poured first. After the bottom agar solidified, $2*10^4$ cells, treated or not with JQ1 for 72h, were seeded in top soft-agar (0.4%) with medium and incubated at 37°C for 21 days. The culture medium was changed twice weekly. Each condition was run in triplicates. Colonies were visualized with an inverted microscope (Leica DMI-6000B microscope, Leica Microsystems Srl) and counted after staining for 1h with 0.005% crystal violet solution. Untreated NThy-ori-3.1 were set at 1.0 and colony units were represented as relative quantification.

High throughput RNA-sequencing and analysis

RNA-sequencing analysis was performed by the Istituto di Genomica Applicata (IGA) in Udine. Briefly, 1.5 µg of good quality RNA (RNA Integrity Number RIN>7) was used for library preparation using the Illumina mRNASeq Sample Prep kit v2.0, following the manufacturer's instructions. Single read sequencing was performed on the HiSeq2000 (Illumina, San Diego, CA, USA) generating 50-base reads. The CASAVA 1.8.2 version of the Illumina pipeline was used for image analysis, base calling, and demultiplexing. Reads were first trimmed in order to remove lower base quality data with ERNE (Vezzi et al. 2012) and adapter sequences were removed with Cutadapt (https://pypi.python.org/pypi/cutadapt/1.3). TopHat (Trapnell et al. 2012) was used for mapping and annotation on the hg19 reference sequence. Differential gene expression analysis was performed according to the experimental design using Cufflinks (Trapnell et al. 2012).

miRNA expression and analysis

Expression analysis of 812 miRNAs was performed by the genetic laboratory of Pharmadiagen Srl, using the NanoString nCounter v2 miRNA Assay kit (NanoString Technologies, Seattle, WA). The nCounter miRNA expression assay allows detection and count of miRNAs through hybridization with fluorescently labeled barcoded probes. Briefly, 280 ng of total RNA was processed following the manufacturer's instructions (NanoString Technologies, Seattle, WA). Subsequent purification and detection of miRNA target were carried out using the nCounter Analysis system.

The total miRNAs counts obtained were elaborated and normalized following the Nanostring's Data Analysis Guide. The background correction was calculated as the geometric mean of negative control plus 2x standard deviation and subtracted to each count. miRNAs expressing less than the background were set as not expressed to overcome basal noise. The technical normalization was performed using the positive control spike counts. The normalization factor was calculated as the ratio

between the average of geometric means and the geometric mean of each sample. The counts of every miRNAs were multiplied by the normalization factor. To be more conservative and avoid false positive miRNA, we set an additional cut off (15 counts) after the above normalization. Fold change was then calculated as JQ1-treated vs vehicle or ATC cell line vs NThy ori 3.1. Only miRNA showing a deregulation greater than two log2-fold change were took into consideration.

Pathway analysis by DIANA miR-Path and GOrilla

The DIANA miRPath v2.0 (diana.imis.athenainnovation.gr/ DianaTools/index.php?r=mirpath/index), a web server established for identification of KEGG pathways corresponding to the networks of miRNA targets by superimposing numerous miRNA-target relationships on the merging and meta-analysis algorithm (Vlachos et al., 2012), was utilized. This program predicts miRNA targets with high accuracy based on the DIANA-microT-CDS algorithm that considers the evolutional conservation of miRNA-binding sites.

The set of miRNA targets was imported into the core analysis tool of GOrilla gene ontology tool (http://cbl-gorilla.cs.technion.ac.il/). It calculated the score P-value that reflects the statistical significance of association between the genes and the pathways and networks by Fisher's exact test. A p-value threshold of 10^{-3} was used to test sensitivity.

Gene expression assays

Total RNA from human cell lines, treated either with 5µM JQ1 or vehicle, was extracted with RNeasy mini kit according with manufacturer's instructions (Qiagen, Hilden, Germany). 500ng of total RNA were reverse transcribed to cDNA using random exaprimers and MMLV reverse transcriptase (Life Technologies, Carlsbad, CA, USA). Real-time PCRs were performed using Platinum Sybr Green QPCR supermix (Life Technologies) with the ABI Prism 7300 Sequence Detection Systems (Applied Biosystems). The ΔΔCT method, by means of the SDS software (Applied Biosystems),

was used to calculate mRNA levels. All oligonucleotide primers were purchased from Sigma Aldrich.

Total mouse RNA (treated either with 0.5μM or vehicle) was extracted with Trizol and reverse transcribed using the Maxima First Strand cDNA Synthesis Kit kit (Thermo Scientific, Waltham, MA). qRT-PCR was performed on a StepOne Plus apparatus using SYBR Green mix (Applied Biosystems) and custom-designed primers *Mcm5* (forward, 5'-CAGAGGCGATTCAAGGAGTTC-3'; reverse, 5'-CGATCCAGTATTCACCCAGGT-3'). Each sample was run in triplicate and 18S was used to control for input RNA. Data analysis was based on the ΔΔCT method, and experiments were repeated at least three times using at least two independent organs or cell pools.

Chromatin immunoprecipitation (ChIP)

In order to perform the ChIP assay, cells were treated for 10 min at 37˚C with formaldehyde added to the culture medium to a 1% final concentration to cross–link the DNA/protein complexes. Glycine was then added for 5 min at room temperature to 0.125 M final concentration to neutralize formaldehyde. Cells were then scraped in PBS with proteinase inhibitors and collected by centrifugation. Pellets were resuspended in cell lysis buffer (1% SDS, 10 mM EDTA, 50 mM Tris-HCl pH 8.1 and protease inhibitors) and sonicated at 6 x 30 seconds burst with 30 seconds break on ice. The sonicated cell suspension was diluted 10 fold in dilution buffer (0.01% SDS, 1.1% Triton X-100, 1.2 mM EDTA, 16.7 mM Tris-HCl pH 8.1, 167 mM NaCl); 10 % of the diluted cell suspension was saved as total input. For immunoprecipitation, samples were incubated with 10 μg of rabbit polyclonal anti-BRD4 (Active Motif) or Rabbit IgG, (Millipore), as negative control, and then samples were incubated with Dynabeads Protein A (Gibco Invitrogen) at 4°C for 4 hours. After washings, the immunocomplexes were eluted with elution buffer (1% SDS, 0.1 M, 50 mM NaHCO3). The DNA was then extracted with phenol/chloroform, the aqueous phase recovered and precipitated. The DNA pellet was resuspended in H_20 and it was used as a template in qPCR with the following primers: *MCM5* Forward Primer

(CCTGTTCTGGCCGTTTGTTC), *MCM5* Reverse Primer (GATCGTCGAATCCCGACATG); *NCR* Forward Primer (TGCTGTTACTTTTTACAGGGAGTT), *NCR* Reverse Primer (TTTGAGCAAAATGTTGAAAACAA); *L7R* Forward Primer (TTCGTGCTGTCATCAGAAGGA), *IL7R* Reverse Primer (TGCCACCAGCAAAAGCTCTT). Fold enrichment was then calculated, as signal over background (IgG). Data are representative of three different experiments.

RNA silencing

For transient silencing of endogenous *MCM5*, TriFECTa RNAi Kit (Integrated DNA Technologies Inc, Coralville, IA, USA) was used. A 'universal' negative control duplex (NC) that targets a site that is absent from human, mouse and rat genomes was used. siRNA oligonucleotides were transfected at a concentration of 5 nM using DharmaFECT1 Transfection reagent (Thermo Scientific Inc, Waltham, MA, USA), according to manufacturer's instructions. The day before transfection, cells were plated in antibiotics-free medium and cells were harvested 72h after transfection. The gene-silencing efficiency was evaluated by mRNA and protein levels analysis. Cell viability was evaluated after 72h transfection as previously described.

Annexin V/Propidium Iodide staining

In order to test the percentage of viable/apoptotic cells after *MCM5* silencing, an Annexin V/Propidium Iodide (AnV/PI) staining was performed. Briefly, cells were washed with cold PBS, transferred to a polystyrene round-bottomed flow tube (Falcon, Becton Dickinson, Franklin Lakes, NY) and resuspended in 195 µL of 1x binding buffer (BB 10 mM; HEPES/NaOH, pH 7.4, 140 mM NaCl, and 2.5 mM CaCl2). 5 µL of Fluorescein-conjugated Annexin V (Annexin V-FITC; Bender Med Systems, Vienna, Austria) was added and samples were incubated for 10 minutes at room temperature. After washing, cells were resuspended in 190 µL of BB in which 10 µL of propidium iodide stock solution (final concentration 1 µg/mL) was added. Flow cytometry analysis was performed on CyAN, Dako Cytomation using the Summit

software (Flow cytometer, Beckman Coulter). Forward scatter (FSC) and side scatter (SSC) were acquired in linear mode. Signals for forward and side scatter and fluorescence were collected for 10^4 cells using the forward light scatter parameter as the master signal. Data are expressed as mean fluorescence intensity (FI) values. All experiments were run in triplicate.

MCM5 over-expression

To over-express MCM5 protein, the TrueClone *MCM5* cDNA cloned in pCMV6-AC, which contains a full open reading frame of the human *MCM5* gene (Origene, Rockville, MD, USA), was utilized. The over-expression vector was transfected with Turbofect reagent (Fisher Scientific S.A.S., Illkirch, France) at 2 µL per well. pCMV-empty vector was used as negative control (NC). Once verified the over-expression by immunoblotting, a rescue experiment was performed, in order to verify the direct involvement of MCM5 in JQ1 mechanism of action. Cells were transfected with pCMV-MCM5 or NC and exposed to 5µM JQ1 or vehicle for 48 h. Cell viability was evaluated by MTT assay, as previously described.

Protein extraction and Western blot

For total protein extraction, briefly, FRO SW1736 and 8505c cells, incubated in vehicle-treated medium (NT, untreated cultures) or with JQ1 5 µM, were harvested by scraping and lysed with total lysis buffer (Tris HCl 50 mM pH8, NaCl 120 mM, EDTA 5 mM, Triton 1%, NP40 1%, protease inhibitors). For subcellular fractionation, pellets were resuspended in buffer A (10 mM Tris-HCl [pH 7.5], 1.5 mM MgCl2, and 10 mM KCl supplemented with 1× protease inhibitor cocktail, 0.5 mM PMSF, 1 mM NaF and 1 mM Na3VO4) and centrifuged at 2,000 × *g* for 10min at 4°C. For nuclear extracts collection, pellets were resuspended in buffer B (20 mM Tris-HCl [pH 7.5], 0.42 M KCl, 1.5 mM MgCl2, 20% [vol/vol] glycerol supplemented with 1× protease inhibitor cocktail, 0.5 mM PMSF, 1 mM NaF, and 1 mM Na3VO4) and centrifuged at 15,000 × *g* for 30min at 4°C. For membrane protein extraction, briefly, cells incubated in

vehicle-treated medium (NT, untreated cultures) or with JQ1 5 µM were harvested by scraping and lysed with membrane extraction buffer (Sucrose 250 mM, HEPES 10 mM, EDTA 1 mM, protease inhibitors). For Western Blot analysis, proteins were electrophoresed on SDS-PAGE of different percentage and then transferred to nitrocellulose membranes, which were saturated with 5% non-fat dry milk in PBS/0.1% Tween 20. The membranes were then incubated overnight with the antibodies enlisted in Table 1.

The day after, membranes were incubated for 2h with anti-rabbit or anti-mouse immunoglobulin coupled to peroxidase 1:4000 (Sigma-Aldrich). The blots were developed using UVITEC Alliance LD (UVITec Limited, Cambridge, UK) with the SuperSignal Technology (Thermo Scientific Inc).

Table 1: Antibodies used in the research project.

Target	*Clonality*	*Host species*	*Diluition*	*Commercial supplier*
cMYC	monoclonal	mouse	1:200	SantaCruz Biotechnology, Heidelberg, Germany
MCM5	polyclonal	rabbit	1:250	Sigma Aldrich
PARP	polyclonal	rabbit	1:400	Abcam
IL7R	polyclonal	rabbit	1:1000	Biorbyt, Cambridge, UK
p21	polyclonal	rabbit	1:500	Santa Cruz Biotechnology, Inc.
phoshpo-STAT3 (Tyr705)	monoclonal	rabbit	1:10000	Merck Millipore, Vimodrone (MI), Italy
p27	polyclonal	rabbit	1:500	Santa Cruz Biotechnology, Inc.
β-actin	polyclonal	rabbit	1:1000	Abcam

Statistical analysis

mRNA and protein levels, cell viability and apoptosis levels were expressed as means ± SD, and significances were determined by a *one-way ANOVA followed by Dunnett's test* performed with GraphPAD Software for Science (San Diego, CA, USA).*P value <0.05 was considered statistically significant.

Results

Biological effects of BET inhibitors on ATC cells

Firstly, the sensitivity of the three ATC cell lines (FRO, SW1736 and 8505c) to BET inhibition was evaluated. As shown in Figure 1, treatments either with JQ1 (Panel A), I-BET762 (Panel B) or I-BET151 (Panel C) significantly reduced ATC cell viability, at different time points. Relying on data obtained, median effective dose of 5µM has been used for further experiments since it gave consistent data for all three cell lines, after 72h treatment.

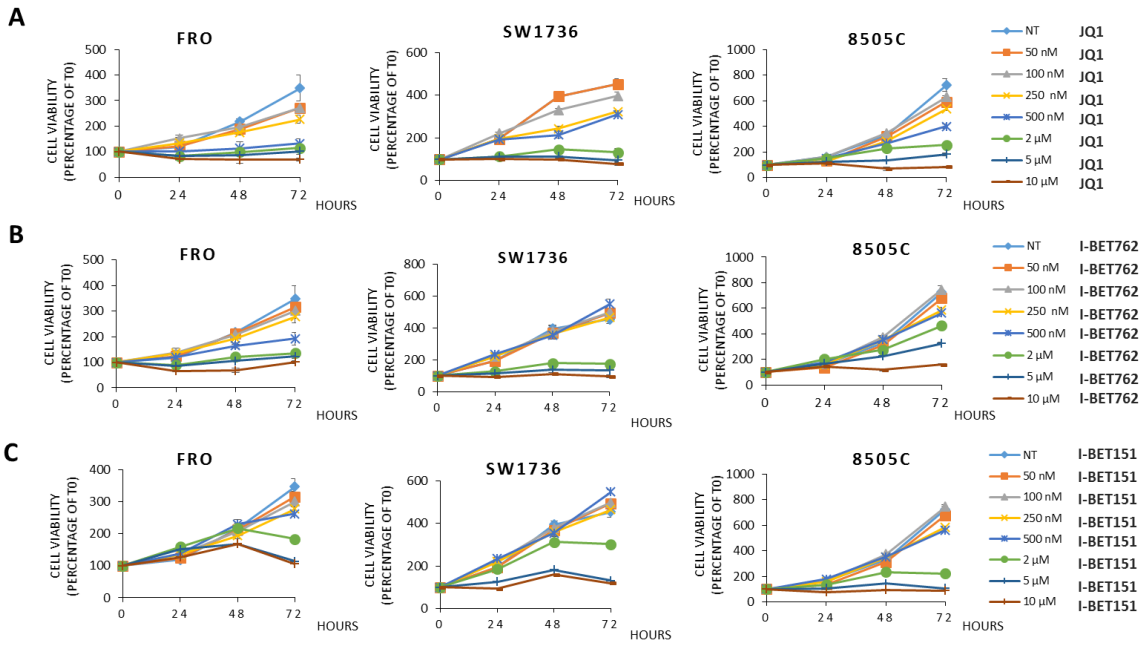

***Figure 1**. BET inhibitors administration decreases proliferation of anaplastic thyroid carcinoma cell lines. FRO, SW1736 and 8505c were exposed to JQ1 (A), I-BET 762 (B) or I-BET151 (C) at different doses (rising from 50nM to 10µM). Cell viability was determined with MTT assay after 0, 24, 48 and 72 h and expressed as a percentage of baseline samples (T0). All samples were run in quadruplicate. Data are representative of 3 independent experiments.*

To assess whether the decrease in cell viability was due to an increase of apoptosis, caspase 3/7 levels were measured after 72h treatment. JQ1 triggers caspases levels in all cell lines in a quite striking manner while I-BET762 and I-BET151 treatments showed a less pronounced effect (Fig.2, Panel A). To assess whether 72h I-BETs treatment elicited a caspase-independent cell death phenomenon, western blot analysis of PARP has been performed. PARP is known to be the substrate for several proteins such as caspases, calpains and cathepsins. It produces several specific cleavage fragments that resemble thesignature patterns of different cell death programs, i.e. apoptosis and necrosis (Gobeil et al. 2001; Chaitanya et al., 2010). As shown in Figure 2 (Panels B and C), ATC cells showed a marked increase of both apoptotic- and necrotic-specific cleaved-PARP bands. Hereinafter, JQ1 treatment was the solely one used for further investigations, as it revealed to be the most effective drug with reliability in all three cell lines.

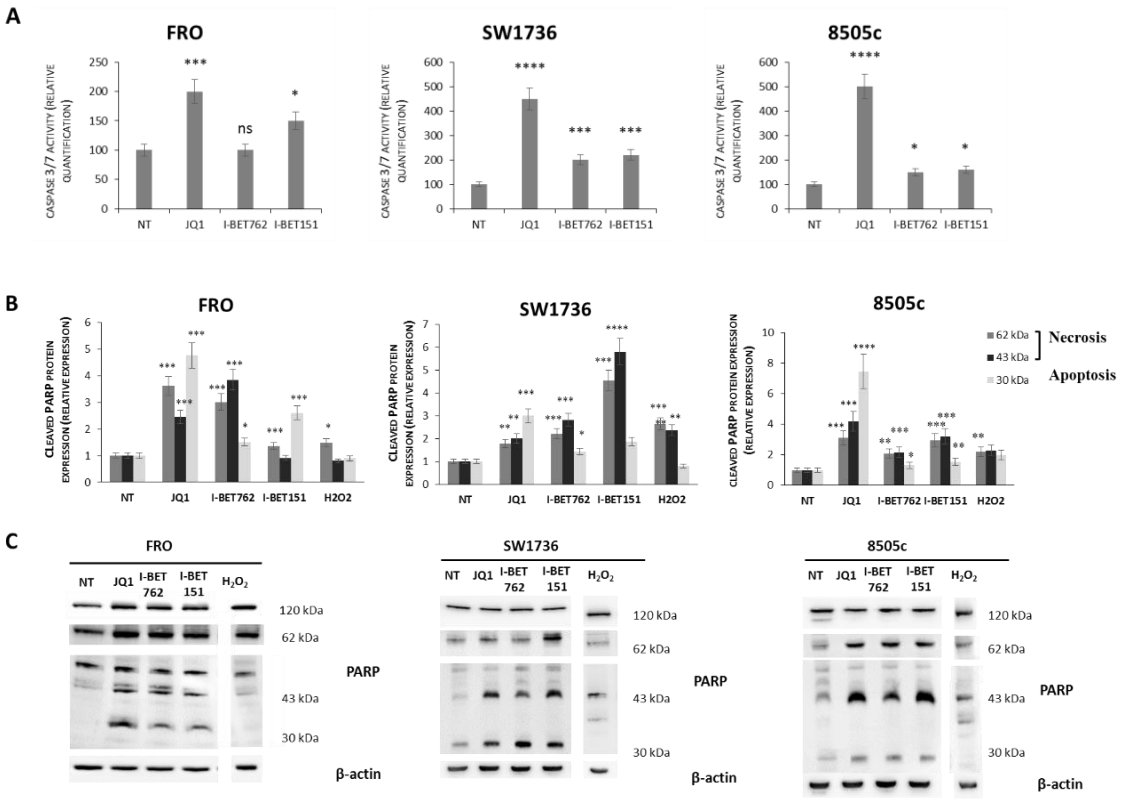

***Figure 2**. BET inhibitors administration increases cell death phenomena in anaplastic thyroid carcinoma cell lines. FRO, SW1736 and 8505c cells were treated either with 5µM JQ1, I-BET762, I-BET151 or vehicle for 72h and caspases 3/7 activity was analyzed (A). Vehicle-treated (NT) cells were arbitrarily set at 100 and caspases activity was expressed as relative expression values. All samples were run in quadruplicate. FRO, SW1736 and 8505c cells were treated either with 5µM JQ1, I-BET762, I-BET151 or vehicle for 72h and PARP protein levels were detected by western blotting (B). Vehicle-treated (NT) cells were arbitrarily set at 1.0 and protein levels were expressed as relative expression values. Hydrogen peroxide (5µM) was used as a positive control for necrosis. Results are shown as mean ± SD. ** p < 0.01, *** p < 0.001, **** p < 0.0001 by ANOVA test. Data are representative of 3 independent experiments.*

As BRD4 activity is linked to cell cycle progression, FACS analysis was performed on cells treated with 5µM JQ1 for 24, 48 and 72h. JQ1 treatment significantly increased the proportion of cells arrested in G0/G1 at each analyzed time point (Fig. 3), specifically leading to a flattened, senescence-like phenotype (Fig.4).

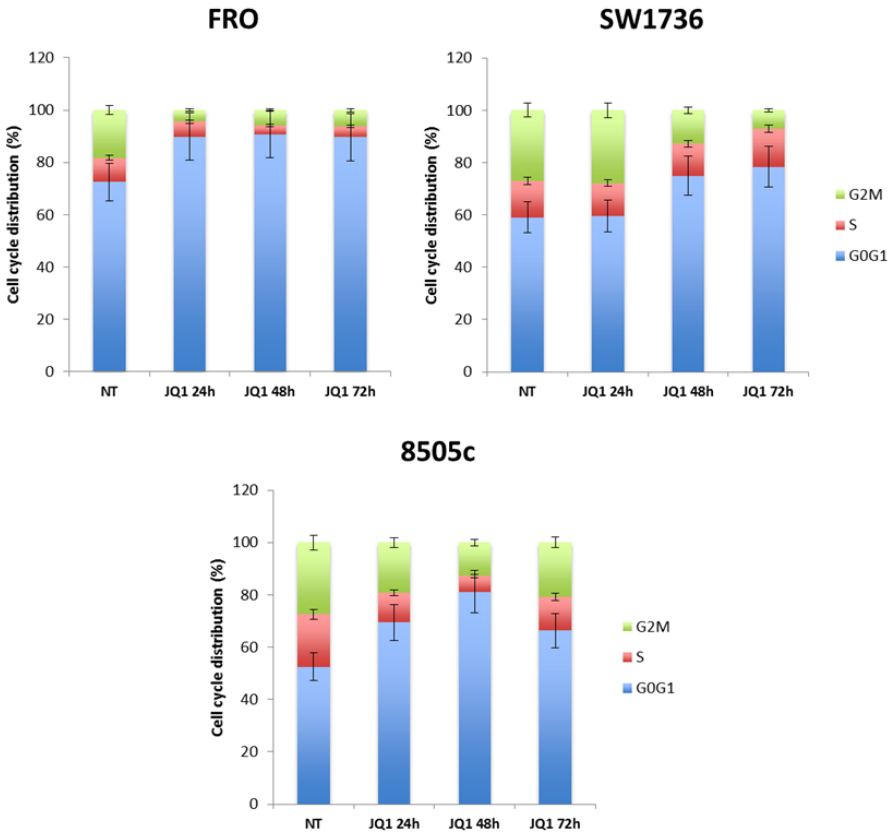

***Figure 3**. Cell cycle analysis after BET inhibition. FRO, SW1736 an 8505c cell cycle distribution was determined after 5µM JQ1 or vehicle administration. Cells were collected after 24, 48 and 72 hours treatments. Data are representative of 3 independent experiment. Results are shown as mean ± SD.*

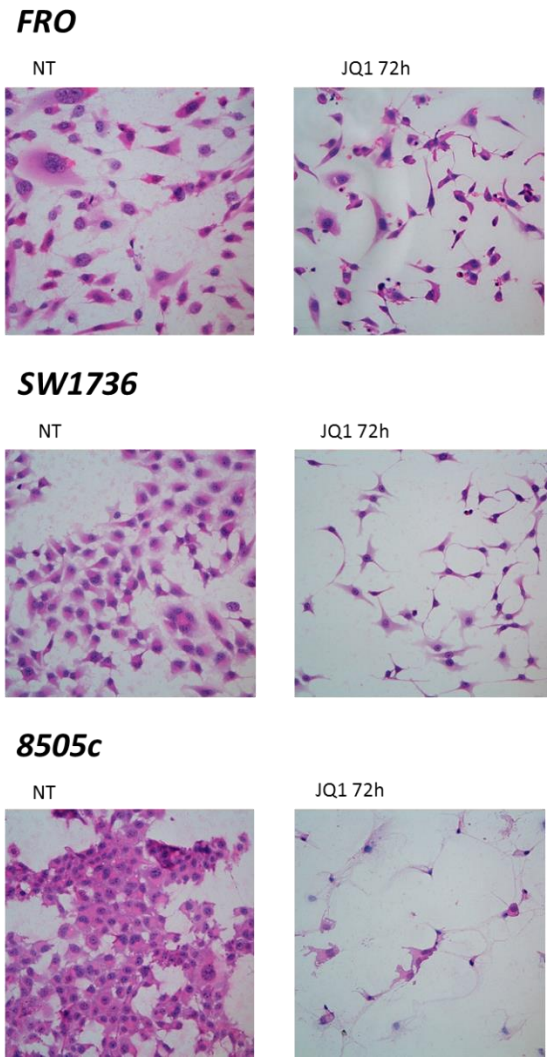

Figure 4. *Changes in cell morphology after BET inhibition. ATC cells phenotype was determined after 5μM JQ1 or vehicle administration. Images were taken after 72 hours treatment at 20x magnification using Leica DMI-6000B microscope.*

BET inhibitors effects on aggressiveness parameters

One of the most common features of aggressive cancer cells is the ability to invade tumor-neighboring tissues. To do that, cells develop different parameters among which motility and clonogenicity are included. In a first set of experiments, the wound healing ability was assessed after treatment with 5μM JQ1 or vehicle. Cells were monitored for 30 h and the wound healing was assessed using an inverted microscope. As shown in Figure 5, JQ1 treatment significantly decreased cell motility when compared to vehicle-treated cells.

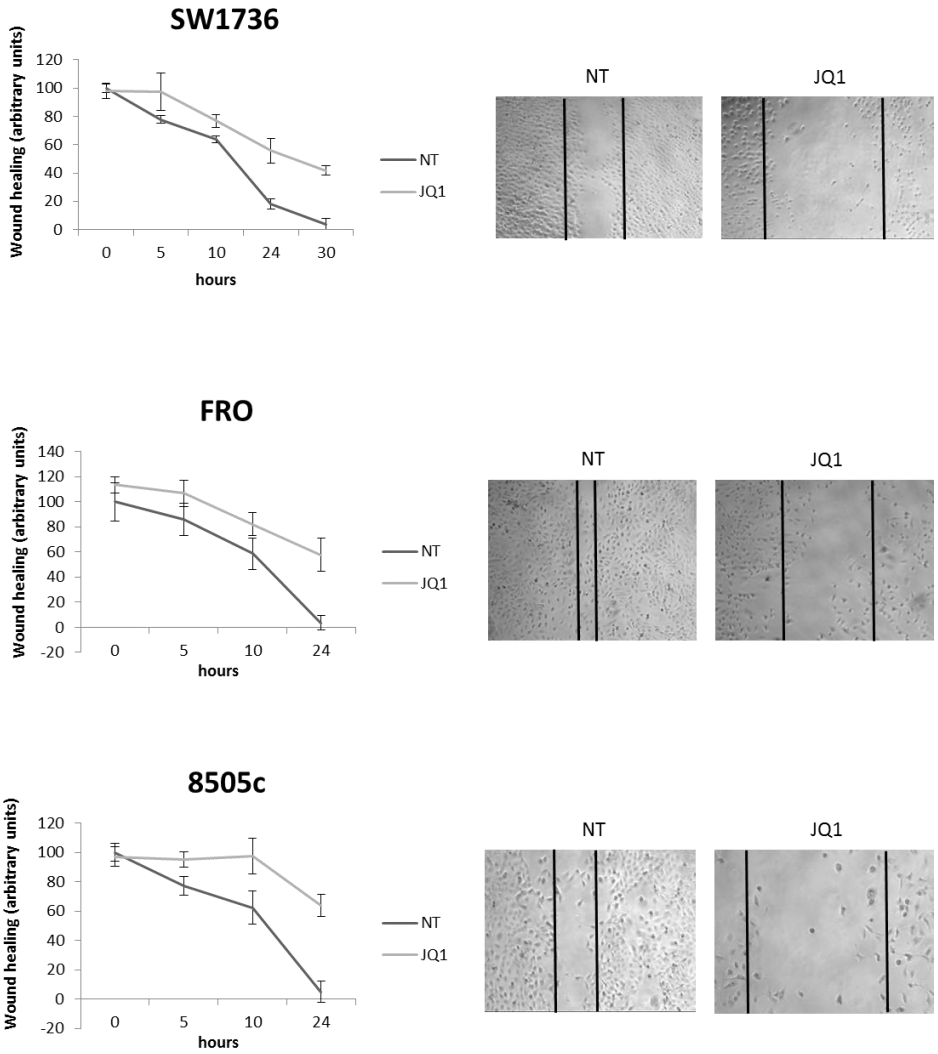

***Figure 5**. BET inhibition decreases ATC cells motility. FRO, SW1736 and 8505c cells were treated with 5μM JQ1 for 24 h and scratched. Wound healing capacity was determined for 30 h and the data were presented as the mean ± SD.*

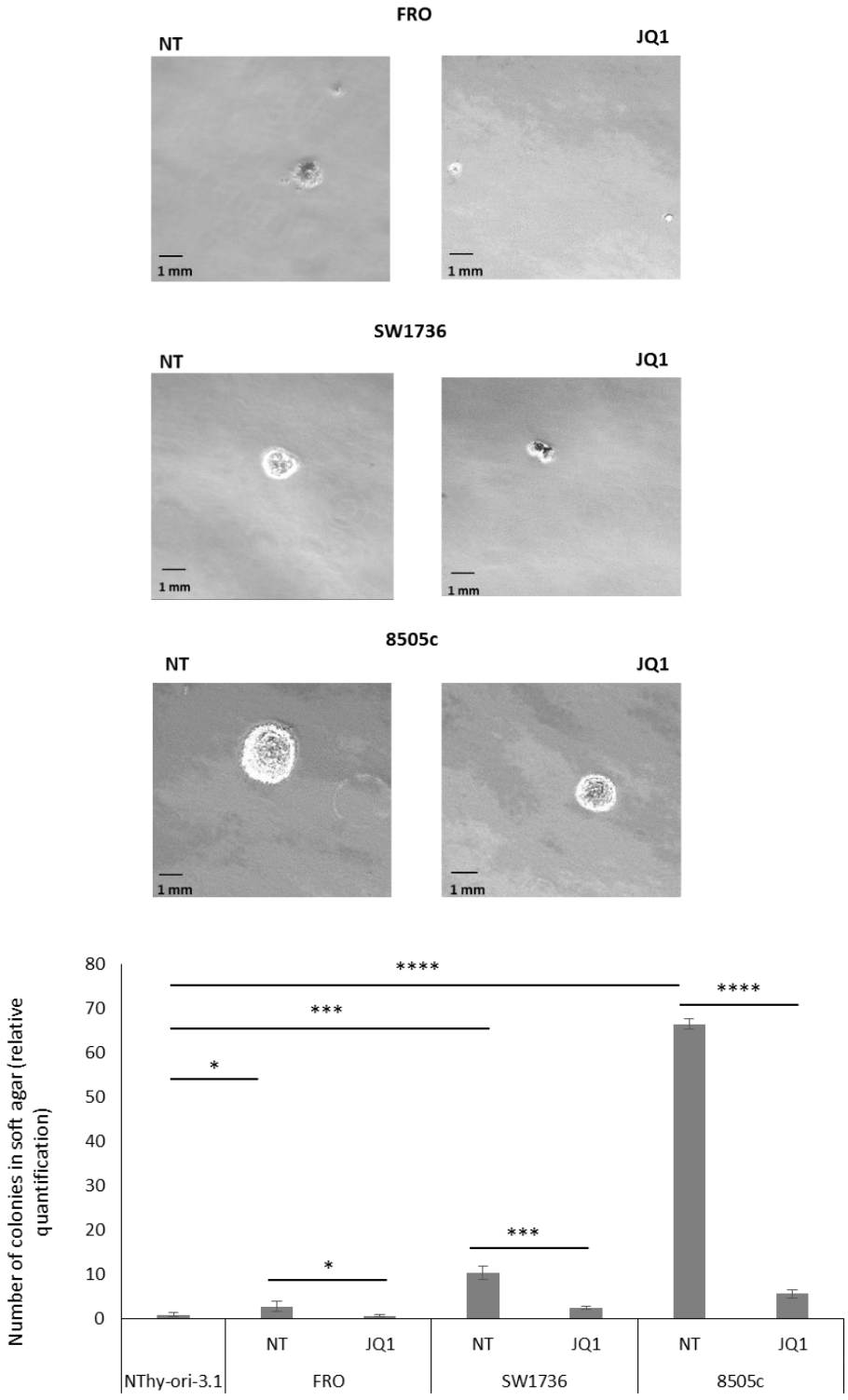

Figure 6. *BET inhibition impairs ATC clonogenic ability. Soft agar colony formation was performed exposing ATC cells to 5μM JQ1 or vehicle. The colony number is illustrated in the right-sided histogram. Non-tumorigenic cells (NThy-ori-3.1) cells were set at 1 and data are presented as relative quantification. Results are shown as mean ± SD. *** p < 0.001, **** p < 0.0001 by ANOVA test. Data are representative of 3 independent experiments.*

Moreover, to evaluate whether a 72 h 5µM JQ1 treatment could reduce ATC clonogenic potential as well, a soft agar assay has been performed. As shown in Figure 6, BET inhibition impaired the ability of ATC cells to form multicellular colonies, as 8505c cells displayed the most dramatic effect. An important feature to point out is that FRO cells showed a weak clonogenic potential when all three ATC cell lines were compared to the non-tumorigenic one (NThy-ori-3.1).

Differential gene expression after BET inhibition

As several studies proposed a possible role of *c-MYC* down-regulation as a major mechanism of BET inhibitors action (Zuber et al 2011; Alderton 2011), it has been assessed if a 5µM JQ1 treatment induced a relevant *c-MYC* modulation in ATC cells. c-Myc is a DNA binding transcription factor involved in the regulation of cell proliferation, differentiation, and apoptosis. High *MYC* expression levels are associated with almost all human cancers (Eilers and Eisenman, 2008). It has been shown that *c-MYC* regulation occurs within short time treatments, thus, ATC cells were exposed to 2, 6 and 24h treatment and mRNA and protein levels were assessed by qPCR and western blotting.

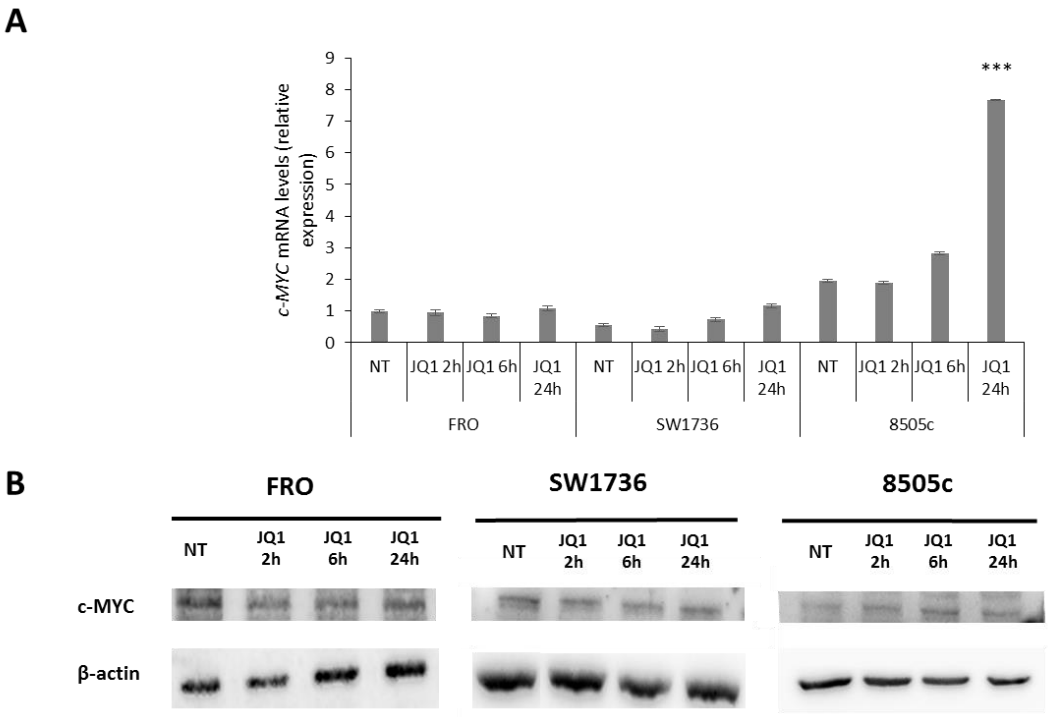

Figure 7. *BET inhibition does not alter c-MYC expression in ATC cells. FRO, SW1736 and 8505c cells were treated either with 5μM JQ1 or vehicle for 2, 6 and 24 hours and c-MYC mRNA expression was evaluated by qPCR (A). All samples were run in triplicate. Vehicle-treated (NT) FRO cells were arbitrarily set at 1.0 and mRNA levels are expressed as relative expression values. FRO, SW1736 and 8505c were treated either with 5μM JQ1 or vehicle for 2, 6 and 24h and c-MYC protein levels were detected by western blotting (B).*

As shown in Figure 7 (Panel A), mRNA levels displayed a high rate of variation for each sample and 5μM JQ1 treatment did not significantly affect *c-MYC* expression levels. As mRNA levels seemed to be unaffected by BET inhibition, similarly no c-MYC protein levels variation could be detected after JQ1 treatment, at any analyzed time point (Panel B).

To identify new potential BETi targets, a high-throughput RNA sequencing analysis and a miRNA expression evaluation were performed.

For this purpose, two different settings were used: the RNA-seq was performed on a non-clonogenic and a clonogenic cell line (FRO and SW1736, respectively) while the miRNA evaluation was performed on the two clonogenic lines (SW1736 and 8505c), as miRNA is involved in tumor aggressiveness and metastatization.

A RNA-seq on FRO and SW1736 treated with 5µM JQ1 or vehicle for 24h was performed in collaboration with the Istituto of Genomica Applicata in Udine. To assess the transcriptional changes induced by BET inhibition, a comparison between vehicle- or JQ1-treated cells was performed. Heat maps representing each analyzed condition are shown in Figure 8 (Panel A). After filtering low quantity reads, approximately 2000 genes were differentially expressed after JQ1 treatment either in FRO or SW1736 cells (at a $\log_2$ fold change >=2). Among them, 768 genes were significantly up-regulated and 1229 were down-regulated in response to JQ1 treatment (Fig.8, Panel B). Venn diagrams showed that the majority of altered genes was specific for each cell line, which likely underlies the differential mRNA profile observed with vehicle treatment. However, there was a core set of 288 genes commonly affected by JQ1 in both cell lines, most of which decreased their expression (n=213).

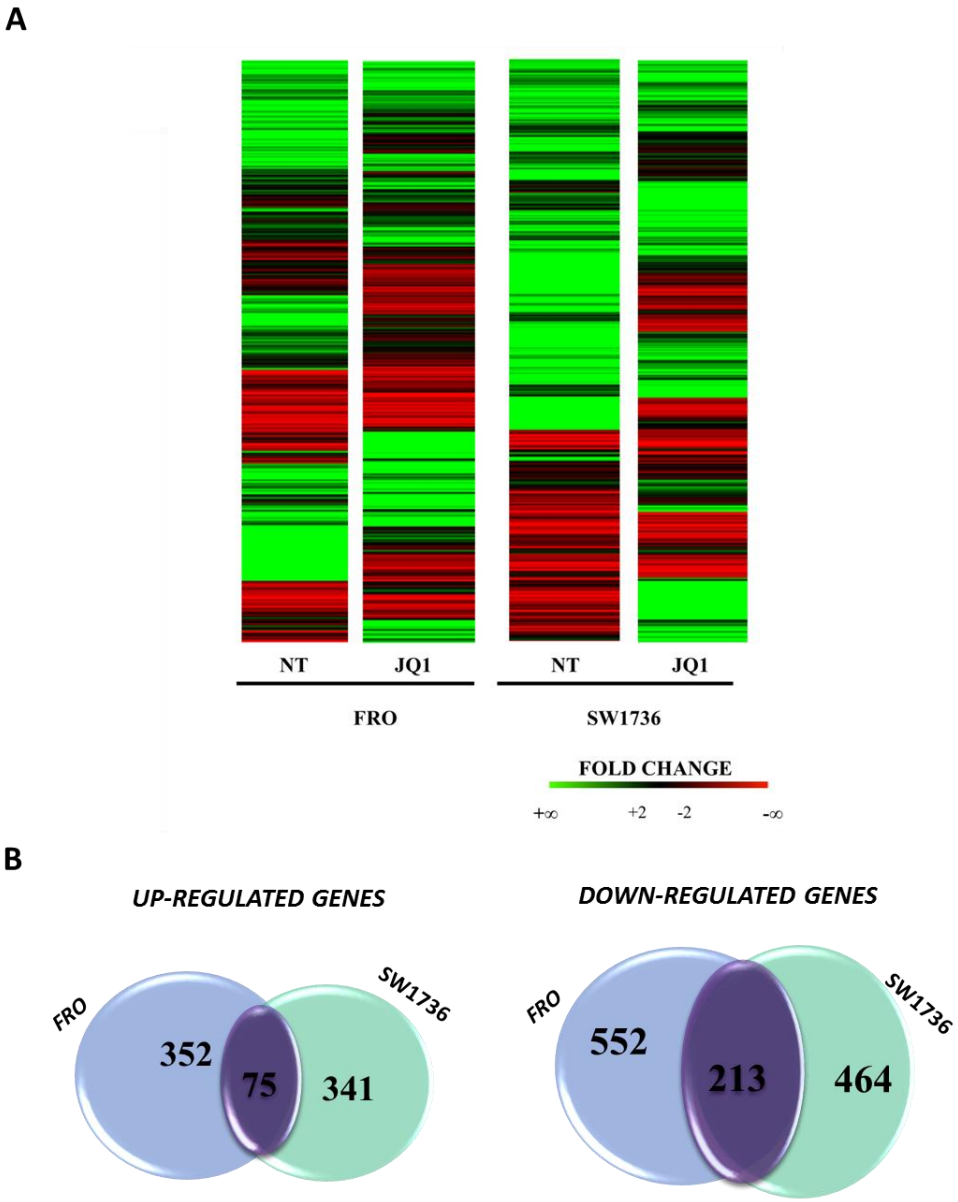

Figure 8. *Gene expression modifications in ATC JQ1-treated cell lines. Heat maps (A) showing the hierarchical clustering of mRNA targets in FRO and SW1736 cell lines. Venn diagrams (B) representing the comparison of both up-regulated (left) and down-regulated (right) genes between FRO and SW1736 cell lines after RNA-seq data analysis. Purple gene clusters represent shared modified genes between FRO and SW1736 cell lines.*

Table 1*:* Top 20 most down-regulated and up-regulated genes after BET inhibition.

DOWN-REGULATED GENES			UP-REGULATED GENES		
GENE	**Log2 (fold_change)**		**GENE**	**Log2 (fold_change)**	
	FRO	**SW1736**		**FRO**	**SW1736**
E2F8	-8.18691	-3.32852	***HIST2H2BE***	5.45681	6.36269
IL7R	-7.92256	-4.28496	***EFR3B***	5.45085	2.31549
SCG5	-7.07872	-5.36462	***HIST1H2BJ***	5.41635	4.29568
MFAP2	-6.55018	-4.00946	***HIST1H2BC***	4.91188	3.90626
KLF17	-5.87194	-2.54046	***AQP3***	4.82547	5.53788
HAS2	-5.61592	-2.59963	***KCNJ2-AS1***	4.77102	2.57414
SP140	-5.51289	-2.76406	***HIST1H2BD***	4.76918	7.37894
SFTA1P	-4.86488	-2.30007	***HIST1H1C***	4.65229	4.36823
APOL3	-4.76234	-3.04492	***MSS51***	4.53001	4.03264
UHRF1	-4.58863	-2.45864	***PROCA1***	4.31851	2.40037
ELFN2	-4.56104	-2.07491	***RNFT2***	4.20444	2.75534
SLC38A5	-4.50203	-3.75806	***ARHGAP4***	4.14859	2.29762
WDR76	-4.50144	-3.32284	***ALS2CR12***	4.07061	5.36388
SEMA6B	-4.46547	-2.00721	***CLU***	4.06906	3.93869
STAP2	-4.43699	-3.34008	***HIST1H2AC***	3.98232	4.03878
RFX8	-4.42127	-3.66572	***BFSP1***	3.77102	2.63104
FMNL1	-4.42127	-2.04374	***ITPR1***	3.6183	7.03299
GINS2	-4.3919	-2.49012	***FAM222A***	3.3286	2.436
HTR1D	-4.32174	-3.30238	***TLL2***	3.24364	2.56248
MCM5	-4.27584	-3.20364	***TM7SF2***	3.20111	7.24837

The shared top 20 differentially expressed genes (Tab.1) were subjected to gene ontology (GO) analysis in order to outline which pathways were mostly affected by BET inhibition. Various signaling cascades turned out to be altered: 'regulation of DNA' and 'metabolic processes' were on top of the list (Fig. 9). The GO analysis identified a large number of JQ1 putative targets in cell cycle-linked pathways. These data are consistent with Da Costa's findings in leukemia cells (Da Costa et al. 2013). Moreover, RNA-seq data confirmed that *c-MYC* does not seems to be a critical factor in JQ1-mediated effects in ATC. BET inhibitors, however, modified the expression of several cell cycle regulators such as *RBs*, *E2Fs* and *CDK*-inhibitors (Tab. 2).

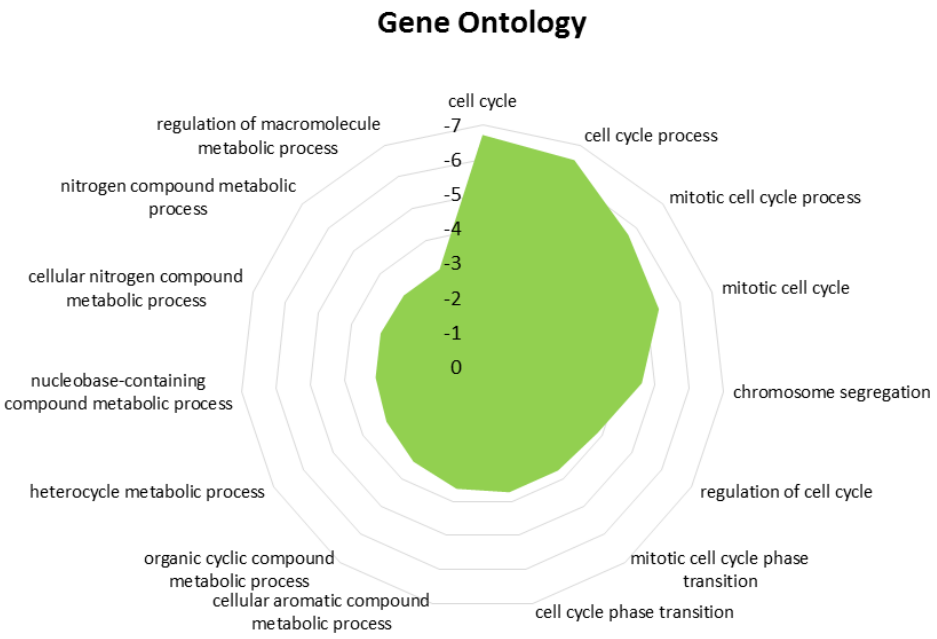

Figure 9. *Gene Ontology analysis. Radar graph representing the most enriched biological pathways associated to BET inhibition. On the y-bar log_{10} p-value is represented.*

Table 2. Cell cycle-linked genes modified by JQ1 treatment (/: no detectable expression)

	Log2 (fold_change)	
GENE	**FRO**	**SW1736**
RBL1	-2.3676	-2.69299
TP53INP1	/	2.16764
TP53TG1	/	2.00806
CDKN1A	/	2.10416
CDKN1C	2.07978	2.66623
CDK1	/	-2.34326
CDK2	-2.12937	/
CDK15	-4.1289	-4.1296
CCNA2	-3.06638	-2.72967
CCNE1	-3.06035	-2.14395
CCNE2	-2.43046	/
E2F1	-3.00569	-2.26302
E2F8	-8.18691	-3.32852
E2F2	-3.96184	-4.19839
E2F1	-3.00569	-2.26302
E2F7	/	-2.35371
MCM5	-4.27584	-3.20364
MCM10	-3.7986	-2.72972
ORC1	-2.22412	-2.65498
CDT1	-2.3867	-3.28703
CDC6	-2.83448	/
CDC45	-2.81054	-3.28352
GINS1	-2.62039	-2.5818
GINS2	-4.3919	-2.49012
GINS3	-2.49263	-3.5349

BET inhibition effects on MCM5

Considering that cell cycle regulation seemed to be the most affected pathway in response to JQ1 treatment, *MCM5* regulation was took into consideration. MCM5 is known to be involved in G1/S cell cycle transition, coordinating origin activation and replication fork progression. It belongs to the minichromosome maintenance complex family, which has been already associated with the highly proliferative phenotype of ATC (Guida et al. 2005). MCM5 protein level has already been proposed as a diagnostic marker of malignancy, i.e. in bladder, esophageal, and gastric cancers (Kebebew et al. 2006). After confirming RNA-seq data on mRNA levels in all three ATC cell lines (Fig.10 Panel A), protein levels were took into consideration, confirming its down-regulation (Fig.10, Panel B-C). To extend and further validate this finding, two murine ATC cell lines derived from tumors developed by a genetically defined mouse model of ATC were used, in collaboration with Prof. Di Cristofano at the Albert Einstein College of Medicine in New York. Treatment of both lines with 0.5µM JQ1 for 72h resulted in a significant down-regulation of *mcm5* RNA (Fig. 10, Panel D).

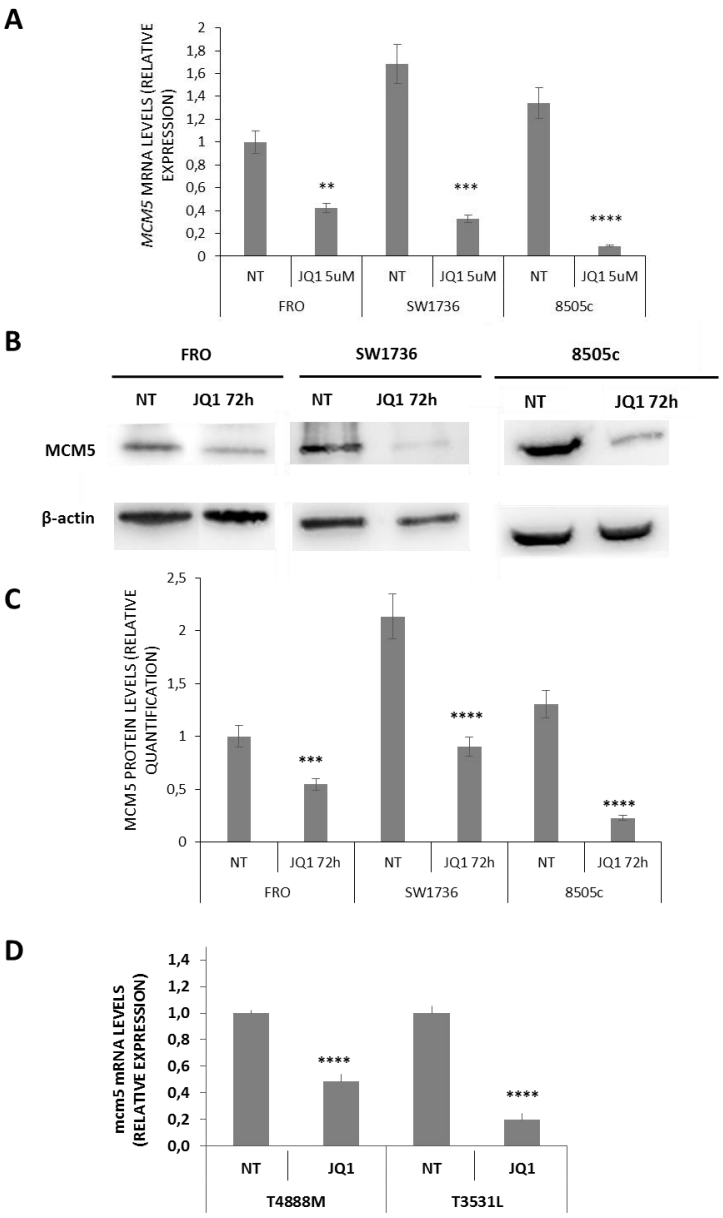

Figure 10*.Down-regulation of MCM5 in human and murine ATC cell lines after JQ1-treatment. FRO, SW1736 and 8505c cells were treated either with 5μM JQ1 or vehicle for 24 hours and MCM5 mRNA expression was evaluated by qPCR (A). All samples were run in triplicate. Vehicle-treated (NT) FRO cells were arbitrarily set at 1.0 and mRNA levels are expressed as relative expression values. ATC cells were treated either with 5μM JQ1 or vehicle for 72h and MCM5 protein levels were detected by western blotting (B). Densitometric analysis of MCM5 protein levels in ATC cells after 5μM JQ1 or vehicle treatment (C). T4888M and T3531L cells were treated either with 0.5μM JQ1 or vehicle for 72 hours and mcm5 mRNA expression was evaluated by qPCR (D). All samples were run in triplicate. Vehicle-treated (NT) T4888M cells were arbitrarily set at 1.0 and mRNA levels are expressed as relative expression values. Results are shown as mean ± SD. *** p < 0.001, **** p < 0.0001 by ANOVA test. Data are representative of 3 independent experiments.*

To evaluate whether *MCM5* is a direct target of BRD4, a ChIP-qPCR analysis was performed. Comparing the BRD4-bound immunoprecipitate to the IgG one, a 5-fold *MCM5* enrichment was observed. To confirm specificity, an intergenic region (*NCR*) has been used as negative control for BRD4-binding (Fig. 11, Panel A). In order to test the biological relevance of *MCM5* gene repression upon BET inhibition, a RNA interference analysis was performed. After observing a nearly total down-regulation of MCM protein levels, especially with siRNA#2 treatment (Fig. 11, Panel B), a significant decrease in cell viability ($p<0.001$) associated to an increase in the percentage of cell death (Fig. 11, Panel C) was witnessed. Moreover, the more MCM5 protein levels decreased, the more increase in cell death was assessed (see siRNA#2 data). To further demonstrate that MCM5 was directly involved in the cell viability reduction observed after BET inhibition, a rescue experiment was performed. FRO and SW1736 cells were treated with pCMV-MCM5 or empty vector (NC) and exposed to JQ1 for 48h. As shown in Fig. 11 Panel D, MCM5 over-expression partially rescued its protein levels in JQ1-treated cells, leading to a slight but significant reduction (10% on average) of JQ1 effects when assessing cell viability (Fig. 11, Panel E). This mild rescue could be reasonably due to the multi-target activity of BET inhibitors, whose effects are mediated by a remarkable number of actors, as shown in the RNA-seq (Fig. 8). Accordingly, poor rescue effects have been obtained when assessing others BETi-single targets (Lockwood et al., 2012; Bandopadhayay et al., 2014).

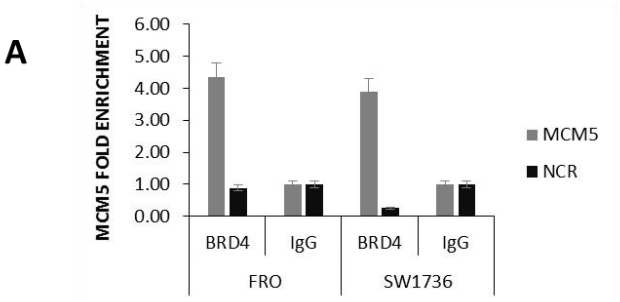
A
MCM5 FOLD ENRICHMENT
6.00
5.00
4.00
3.00
2.00
1.00
0.00
MCM5
NCR
BRD4
IgG
BRD4
IgG
FRO
SW1736

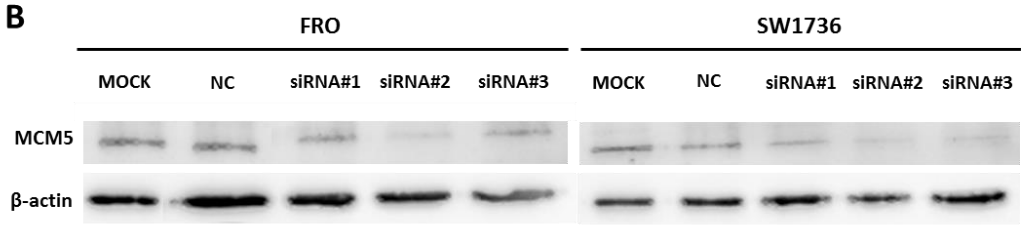
B
FRO
SW1736
MOCK
NC
siRNA#1
siRNA#2
siRNA#3
MOCK
NC
siRNA#1
siRNA#2
siRNA#3
MCM5
β-actin

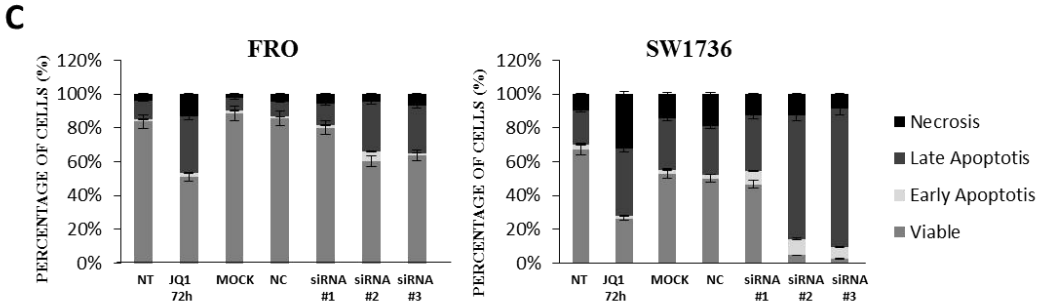
C
FRO
SW1736
PERCENTAGE OF CELLS (%)
120%
100%
80%
60%
40%
20%
0%
NT
JQ1 72h
MOCK
NC
siRNA #1
siRNA #2
siRNA #3
Necrosis
Late Apoptotis
Early Apoptotis
Viable

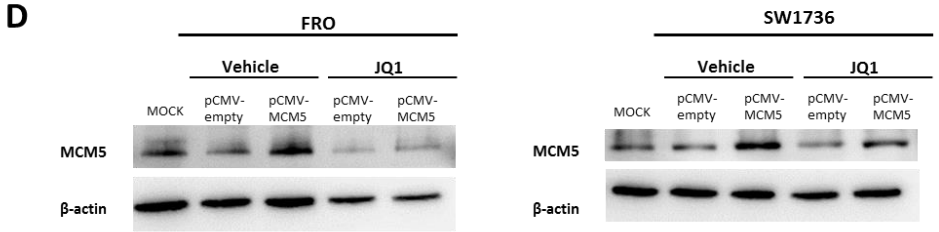
D
FRO
SW1736
Vehicle
JQ1
MOCK
pCMV-empty
pCMV-MCM5
pCMV-empty
pCMV-MCM5
MCM5
β-actin

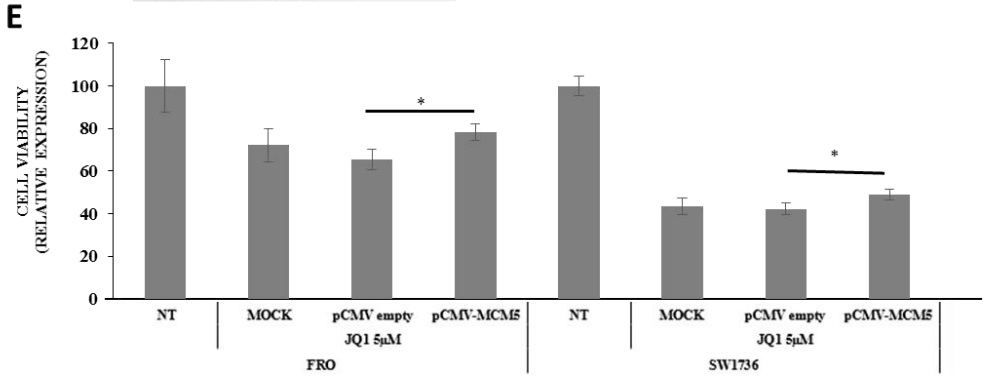
E
CELL VIABILITY (RELATIVE EXPRESSION)
120
100
80
60
40
20
0
*
*
NT
MOCK
pCMV empty
pCMV-MCM5
JQ1 5μM
FRO
NT
MOCK
pCMV empty
pCMV-MCM5
JQ1 5μM
SW1736

Figure 11. *MCM5 is directly involved in BET inhibitors effects in human ATC cell lines. Chromatin immunoprecipitation in ATC cells performed with BRD4 or IgG antibodies (A). MCM5 DNA was amplified using promoter-specific primers and analyzed by qPCR. All samples were run in triplicate. IgG-immunoprecipitate was arbitrarily set at 1.0 and the enrichment was expressed as relative expression value. An intergenic region (NCR) was used as negative control for BRD4-binding. FRO and SW1736 cells were treated with non-targeting siRNA (NC, negative control) or three different MCM5-specific siRNA (5nM). Cells were collected after 72h treatment and MCM5 protein levels were analyzed (B). FRO and SW1736 were exposed to either siRNA targeting MCM5 or negative control for 72 hours and apoptosis levels was analyzed by Annexin V staining (C). FRO and SW1736 cells were treated with pCMV empty vector (NC, negative control) or pCMV vector specific for MCM5 (1.3 µg). Cells were collected after 48 h treatment and MCM5 protein levels were analyzed (D). FRO and SW1736 were treated with 0.01 µg p-CMV-MCM5 or empty vector and exposed to 5µM JQ1 or vehicle. Cell viability was determined by MTT assay after 48h (E). NT was arbitrarily set at 100 and cell viability was expressed as relative expression value. All samples were run in quadruplicate. Results are shown as mean ± SD. *** p < 0.001, **** p < 0.0001 by ANOVA test. Data are representative of 3 independent experiments.*

In vivo MCM5 levels evaluation

Data presented so far highlighted the relevance of MCM5 in thyroid cancer cells growth. Thus, MCM5 expression was evaluated in a tissue microarray composed by 12 NTs, 25 FAs, 23 FTCs, 36 PTCs and 8 ATCs. Representative images of MCM5 staining are shown in Figure 12 (Panel A). Normal thyroid tissue and in FAs displayed a faded MCM5 expression. PTCs showed a dual behavior: some samples exhibited an intense and high MCM5 nuclear staining, while some others a much lesser one, with only a cytoplasmic signal. FTCs showed a predominant cytoplasmic MCM5 staining. ATCs, instead, presented a striking nuclear MCM5 localization. No significant differences were observed in terms of MCM5 nuclear or cytoplasmic staining intensity among different areas of each tumor. Quantification of the nuclear immunohistochemical signal was obtained by computing percentage of cell positivity and intensity of signal (Fig. 12, Panel B).

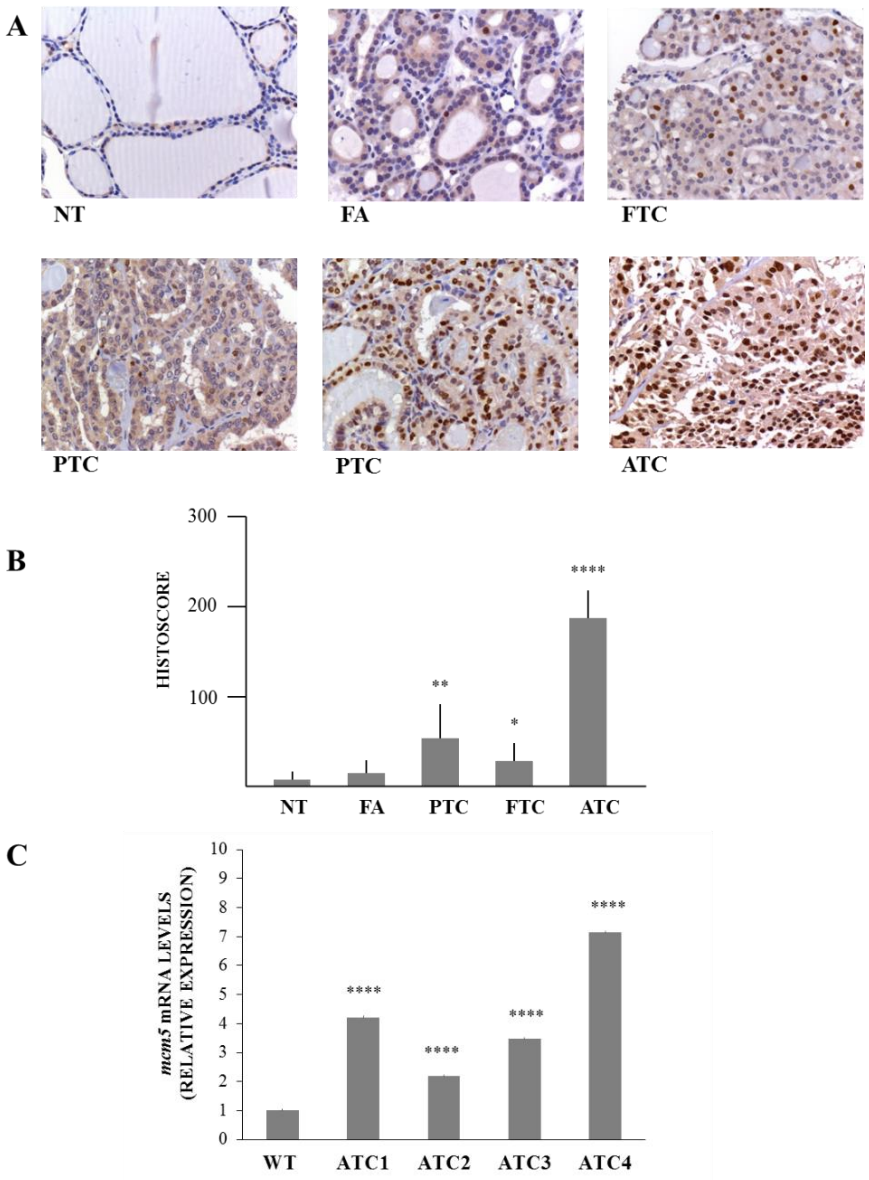

Figure 12. *MCM5 expression in thyroid tumors. Representative images (A) of MCM5 expression in normal thyroid tissues (NT), FAs, PTCs, FTCs and ATCs. Quantification of MCM5 expression in normal and neoplastic thyroid tissues (B). Quantification was obtained by using the IHC score, calculated as described in Materials and Methods section. Mcm5 expression was evaluated by qPCR (C) in control thyroids from wild type mice and primary ATCs from [Pten, Tp53]$^{thyr-/-}$ mice. All samples were run in triplicate. Wild type (WT) expression was set at 1.0 and mRNA levels are expressed as relative expression values. Results are shown as mean ± SD. * $p < 0.05$, ** $p < 0.01$, **** $p < 0.0001$ by ANOVA test.*

Since cytoplasmic MCM5 protein represents the inactive MCM5 isoform (Abe et al. 2012), the strong nuclear staining observed in all ATCs and several PTCs would suggest its hyper-activation. Finally, the expression of mcm5 in four primary ATCs developed by [*Pten, Tp53*]$^{thyr-/-}$ mice (Antico Arciuch et al. 2011) was measured (Prof. Di Cristofano). In agreement with the human data, mcm5 was found significantly overexpressed in mouse ATCs, compared to normal thyroids (Fig. 12, Panel C).

BET inhibition effects on IL7R

After validating MCM5 as a direct target of BET inhibitors, IL7R modulation was took into consideration. The IL7-related signal cascade is crucial for normal development and maintenance of the immune system. In non-hematopoietic tissues, interleukin 7 receptor (*IL7R*) expression has been identified in a small subset of tissues, i.e. central nervous system, lung, renal, colorectal cancers and melanoma (Cosenza et al., 2002). Recently, Ott at al. observed that JQ1 treatment decreased *IL7R* expression in leukaemic cell lines, both at mRNA and protein levels (Ott et al. 2012). The RNA-seq analysis showed a marked decrease of IL7R in FRO and SW1736 cells after a 5µM JQ1 treatment (see Tab. 1). The significant down-regulation of IL7R mRNA levels was confirmed by qPCR, but this reduction was not confirmed analyzing protein levels. All these data are presented in Figure 13.

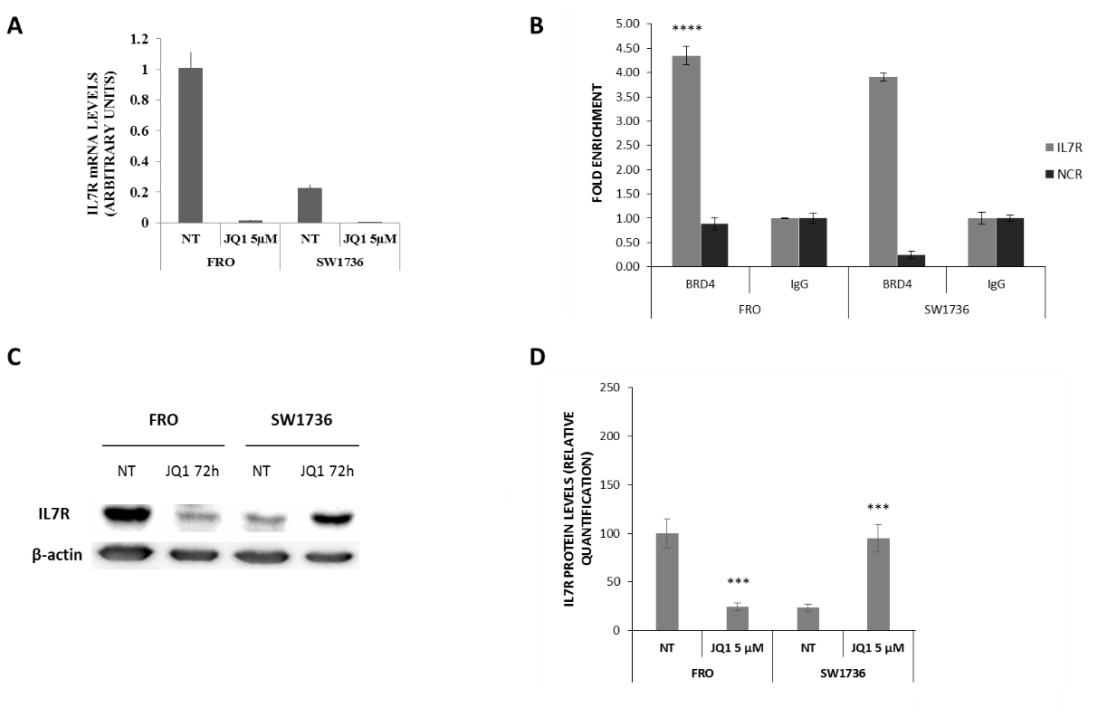

Figure 13*. JQ1-induced modification of IL7R expression in human ATC cell lines. FRO, SW1736 and 8505c cells were treated either with 5μM JQ1 or vehicle for 24 hours and IL7R mRNA expression was evaluated by qPCR (A). All samples were run in triplicate. Vehicle-treated (NT) FRO cells were arbitrarily set at 1.0 and mRNA levels are expressed as relative expression values. Chromatin was isolated from ATC cell lines and immunoprecipitated with BRD4 or IgG antibodies (B). IL7R DNA was amplified using promoter-specific primers and analyzed by qPCR. All samples were run in triplicate. IgG-immunoprecipitate was arbitrarily set at 1.0 and the enrichment was expressed as relative expression value. An intergenic region (NCR) was used as a negative control for BRD4-binding. FRO, SW1736 and 8505c cells were treated either with 5μM JQ1 or vehicle for 72h and IL7R protein levels were detected by western blotting (C). Densitometric analysis of IL7R protein levels in ATC cells after 5μM JQ1 or vehicle treatment (D). Results are shown as mean ± SD. *** p < 0.001, by ANOVA test. Data are representative of 3 independent experiments.*

Even if *IL7R* is a direct target of BRD4, as shown in the ChIP –qPCR experiment (Fig. 13, Panel B), the endogenous IL7R protein was not so abundant in these cell lines and, therefore, the misregulation of a protein involved in during lymphocyte development seemed not to perform a substantial role in JQ1 effects in thyroid cancer cells. Moreover, it has been previously reported a discordance between mRNA and protein levels, suggesting that IL7R levels could be unstable (Cosenza et al., 2002). The results obtained on IL7R modulation after BET inhibition seemed to support this idea.

BET inhibition modifies miRNA expression in ATC cells

Data presented so far clearly demonstrated the anti-neoplastic activity of BET inhibitors in ATC cells. As the RNA-seq analysis proved the pleiotropic effect of JQ1 treatment and being ncRNAs key features governing aggressive cancer subtypes (Grotenhuis et al., 2012), we focused on a possible JQ1-dependent miRNA regulation. There are multiple reports revealing how EMT is affected by various miRNAs demonstrating an inter-connectivity between miRNAs, EMT and cancer progression. Various miRNA signatures can accurately discriminate tumor from normal tissue, as well as various cancer sub-types among them. Furthermore, it is now well established that miRNAs can serve as candidate biomarkers for diagnostic and prognostic purposes (Zaravinos, 2015; Prokopi et al., 2015).

The identification of putative miRNAs involved in BET inhibitors effects on ATC cells was assessed through the nCounter miRNA Expression Assay Kit, a novel digital color-coded barcode technology based on direct multiplexed measurement of gene expression. Relying on the data on ATC aggressiveness, SW1736 and 8505c were used for further investigations, as these cell lines displayed the highest clonogenic ability. ATC samples, 5µM JQ1 or vehicle-treated for either 48 or 72 hours, were run on the Nanostring platform in collaboration with the genetic lab of Pharmadiagen srl (PN).

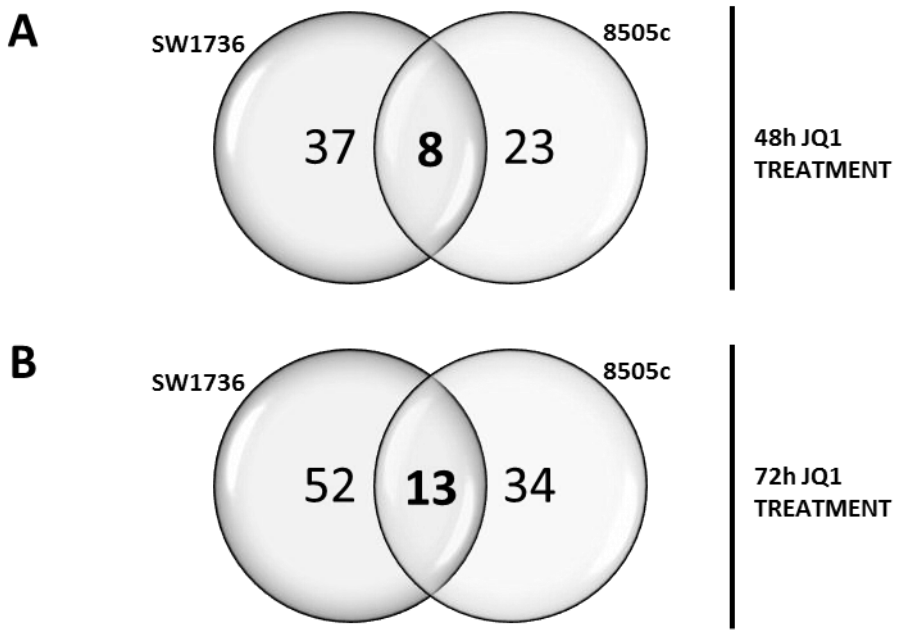

Figure 14. *miRNAs alteration due to BET inhibition in ATC cells. SW1736 and 8505c treated with 5μM JQ1 or vehicle for 48h were subjected to Nanostring platform miRNAs evaluation (A). 45 and 31 miRNAs turned out to be up-regulated by BET inhibition in SW1736 and 8505c, respectively. 8 miRNAs shared a common alteration in both cell lines. SW1736 and 8505c treated with 5μM JQ1 or vehicle for 72h were subjected to Nanostring platform miRNAs evaluation (B). 65 and 47 miRNAs turned out to be up-regulated by BET inhibition in SW1736 and 8505c, respectively. 13 miRNAs shared a common alteration in both cell lines.*

Of the 812 miRNAs analyzed, 45 and 31 miRNAs turned out to be deregulated after 48h JQ1 treatment in SW1736 and 8505c cells, respectively. As shown in Figure 14, Panel A, 8 miRNAs displayed a common up-regulation in both cell lines. After a 72h JQ1 treatment, instead, 65 and 47 miRNAs proved to be deregulated in SW1736 and 8505c cells, respectively. 13 miRNAs showed a common up-regulation in the two cell lines (Fig. 14, Panel B). In order to delineate capital miRNAs in JQ1 mediated effects, we compared 48h and 72h common miRNAs, highlighting a pool of 7 miRNAs commonly up-regulated in both SW1736 and 8505c after both 48 and 72h JQ1 treatment (Tab. 3).

Table 3. Shared miRNAs altered after 5μM treatment in ATC cells.

48-72h shared up-regulated miRNAs
hsa-miR-182-5p
hsa-miR-4516
hsa-miR-1234
hsa-miR-30c-5p
hsa-miR-4488
hsa-miR-4532
hsa-miR-548t-5p

JQ1 up-regulates miRNAs involved in STAT3 and PTEN signal transduction pathways

In order to elucidate potential mechanisms controlled by the pool of 7 miRNAs identified, the bioinformatic softwares available online have been exploited. The approach used is depicted in Figure 15.

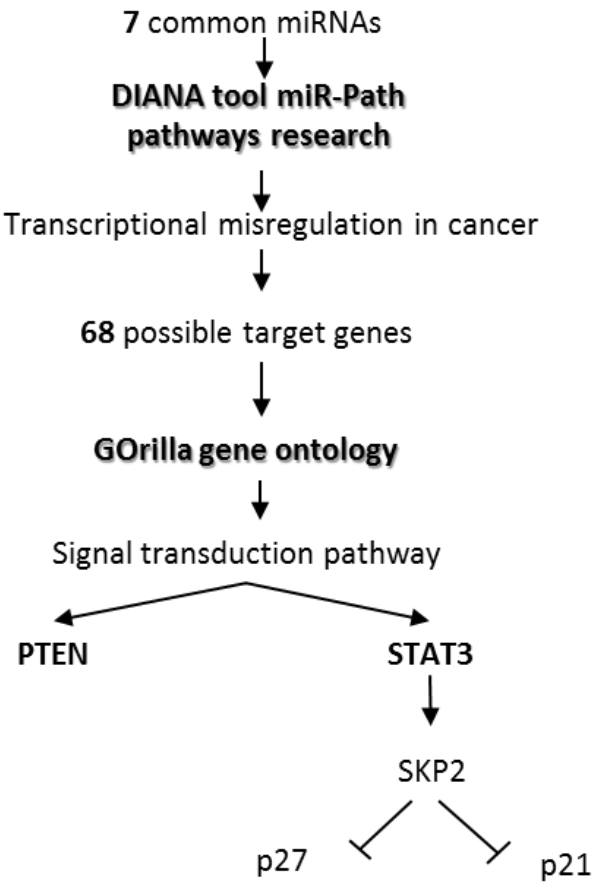

Figure 15. *Experimental approach used to identify altered pathways due to JQ1-dependent up-regulated miRNAs.*

The shared 7 miRNAs were subjected to a pathways analysis using the mirPath algorithm offered by DIANA tools (http://diana.imis.athena-innovation.gr/DianaTools/index.php?r=mirpath/index), which suggested 'transcriptional misregulation in cancer' as one of the most significantly associated enriched pathways. The database takes advantage of an algorithm to enlist the putative miRNA-associated gene targets and, for the submitted query, the algorithm proposed 68 targets. These putative miRNA-associated genes have been subjected to a gene ontology analysis, in order to outline the biological pathways in which these miRNAs are involved (Fig. 16). The analysis showed a strong enrichment in the 'signal transduction' pathway, in which STAT3 and PTEN are involved.

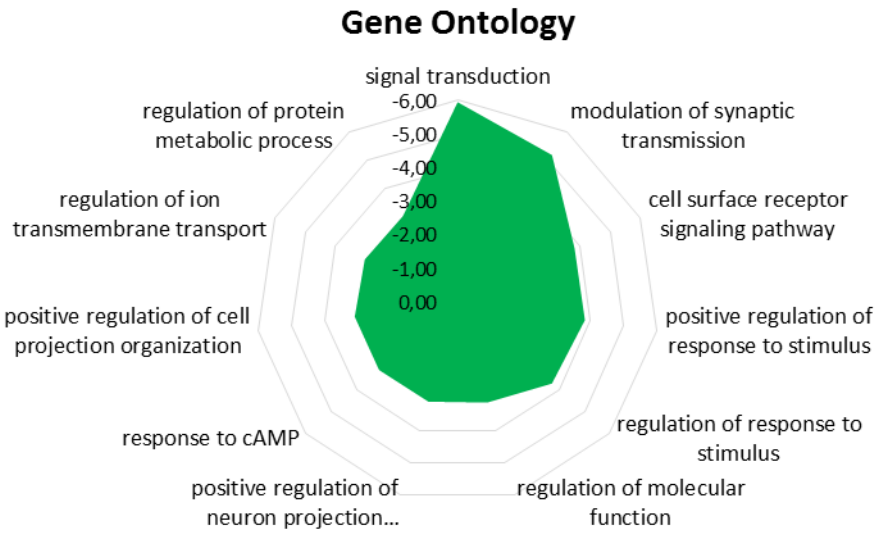

Figure 16. *Gene Ontology analysis. Radar graph representing the most enriched biological pathways associated to miRNA-related target genes. On the y-bar log_{10} p-value is represented.*

In order to validate this computational approach, mRNA and/or protein levels of capital elements involved in this cascade have been evaluated. PTEN is a known tumor-suppressor in thyroid cancer that modulates the cell cycle progression and cell survival drive associated to the activation of the PI3K-AKT signaling pathway (Charles et al., 2014). As shown in Figure 17, Panel A, *PTEN* mRNA levels displayed a 2 to 5-fold up-regulation in both ATC cell lines after 48 and 72h JQ1 treatment.

STAT3 is a member of the signal transducer and activator of transcription (STAT) family of proteins that are phosphorylated in response to diverse stimuli by the receptor-associated kinases, forming homo- or heterodimers that translocate to the cell nucleus where they act as transcription activators. Once activated, STAT3 induces the expression of *SKP2* (S-phase kinase-associated protein 2), a member of the F-box protein family that mediates the ubiquitination of p21 (*CDKN1A*) and p27 (*CDKN1B*) (Lee et al., 2014). BETi-treated 8505c cells displayed a strong decrease in phospho-STAT3 (p-STAT3) protein levels when compared to vehicle-treated cells. SW1736, instead, did not show any detectable variations in p-STAT3 protein levels after treatment. This is possibly due to the scarce basal p-STAT3 level, which made it challenging to detect any variation, or, most probably, to a different site of

phosphorilation in SW1736, not detectable with the antibody adapted (Fig. 17, Panel B-C). Then, the variation in *SKP2* mRNA levels has been evaluated. After both 48h and 72h JQ1 treatments, ATC cells displayed a significant decrease in *SKP2* mRNA levels (Fig. 17, Panel A), suggesting the possible STAT3-dependent cascade alteration. The JQ1 dependent up-regulation of the ultimate targets of this signal cascade were sequently evaluated. Both SW1736 and 8505c showed a striking increase in both p21 and p27 protein levels (Fig.17, Panel B-C), trend that is supported by a post-transcriptional regulation of these proteins by SPK2, as previously reported by Lee et al., 2014. Moreover, p21 mRNA levels were significantly increased after BET inhibition, suggesting a second signaling cascade involved in the regulation of its gene expression (Fig. 17, Panel A).

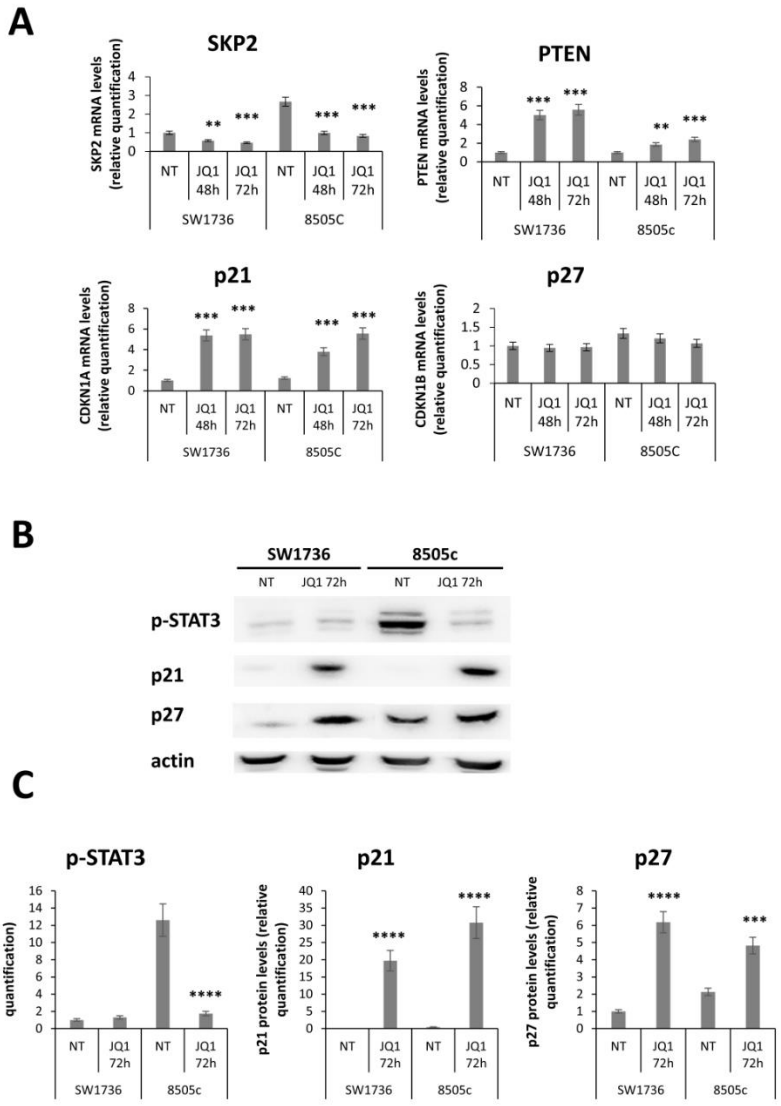

Figure 17. *ATC-shared miRNAs, up-regulated after BET inhibition, regulates signal transduction pathway members. SW1736 and 8505c were treated with 5μM JQ1 or vehicle for 48h and 72h. Cells were collected and SKP2, PTEN, CDKN1A and CDKN1B mRNA levels were evaluated (A). All samples were run in triplicate. Vehicle-treated (NT) SW1736 cells were arbitrarily set at 1.0 and mRNA levels are expressed as relative expression values. Results are shown as mean ± SD. *** p < 0.001, **** p < 0.0001 by ANOVA test. Data are representative of 3 independent experiments. SW1736 and 8505c were treated with 5μM JQ1 or vehicle for 72h. Cells were collected and p-STAT3, p21 and p27 protein levels were evaluated (B). Densitometric analysis of p-STAT3, p21 and p27 protein levels in ATC cells after 5μM JQ1 or vehicle treatment (D). Vehicle-treated (NT) SW1736 cells were arbitrarily set at 1.0 and protein levels were expressed as relative expression value. Results are shown as mean ± SD. *** p < 0.001, **** p < 0.0001 by ANOVA test.*

Differentially expressed miRNAs between ATC and normal thyroid tissue

Finally, to identify chief miRNAs differentially expressed between ATC cells and normal ones, SW1736, 8505c and NThy ori 3.1 RNAs were run on the Nanostring platform. Considering the 812 miRNAs analyzed, 65 and 96 miRNAs turned out to be deregulated in SW1736 and 8505c cells, respectively, when compared to thyroid epithelial cells. 35 miRNAs showed a common regulation in the two ATC cell lines (Fig. 18) and are enlisted in Table 4.

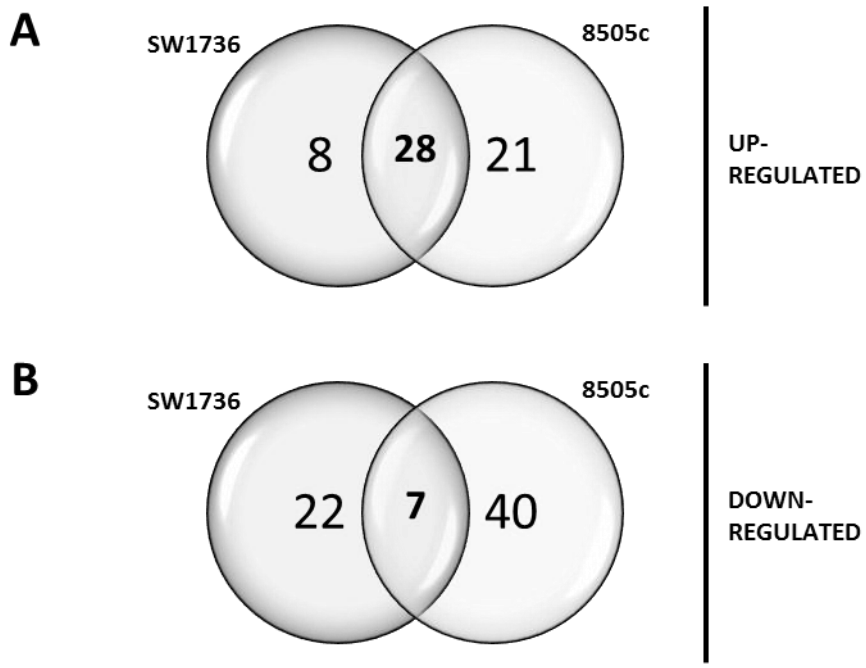

Figure 18. *miRNA alteration in ATC cells compared to normal ones. SW1736, 8505c and NThy ori 3.1 were subjected to Nanostring platform miRNAs evaluation. 36 and 49 miRNAs turned out to be up-regulated in SW1736 and 8505c, respectively, compared to NThy ori 3.1. 28 miRNAs shared a common up-regulation in both cell lines (A). 29 and 47 miRNAs turned out to be down-regulated in SW1736 and 8505c, respectively, compared to NThy ori 3.1. 7 miRNAs shared a common down-regulation in both cell lines (B).*

Table 4. Altered miRNAs in ATC cell lines.

miRNAs COMMONLY DEREGULATED IN ATC CELLS	
UP-REGULATED	**DOWN-REGULATED**
hsa-miR-1	hsa-miR-1234
hsa-miR-100-5p	hsa-miR-1268a
hsa-miR-1226-3p	hsa-miR-127-3p
hsa-miR-1257	hsa-miR-193b-3p
hsa-miR-125b-5p	hsa-miR-34a-5p
hsa-miR-139-3p	hsa-miR-4488
hsa-miR-146a-5p	hsa-miR-4516
hsa-miR-183-5p	
hsa-miR-221-3p	
hsa-miR-29b-3p	
hsa-miR-302f	
hsa-miR-31-5p	
hsa-miR-335-5p	
hsa-miR-337-3p	
hsa-miR-337-5p	
hsa-miR-33a-5p	
hsa-miR-412	
hsa-miR-4286	
hsa-miR-450a-5p	
hsa-miR-502-5p	
hsa-miR-504	
hsa-miR-512-3p	

hsa-miR-512-5p	
hsa-miR-548a-5p	
hsa-miR-548am-3p	
hsa-miR-548d-3p	
hsa-miR-7-5p	
hsa-miR-936	

Several miRNAs highlighted in this analysis have been already described as up-regulated in thyroid cancer; among them miR-221/222 have undoubtedly been correlated to thyroid cancer aggressiveness (Kentwell et al., 2014; Fuziwara and Kimura, 2014).

Crosschecking Table 3 and Table 4, a very peculiar behavior could be highlighted. hsa-miR-4516, hsa-miR-1234 and hsa-miR-4488 were down-regulated in ATC cells when compared to NThy ori 3.1 and turned out to be up-regulated in ATC after BET inhibition (both 48 and 72 h JQ1 treatments).

Discussion

Nowadays, the cross talk between genomic and epigenomic elements in driving insurgence and progression of both hematologic malignancies and solid tumors have been extensively emphasized (Martín-Subero et al. 2013). Among different epigenetic anticancer drugs, those targeting BET proteins have gained researchers' attention as promising therapeutics in a remarkable range of diseases (Shi and Vakoc 2014; Wee et al. 2014). ATC is the thyroid cancer sub-type burdened by the worse outcome. It possesses different and poor clinical and pathological features compared to other sub-types of thyroid cancer. A standard therapy is still missing and radioiodine fails to hinder the poor prognosis and high rate of metastases associated to it. ATC cell lines were used as a model of highly aggressive carcinoma to test the antineoplastic activity of BET inhibition, focusing on the mechanisms pursuing this outcome. As expected, human ATC cell lines FRO, SW1736 and 8505c, treated with three different BET inhibitors, displayed a decrease in cell viability associated to an increase in cell death phenomena. In this experimental model, BET inhibition activated a multi-target cascade resulting in considerable biological effects, as demonstrated by both mRNA and miRNA sequencing data. The identification of genes mediating BET inhibitors anti-proliferative effect could provide innovative therapeutic targets. The majority of JQ1-related deregulated genes belong to cell cycle regulators and apoptosis, i.e. E2Fs, CDKs and CDK inhibitors, and other TP53 pathway-related elements (Møller 2003; Smallridge et al. 2009). These data are similar to those previously published in medulloblastoma and metastatic melanoma (Segura et al. 2013; Henssen et al. 2013). All these findings corroborate the hypothesis that BET inhibitors unsettled cell cycle control, driving G0/G1 arrest and inducing cell death, acting on multiple targets.

BET inhibition induced a basal 10-fold down-regulation of MCM5 expression, suggesting its essential role in mediating BET inhibitors' effects. As further proof, *MCM5* proved to be a direct target of BRD4, as highlighted in the ChIP-qPCR assay, and its overexpression moderately attenuated ATC drug sensitivity, in terms of cell

viability, as shown in the rescue experiment (Fig. 11, Panel E). This slight effect was reasonably due to the multi-target activity of epigenetic drugs in general, which acted simultaneously on a wide range of targets, demonstrated by sequencing data. Consequently, poor rescue effects have been obtained for other targets of BET inhibitors (Lockwood et al., 2012; Bandopadhayay et al., 2014). MCM5 belongs to the minichromosome maintenance complex, which includes elements essential for DNA replication. MCM proteins are considered licensing components for the S-phase initiation. MCMs oscillated between nuclear and cytoplasmic localizations. Nuclear MCMs associate with DNA during G1 and early S-phase, allowing the control of replication origin firing, in order to restrict the chromosome replication to only one round per cell cycle. MCMs are restricted, instead, to cytoplasm during G2/M phase in order to prevent re-replication phenomena (Laskey 2005). Lately, components of MCM family have been described as aberrantly expressed in many malignancies, including thyroid carcinomas (Giaginis et al. 2010). In agreement with these findings and corroborating the *in vitro* and *in vivo* results, ATCs displayed a higher MCM5-staining when compared to the normal thyroid gland (Fig.12). Several studies have linked MCM5 expression to different pathways (Guida et al. 2005; Abe et al. 2012; Noseda and Karsan 2006; Laskey 2005) and Figure 19 attempted to summarize the major players controlling *MCM5* gene expression, considering their functional interactions. By comparing Figure 19 and Table 2, it is undisputable that many proteins regulating MCM5 expression are also altered by BET inhibition. JQ1, down-regulating the expression of MCM5 and other key elements involved in the replication fork assembly, was able to impair cell cycle mechanisms leading to, first, G0/G1 arrest (see Fig.3) and ultimately cell death (see Fig. 2).

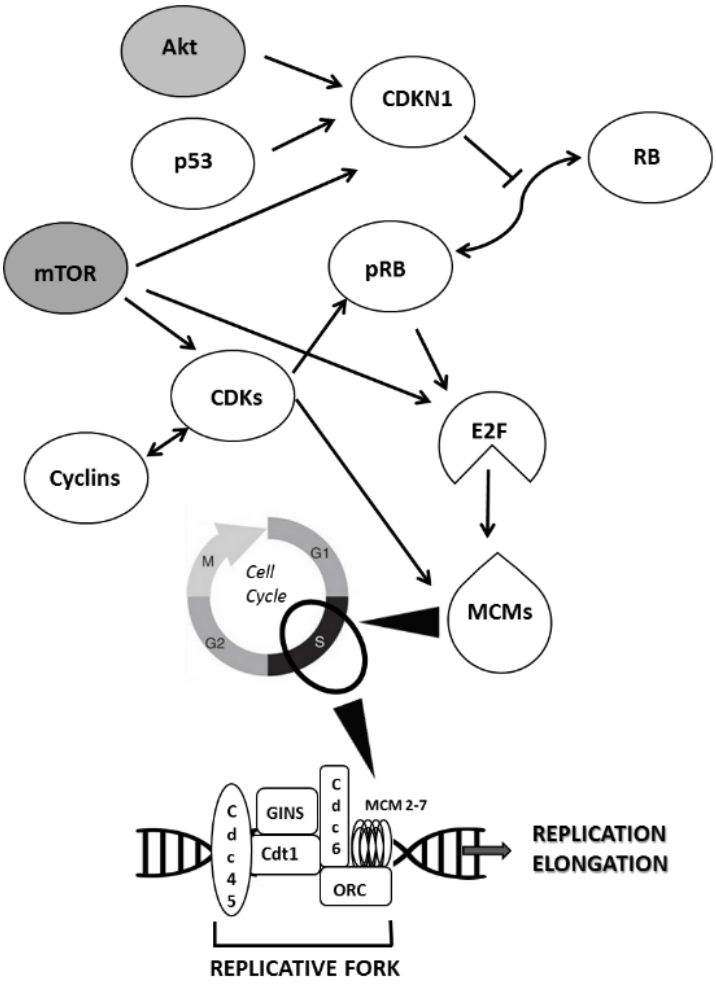

Figure 19. *Biological network related to MCMs protein function. Network diagram (upper part) showing key molecules controlling MCMs protein levels. White symbols represent proteins whose mRNA levels are modulated by BET inhibitors in our transcriptome analysis; gray symbols indicate proteins whose mRNA are not included in the RNA-seq. Arrows indicate functional relationship between proteins (delineated in Guida et al. 2005; Abe et al. 2012; Laskey 2005). The lower part indicates factors cooperating with MCM proteins in the replicative fork assembly. Arrowheads show the relationship between MCMs and cell cycle phases.*

IL7 is a cytokine that is considered crucial for the normal development and the maintenance of the immune system. Its binding with IL7R stimulates hematopoietic stem cell differentiation, homeostasis of lymphoid cells, etc (Kim et al., 2013). In contrast with the constitutive transcription of *IL7*, IL7R expression is strictly balanced in response to differentiation stimuli. IL7R was shown to be misregulated in leukaemic cell lines, both at mRNA and protein levels, after BET inhibition (Ott et al.

2012). In anaplastic thyroid cell lines a 24h JQ1 treatment exhibited a significant down-regulation decrease in *IL7R* mRNA levels that is not matched to a consistent protein level reduction (Fig. 13). These data are consistent with the ones published by Cosenza et al.: if *IL7R* mRNA levels could be detected in central nervous system, lung, renal, colorectal and breast cancers, though a discordance with protein expression has been reported (Cosenza et al., 2002). This could suggest that *IL7R* mRNA is unstable and not able to lead to a consistent protein product.

After focusing on global gene expression, the non-coding RNAs were taken into consideration. Recently, the investigation of BET inhibitors-derived miRNA regulation has gained the attention of a good slice of the scientific audience. Hitherto, only focused studies are available (Xu et al., 2016) and a quest on global BET inhibitors-induced miRNA modulation has not been pursued yet. In thyroid cancer, miRNAs deregulation have been reported to contribute to tumor progression. ATC cells treated with 5µM JQ1 showed a marked miRNA deregulation at both 48 and 72h exposure, with a pool of 7 miRNAs substantially up-regulated after sustained BET inhibition in ATC cells. Some of these miRNAs have already been associated to inhibition of proliferation and apoptosis, moreover, they have been correlated with survival in different solid tumor models (Xu et al., 2014; Liu et al., 2014).

Exploiting the emerging bioinformatics tools available online, some putative miRNA-related targets have been identified. The chief associated pathway have been explored, i.e. the signal transduction cascade, and two associated key players, STAT3 and PTEN, have been investigated. PTEN is a known tumor suppressor whose expression prove to be altered in thyroid cancer (Jolly et al., 2016). The primary function of PTEN is the negative regulation of the PI3K pathway, which has been linked to cell proliferation and survival. As expected, ATC cells treated with 5µM JQ1 displayed a 2-5 fold increase in *PTEN* mRNA levels, confirming a possible miRNA-dependent regulation. STAT3 is a transcription factor that is phosphorylated upon activation; it transfers into the nucleus and activates target genes. This protein plays an important role in cellular transformation and tumorigenesis and is constitutively

activated in about 70% of solid and hematological cancers. Increased expression and activation of STAT3 have been described in thyroid cancer tissues and inhibition of STAT3 signaling pathway has been considered a promising therapeutic approach to treat human cancers that harbor aberrantly active STAT3 (Sosonkina et al., 2014). Several miRNAs included in this analysis turned out to be associated to STAT3 signaling pathways, miR-1234 and mir-4516 being the most characterized. STAT3 positively regulates *SPK2* gene expression, which is an ubiquitin ligase that induced the degradation of the CDK inhibitors $p21^{Cip1}$, $p27^{Kip1}$, p57 (*CDKN1C*), and forkhead box O1 (FoxO1). SKP2 is known to be overexpressed in ATC (Chiappetta et al., 2007). BET inhibition displayed a decrease in *SKP2* expression correlated to an increase in p21 and p27 protein levels, in both ATC cell lines. It must be pointed out that SPK2-dependent p21 regulation acts at post-translational level. Nevertheless, a p21 gene expression regulation was disclosed, possibly due to other miRNAs-related activities. In fact, some of the miRNAs up-regulated by JQ1 treatment are known to regulate p21 transcript levels, i.e. miR-34c, miR-302, miR-218. Moreover, miR-4516 and miR-4488 are predicted to bind CDKN1A mRNA by the algorithm employed by miRBD, an online database for miRNA target prediction and functional annotations (http://mirdb.org/miRDB/). STAT3 phosphorylation was subjected to a strong decrease in 8505c, while was undetectable in SW1736. The lack in misregulation in phospho-STAT3 in SW1736 after BET inhibition was probably due to a different site of phosphorylation not detectable with the antibody used for this analysis. Indubitably, further investigations are required to better elucidate JQ1-dependent miRNAs regulation on these pathways, analyzing a wider spectrum of targets and taking advantage of the newly designed antago-miRs and miR-mimic.

An interesting event could be disclosed comparing JQ1-regulated and ATC-linked miRNAs: three miRNAs (hsa-miR-4516, hsa-miR-1234, hsa-miR-4488) proved to be down-regulated in both ATC cell lines when compared to NThy ori 3.1 and, then, turned out to be up-regulated by JQ1 treatment, in both time points (48 and 72h

exposure). These data could support the possible antineoplastic activity of BET inhibition in thyroid cancer cells.

Taken together, all these data pointed to a robust multi-target JQ1 activity in ATC cell lines. As BRD4 displays a relevant role in RNApol II dependent transcription, an intriguing future perspective could rely in profiling cancer-related BRD4-dependent enhancement in order to discover new potential molecular markers able to discriminate thyroid cancer subtypes with a different grade of aggressiveness, highlighting a new set of potential therapeutic targets in the management of thyroid cancers.

Acknowledgements

I thank Slobodanka Radovic, Manager Biological Applications of NGS at the Istituto di Genomica Applicata (UD), for the RNA-seq data analysis, Emanuele Cettul and Luciana Gualdi from Pharmadiagen Srl Genetics Lab (PN) for the miRNA-seq data analysis, Barbara Toffoletto for all the FACS analysis.

I thank Prof. Carla Di Loreto for the opportunity she gave me. I am grateful to Prof. Giuseppe Damante for all his invaluable support during my PhD.

I thank all the Genetics Lab for being my family for three years.

Abbreviations

Ago: Argonauta

AKT: v-Akt murine thymoma viral oncogene homolog

ALL: acute lymphoblastic leukaemia

AML: acute myeloid leukaemia

AnV: annexin V

ARID1A: AT-rich interactive domain-containing protein 1A

Asn: asparagine

ATC: anaplastic thyroid cancer

ATP: adenosine triphosphate

ATRX: α-thalassemia X-linked mental retardation

BET: bromodomain and extra-terminal protein

BETi: BET inhibitors

BRAF: B-raf proto-oncogene, serine/threonine kinase

BRD: bromodomain

CDK: cyclin-dependent kinase

CDKN1A: cyclin dependent kinase inhibitor 1A or p21

CDKN1B: cyclin dependent kinase inhibitor 1B or p27

CDKN1C: cyclin dependent kinase inhibitor 1C or p57

CDKN2A: cyclin dependent kinase inhibitor 2A or p16

CHD4: NuRD nucleosome remodeling complex

Chromo: chromodomain

circRNA: circular RNA

COFS: cerebro-oculo-facio-skeletal syndrome

CREBBP: CREB binding protein

CTD: C-terminal domain

DAPK1: death-associated protein kinase 1

DBP: DNA binding protein

DNMT: DNA methyltransferase

DNMTi: DNA methyltransferase inhibitor

DTC: differentiated thyroid cancer

E2F: E2 transcription factor

EBRT: external beam radiation therapy

EC50: half maximal effective concentration

EP300: E1A binding protein p300

EZH2: Enhancer of Zeste homolog 2

FA: follicular adenoma

FDA: food and drug administration

FGFR: fibroblast growth factor receptor

FNA: fine-needle aspiration

FOXO1:forkhead box O1

FTC: follicular thyroid cancer

FVPTC: follicular variant of papillary thyroid cancer

GLTSCR1: glioma tumor suppressor candidate region gene 1

GO: gene ontology

GSTP1: glutathione S-transferase P

H3F3A: histone variant H3.3

HAT: histone acetyltransferase

HATi: histone acetyltransferase inhibitor
HBD: histone-binding domain
HDAC: histone deacetylase
HDACi: histone deacetylase inhibitor
HMT: histone methyltransferase
HMTi: histone methyltransferase inhibitor
I^-: iodide ion
I_2: iodine
IDH1: isocitrate dehydrogenase 1
IL7R: interleukin 7 receptor
JMJD6: histone arginine demethylase
Kac: acetyl-lysine
KD: Dissociation constant
KDM: histone lysine demethylase
KMT2A: lysine methyltransferase 2A
lncRNA: long non coding RNA
LPS: lipopolysaccharide
MAGEA4melanoma-associated antigen 4
MAPK: mitogen-activated protein kinases
MBT: malignant brain tumor
MCM5: minichromosome manteinance complex 5
MEN: multiple endocrine neoplasia
MGMT: O^6-methylguanine DNA methyltransferase
miR: microRNA
miRNA: microRNA
MTC: medullary thyroid carcinoma
MYC: v-myc avian myelocitomatosis viral oncogene
NAMA: non-protein coding RNA associated with MAP Kinase pathway and growth arrest
NCR: negative control intergenic region
ncRNA: non coding RNA
NGS: next-generation sequencing
NMC: MUT midline carcinoma
NSD3: SET domain-containing histone methyltransferase
NT: normal thyroid gland
NUT: nuclear protein in testis
PARP: poly (ADP-ribose) polymerase
PARPi: poly (ADP-ribose) polymerase inhibitor
PAX8: paired-box gene 8
PCR2: Polycomb Repressive Complex 2
PDGFR: platelet-derived growth factor receptor
PDTC: poorly differentiated thyroid cancer
PDTC: poorly differentiated thyroid carcinoma
PI: propidium iodide
PI3K: phosphoinositide 3-kinase
PIK3CA: phosphatidylinositol-4,5-bisphosphate 3-kinase
piRNA: piwi-interacting RNA
p-STAT: phospho-signal transducer and activator of transcription
PTC: papillary thyroid cancer
PTCSC3AA: PTC susceptibility candidate 3
P-TEFb: positive transcription elongation factor complex

PTEN: phosphatase and tensin homolog

PTH: parathyroid hormone

PTM: post translational modification

RAI: adjuvant radioactive iodine ^{131}-I

RAS: v-ras oncogene homologue

RDM: histone arginine demethylase

RET: rearranged during transfection

RISC: RNA-induced silencing complex

RNApol II: RNA polymerase II

RNA-seq: RNA sequencing

RNP: ribonuclear protein

rRNA: ribosomal RNA

SAHA: suberoylanide hyroxamic acid

SE: super enhancer

siRNA: small interfering RNA

SKP2: S-phase kinase-associated protein 2

SLC5A8: solute carrier family 5 member 8

snoRNAs: small nucleolar RNAs

snRNA: small nuclear RNA

STAT: signal transducer and activator of transcription

STR: single tandem repeats

T0: baseline time point

T3: triiodothyronine

T4: thyroxine

TCGA: the cancer genome atlas

TE: transposable element

TERT: telomerase reverse transcriptase

TG: thyroglobulin

TIMP3: tissue inhibitor of metalloproteinases 3

TK: tyrosine kinase

TKi: tyrosine kinase inhibitor

TKR: tyrosine kinase receptor

TRH: thyrotropin-releasing hormone

TSH: thyroid-stimulating hormone

UC: undifferentiated carcinoma

UCHL1: ubiquitin carboxy-terminal hydrolase L1

VEGFR: vascular endothelial growth factor receptor

Publications

- Mio C, Lavarone E, Conzatti K, Baldan F, Toffoletto B, Puppin C, Filetti S, Durante C, Russo D, Orlacchio A, Di Cristofano A, Di Loreto C, Damante G. 2016 **MCM5 as a target of BET inhibitors in thyroid cancer cells**. Endocr Relat Cancer. Endocr Relat Cancer; 23(4):335-47. doi: 10.1530/ERC-15-0322.
- Celano M, Mio C, Sponziello M, Verrienti A, Bullotta S, Durante C, Damante G, Russo D. 2017 **Targeting post-translational histone modifications for the treatment of non-medullary thyroid cancer**. Mol Cell Endocrinol; submitted
- Allegri L, Baldan F, Mio C, Puppin C, Russo D, Kryštof V, Damante G. 2016 **Effects of BP-14, a novel cyclin-dependent kinase inhibitor, on anaplastic thyroid cancer cells**. Oncol Rep; 35(4):2413-8. doi: 10.3892/or.2016.4614.
- Baldan F, Mio C, Allegri L, Conzatti K, Toffoletto B, Puppin C, Radovic S, Vascotto C, Russo D, Di Loreto C, Damante G. 2016 **Identification of functional and interaction targets of the RNA-binding protein HuR in thyroid cell lines**. Oncotarget; 7(39):63388-63407. doi: 10.18632/oncotarget.11255.
- Rosignolo F, Sponziello M, Durante C, Puppin C, Mio C, Baldan F, Di Loreto C, Russo D, Filetti S, Damante G. 2016 **Expression of PAX8 target genes in papillary thyroid carcinoma**. PLoS One; 11(6):e0156658. doi: 10.1371/journal.pone.0156658.
- Baldan F, Mio C, Lavarone E, Di Loreto C, Puglisi F, Damante G, Puppin C. 2015 **Epigenetic bivalent marking is permissive to the synergy of HDAC and PARP inhibitors on TXNIP expression in breast cancer cells**. Oncol Rep; 33(5):2199-206. doi: 10.3892/or.2015.3873.
- Baldan F, Mio C, Allegri L, Puppin C, Russo D, Filetti S, Damante G. 2015 **Synergy between HDAC and PARP Inhibitors on Proliferation of a Human Anaplastic Thyroid Cancer-Derived Cell Line**. Int J Endocrinol; 2015: 978371. doi: 10.1155/2015/978371.

Posters

- **ESHG 2015**: Alessandra Franzoni, Elitza Markova-Car, Sanja Dević-Pavlić, Davor Jurišić, Cinzia Puppin, Catia Mio, Marila De Luca, Giulia Petruz, Sandra Kraljević Pavelić , Giuseppe Damante, **'A polymorphic ggc repeat in the npas2 gene and its association with melanoma**'.
- **SIBBM 2015**: Catia Mio, Elisa Lavarone, Federica Baldan, Barbara Toffoletto, Cinzia Puppin, Sebastiano Filetti, Cosimo Durante, Diego Russo, Carla Di Loreto, Giuseppe Damante, **'MCM5 as a target of BET inhibitors in thyroid cancer cells'.**

References

- Abe S, Kurata M, Suzuki S et al. (2012) Minichromosome Maintenance 2 Bound with Retroviral Gp70 Is Localized to Cytoplasm and Enhances DNA-Damage-Induced Apoptosis. PLoS One. 7: 40129.
- Alderton GK. (2011) Targeting MYC? You BET. Nat Rev Drug Discov. 10: 732-3.
- Antico Arciuch VG, Russo MA, Dima M et al. (2011) Thyrocyte-specific inactivation of p53 and Pten results in anaplastic thyroid carcinomas faithfully recapitulating human tumors. Oncotarget. 2: 1109–1126.
- Arturi F, Russo D, Giuffrida D, et al. (2000) Sodium-iodide symporter (NIS) gene expression in lymph-node metastases of papillary thyroid carcinomas. Eur. J. Endocrinol. 143(5):623-7.
- Baldan F, Mio C, Allegri L, et al. (2015) Synergy between HDAC and PARP Inhibitors on Proliferation of a Human Anaplastic Thyroid Cancer-Derived Cell Line. Int. J. Endocrinol. 2015:978371. doi: 10.1155/2015/978371.
- Baldan F, Mio C, Lavarone E, et al. (2015) Epigenetic bivalent marking is permissive to the synergy of HDAC and PARP inhibitors on TXNIP expression in breast cancer cells. Oncol. Rep. 33(5):2199-206. doi: 10.3892/or.2015.3873.
- Bamborough P, Chung CW. (2015) Fragments in bromodomain drug discovery. Med. Chem. Commun, 6: 1587-1604. doi: 10.1039/C5MD00209E.
- Bandopadhayay P, Bergthold G, Nguyen B, et al. (2014) BET bromodomain inhibition of MYC-amplified medulloblastoma. Clin Cancer Res. 20: 912-25.
- Bartholomew B. (2014) Regulating the Chromatin Landscape: Structural and Mechanistic Perspectives. Annu. Rev. Biochem. 83: 671–696. doi: 10.1146/annurev-biochem-051810-093157.
- Baselga J, Cortes J, Kim SB, et al. (2012) Pertuzumab plus trastuzumab plus docetaxel for metastatic breast cancer. N. Engl. J. Med. 366(2):109–119.
- Baumann C, Schmidtmann A, Muegge K, et al. (2008) Association of ATRX with pericentric heterochromatin and the Y chromosome of neonatal mouse spermatogonia. BMC Mol. Biol. 9:29.
- Begum S, Rosenbaum E, Henrique R, et al. (2004) BRAF mutations in anaplastic thyroid carcinoma: implications for tumor origin, diagnosis and treatment. Mod. Pathol. 17(11):1359-63.
- Belkina AC, Denis GV. (2012) BET domain co-regulators in obesity, inflammation and cancer. Nat. Rev. Cancer. 12(7): 465–477. doi: 10.1038/nrc3256.
- Belkina AC, Nikolajczyk BS, Denis GV. (2013) BET protein function is required for inflammation: Brd2 genetic disruption and BET inhibitor JQ1 impair mouse macrophage inflammatory responses. J. Immunol. 190: 3670–3678.
- Bellantone R, Lombardi CP, Bossola M, et al. (2002) Total thyroidectomy for management of benign thyroid disease: review of 526 cases. World Journal of Surgery. 26(12):1468–1471. doi: 10.1007/s00268-002-6426-1.
- Bernstein BE, Meissner A, Lander ES. (2007) The mammalian epigenome. Cell. 128: 669-681. doi: 10.1016/j.cell.2007.01.033.

- Blanke CD, Rankin C, Demetri GD, et al. (2008) Phase III randomized, intergroup trial assessing imatinib mesylate at two dose levels in patients with unresectable or metastatic gastrointestinal stromal tumors expressing the kit receptor tyrosine kinase: S0033. J. Clin. Oncol. 26(4):626–632.
- Brand M, Measures AM, Wilson BG, et al. (2015) Small molecule inhibitors of bromodomain-acetyl-lysine interactions. ACS Chem. Biol. 10: 22–39.
- Brown RL, de Souza JA, Cohen EE. (2011) Thyroid cancer: burden of illness and management of disease. J Cancer. 2:193-9.
- Cancer Genome Atlas Research Network (2014) Integrated genomic characterization of papillary thyroid carcinoma. Cell. 159(3):676–690
- Catalano MG, Fortunati N, Boccuzzi G. (2012) Epigenetics modifications and therapeutic prospects in human thyroid cancer. Front Endocrinol. (Lausanne). 3:40.
- Chaidos A, Caputo V, Karadimitris A. (2015) Inhibition of bromodomain and extra-terminal proteins (BET) as a potential therapeutic approach in haematological malignancies: emerging preclinical and clinical evidence. Ther. Adv. Hematol. 6(3): 128–141. doi: 10.1177/2040620715576662.
- Chaitanya GV, Steven AJ, Babu PP. (2010) PARP-1 cleavage fragments: signatures of cell-death proteases in neurodegeneration. Cell Commun Signal. 22: 8-31.
- Champa D, Di Cristofano A. (2015) Modeling anaplastic thyroid carcinoma in the mouse. Horm. Cancer. 6(1):37-44. doi: 10.1007/s12672-014-0208-8.
- Charles RP, Silva J, Iezza G et al. (2014) Activating BRAF and PIK3CA mutations cooperate to promote anaplastic thyroid carcinogenesis. Mol Cancer Res. 12:979-86.
- Chiappetta G, De Marco C, Quintiero A et al. (2007) Overexpression of the S-phase kinase-associated protein 2 in thyroid cancer. Endocr Relat Cancer. 14:405-20.
- Citterio E, Van Den Boom V, Schnitzler G, et al. (2000) ATP-dependent chromatin remodeling by the Cockayne syndrome B DNA repair-transcription-coupling factor. Mol. Cell. Biol. 20:7643–53.
- Clapier CR, Cairns BR. (2009) The biology of chromatin remodeling complexes. Annu. Rev. Biochem. 78:273-304. doi:10.1146/annurev.biochem.77.062706.153223.
- Cosenza L, Gorgun G, Urbano A et al. (2002) Interleukin-7 receptor expression and activation in nonhaematopoietic neoplastic cell lines. Cell Signal. 14 :317-25.
- Cosgrove MS, Boeke JD, Wolberger C. (2004) Regulated nucleosome mobility and the histone code. Nat Struct Mol Biol. 11(11):1037-43.
- Costa R, Carneiro BA, Chandra S, et al. (2016) Spotlight on lenvatinib in the treatment of thyroid cancer: patient selection and perspectives. Drug Des. Devel. Ther. 10: 873-84. doi: 10.2147/DDDT.S93459.
- Da Costa D, Agathanggelou A, Perry T, et al. (2013) BET inhibition as a single or combined therapeutic approach in primary paediatric B-precursor acute lymphoblastic leukaemia. Blood Cancer J. 3:e126.
- Dawson M, Prinjha RK, Dittmann A, et al. (2011) Inhibition of BET recruitment to chromatin as an effective treatment for MLL-fusion leukaemia. Nature. 478: 529–533.
- Dawson MA, Kouzarides T, Huntly BJ. (2012) Targeting epigenetic readers in cancer. N. Engl. J. Med. 367:647–657.

- Day JJ, Sweatt JD. (2010) DNA methylation and memory formation. Nat Neurosci. 13(11):1319-23. doi: 10.1038/nn.2666.
- Della Ragione F, Gagliardi M, D'Esposito M, et al. (2014) Non-coding RNAs in chromatin disease involving neurological defects. Front. Cel.l Neurosci. 8:54. doi: 10.3389/fncel.2014.00054.
- Denis GV, McComb ME, Faller DV, et al. (2006) Identification of transcription complexes that contain the double bromodomain protein Brd2 and chromatin remodeling machines. J Proteome Res. 5:502–511.
- Devaiah BN, Singer DS. (2012) Two faces of BRD4. Mitotic bookmark and transcriptional lynchpin. Transcription. 4(1): 13–17. doi: 10.4161/trns.22542.
- DeWoskin VA, Million RP. (2013) The epigenetics pipeline. Nat. Rev. Drug Discov. 12: 661–662.
- Dhalluin C, Carlson JE, Zeng L, et al. (1999) Structure and ligand of a histone acetyltransferase bromodomain. Nature. 399(6735):491–6.
- Diederichs S, Bartsch L, Berkmann JC, et al. (2016) The dark matter of the cancer genome: aberrations in regulatory elements, untranslated regions, splice sites, non-coding RNA and synonymous mutations. EMBO Mol. Med. pii: e201506055. doi: 10.15252/emmm.201506055. [Epub ahead of print]
- Durante C, Haddy N, Baudin E, et al. (2006) Long-term outcome of 444 patients with distant metastases from papillary and follicular thyroid carcinoma: benefits and limits of radioiodine therapy. J. Clin. Endocrinol. Metab. 91(8):2892-9.
- Egger G, Liang G, Aparicio A, et al. (2004) Epigenetics in human disease and prospects for epigenetic therapy. Nature. 429:457–463.
- Eilers M, Eisenman RN. (2008) Myc's broad reach. Genes Dev. 22: 2755-66. doi: 10.1101/gad.1712408.
- Elisei R, Viola D, Torregrossa L, et al. (2012) The BRAF(V600E) mutation is an independent, poor prognostic factor for the outcome of patients with low-risk intrathyroid papillary thyroid carcinoma: single-institution results from a large cohort study. J. Clin. Endocrinol. Metab. 97(12):4390-8. doi: 10.1210/jc.2012-1775.
- Elisei R. (2012) Anaplastic thyroid cancer therapy: dream or reality? Endocrine. 42(3):468-70. doi: 10.1007/s12020-012-9785-x.
- Esteller M, Garcia-Foncillas J, Andion E, et al. (2012) Inactivation of the DNA-repair gene MGMT and the clinical response of gliomas to alkylating agents. N. Engl. J. Med. 343:1350-1354.
- Fallahi P, Mazzi V, Vita R, et al. (2015) New therapies for dedifferentiated papillary thyroid cancer. Int. J. Mol. Sci. 16(3):6153-82. doi: 10.3390/ijms16036153.
- Ferrari SM, Fallahi P, Politti U, et al. (2015) Molecular Targeted Therapies of Aggressive Thyroid Cancer. Front Endocrinol. (Lausanne). 6:176. doi: 10.3389/fendo.2015.00176.
- Ferri E, Petosa C, McKenna CE. (2016) Bromodomains: Structure, function and pharmacology of inhibition. Biochem Pharmacol. 106:1-18. doi:10.1016/j.bcp.2015.12.005.
- Filippakopoulos P, Knapp S. (2012) The bromodomain interaction module. FEBS Lett. 586(17):2692-704. doi: 10.1016/j.febslet.2012.04.045.

- Filippakopoulos P, Knapp S. (2014) Targeting bromodomains: epigenetic readers of lysine acetylation. Nat. Rev. Drug Discov. 13(5):337-56. doi: 10.1038/nrd4286.
- Filippakopoulos P, Picaud S, Fedorov O, et al. (2012) Benzodiazepines and benzotriazepines as protein interaction inhibitors targeting bromodomains of the BET family. Bioorg. Med. Chem. 20(6):1878-86. doi: 10.1016/j.bmc.2011.10.080.
- Filippakopoulos P, Qi J, Picaud S, et al. (2010) Selective inhibition of BET bromodomains. Nature. 468(7327):1067-73. doi: 10.1038/nature09504.
- Florence B, Faller DV. (2001) You bet-cha: a novel family of transcriptional regulators. Front. Biosci. 6:D1008–D1018.
- Fu LL, Tian M, Li X, et al. (2015) Inhibition of BET bromodomains as a therapeutic strategy for cancer drug discovery. Oncotarget. 6(8):5501-16.
- Fuks F, Hurd PJ, Deplus R, et al. (2003) The DNA methyltransferases associate with hp1 and the suv39h1 histone methyltransferase. Nucleic Acids Res. 31:2305–2312.
- Fuziwara CS, Kimura ET. (2014) MicroRNA Deregulation in Anaplastic Thyroid Cancer Biology. Int. J. Endocrinol. 2014:743450. doi: 10.1155/2014/743450.
- Gaspar-Maia A, Alajem A, Meshorer E, et al. (2011) Open chromatin in pluripotency and reprogramming. Nat. Rev. Mol. Cell Biol. 12(1):36-47. doi: 10.1038/nrm3036.
- Giaginis C, Vgenopoulou S, Vielh P, et al. (2010) MCM proteins as diagnostic and prognostic tumor markers in the clinical setting. Histol Histopathol. 25: 351-70.
- Gillette TG, Hill JA. (2015) Readers, writers, and erasers: chromatin as the whiteboard of heart disease. Circ Res. 116(7):1245-53. doi:10.1161/CIRCRESAHA.116.303630.
- Girard A, Sachidanandam R, Hannon GJ, et al. (2006) A germline-specific class of small RNAs binds mammalian Piwi proteins. Nature. 442: 199–202.
- Gobeil S, Boucher CC, Nadeau D, et al. (2001) Characterization of the necrotic cleavage of poly(ADP-ribose) polymerase (PARP-1): implication of lysosomal proteases. Cell Death Differ. 8: 588-94.
- Grotenhuis BA, Wijnhoven BP, van Lanschot JJ. (2012) Cancer stem cells and their potential implications for the treatment of solid tumors. J Surg Oncol. 106: 209-15. doi: 10.1002/jso.23069.
- Guida T, Salvatore G, Faviana P et al. (2005) Mitogenic effects of the up-regulation of minichromosome maintenance proteins in anaplastic thyroid carcinoma. J Clin Endocrinol Metab. 90: 4703-9.
- Heerboth S, Lapinska K, Snyder N, et al. (2014) Use of epigenetic drugs in disease: an overview. Genet. Epigenet. 6:9-19. doi: 10.4137/GEG.S12270.
- Henssen A, Thor T, Odersky A et al. (2013) BET bromodomain protein inhibition is a therapeutic option for medulloblastoma. Oncotarget. 4: 2080-95.
- Hu W, Alvarez-Dominguez JR, Lodish HF. (2012) Regulation of mammalian cell differentiation by long non-coding RNAs. EMBO reports. 13: 971-983. doi:10.1038/embor.2012.145.
- Imielinski M, Berger AH, Hammerman PS, et al. (2012) Mapping the hallmarks of lung adenocarcinoma with massively parallel sequencing. Cell. 150:1107-1120
- James LI, Frye SV. (2013) Targeting Chromatin Readers. Clin Pharmacol Ther. 93(4): 312–314.

- Janzen WP, Wigle T, Jin J, et al. (2010) Epigenetics: Tools and Technologies. Drug Discov Today Technol. 7(1):e59-e65.
- Jolly LA, Novitskiy SV, Owens P et al. (2016) Fibroblast-mediated collagen remodeling within the tumor microenvironment facilitates progression of thyroid cancers driven by BrafV600E and Pten loss. Cancer Res. pii: canres.2351.2015.
- Jones PA, Archer TK, Baylin SB, et al. (2008) Moving AHEAD with an international human epigenome project. Nature. 454(7205):711-5. doi: 10.1038/454711a.
- Kahn SA, Reddy D, Gupta S. (2015) Global histone post-translational modifications and cancer: Biomarkers for diagnosis, prognosis and treatment? World J Biol Chem. 6(4): 333–345. doi: 10.4331/wjbc.v6.i4.333.
- Kanno T, Kanno Y, Siegel RM, et al. (2004) Selective recognition of acetylated histones by bromodomain proteins visualized in living cells. Mol. Cell. 13:33–43.
- Kebebew E, Peng M, Reiff E et al. 2006. Diagnostic and prognostic value of cell-cycle regulatory genes in malignant thyroid neoplasms. World J Surg. 30: 767-74.
- Kentwell J, Gundara JS, Sidhu SB. (2014) Noncoding RNAs in endocrine malignancy. Oncologist. 19 483–491. doi:10.1634/theoncologist.2013-0458.
- Kim MS, Chung NG, Kim MS et al. (2012) Somatic mutation of IL7R exon 6 in acute leukemias and solid cancers. Hum Pathol. 44: 551-5. doi: 10.1016/j.humpath.2012.06.017.
- Kim MY, Mauro S, Gervy N, et al. (2004) NAD+ dependent modulation of chromatin structure and transcription by nucleosome binding properties of PARP-1. Cell. 119: 803-814.
- Längst G, Manelyte L. (2015) Chromatin Remodelers: From Function to Dysfunction. Genes (Basel). 6(2):299-324. doi: 10.3390/genes6020299.
- Larkin J, Del Vecchio M, Ascierto PA, et al. (2014) Vemurafenib in patients with BRAF(V600) mutated metastatic melanoma: an open-label, multicentre, safety study. Lancet Oncol. 15(4):436–444.
- Laskey R. (2005) The Croonian Lecture 2001 hunting the antisocial cancer cell: MCM proteins and their exploitation. Philos Trans R Soc Lond B Biol Sci. 360: 1119-32.
- Latham JA, Dent SYR. (2007) Cross-regulation of histone modifications. Nat. Struct. Mol. Biol. 14: 1017 – 1024. doi:10.1038/nsmb1307.
- Lavarone E, Puppin C, Passon N, et al. (2013) The PARP inhibitor PJ34 modifies proliferation, NIS expression and epigenetic marks in thyroid cancer cell lines. Mol. Cell. Endocrinol. 365(1):1-10. doi: 10.1016/j.mce.2012.08.019.
- Lebastchi AH, Callender GG. (2014) Thyroid cancer. Curr. Probl. Cancer. 38(2):48-74. doi: 10.1016/j.currproblcancer.2014.04.001.
- Lee JJ, Lee JS, Cui MN et al. (2014) BIS targeting induces cellular senescence through the regulation of 14-3-3 zeta/STAT3/SKP2/p27 in glioblastoma cells. Cell Death Dis. 5:e1537
- Lee WH, Morton RA, Epstein JI, et al. (1994) Cytidine methylation of regulatory sequences near the pi-class glutathione S-transferase gene accompanies human prostatic carcinogenesis. Proc. Natl Acad. Sci. USA. 91:11733-11737.
- Ley TJ, Ding L, Walter MJ, et al. (2010) DNMT3A mutations in acute myeloid leukemia. N. Engl. J. Med. 363:2424-2433.

- Lin CY, Lovén J, Rahl PB, et al. (2012) Transcriptional amplification in tumor cells with elevated c-Myc. Cell. 56–67.
- Liu N, Cui RX, Sun Y et al. (2014) A four-miRNA signature identified from genome-wide serum miRNA profiling predicts survival in patients with nasopharyngeal carcinoma. Int J Cancer. 134:1359-68.
- Lockwood WW, Zejnullahu K, Bradner JE et al. (2012) Sensitivity of human lung adenocarcinoma cell lines to targeted inhibition of BET epigenetic signaling proteins. Proc Natl Acad Sci U S A. 109: 19408-13.
- Loven J, Hoke HA, Lin CY, et al. (2013) Selective inhibition of tumor oncogenes by disruption of super-enhancers. Cell 153: 320–334.
- Luong QT, O'Kelly J, Braunstein GD, et al. (2006) Antitumor activity of suberoylanilide hydroxamic acid against thyroid cancer cell lines in vitro and in vivo. Clin. Cancer Res. 12(18):5570-7.
- Martín-Subero JI, López-Otín, C, Campo E. (2013) Genetic and epigenetic basis of chronic lymphocytic leukemia. Curr Opin Hematol. 20: 362-8.
- McIver B, Hay ID, Giuffrida DF, et al. (2001) Anaplastic thyroid carcinoma: a 50-year experience at a single institution. Surgery, 130 (6) 1028–1034.
- Melo M, da Rocha AG, Vinagre J, et al. (2014) TERT promoter mutations are a major indicator of poor outcome in differentiated thyroid carcinomas. J. Clin. Endocrinol. Metab. 99(5):E754-65. doi: 10.1210/jc.2013-3734.
- Mio C, Lavarone E, Conzatti K, et al. (2016) MCM5 as a target of BET inhibitors in thyroid cancer cells. Endocr Relat Cancer. pii: ERC-15-0322.
- Mirguet O, Lamotte Y, Donche F, et al. (2012) From ApoA1 upregulation to BET family bromodomain inhibition: discovery of I-BET151. Bioorg. Med. Chem. Lett. 22: 2963–2967.
- Møller MB. (2003) Molecular control of the cell cycle in cancer: biological and clinical aspects. Dan Med Bull. 50: 118-38.
- Morceau F, Chateauvieux S, Gaigneaux A, et al. (2013) Long and Short Non-Coding RNAs as Regulators of Hematopoietic Differentiation. Int. J. Mol. Sci. 14(7): 14744-14770. doi:10.3390/ijms140714744.
- Muller S, Filippakopoulos P, Knapp S. (2011) Bromodomains as therapeutic targets. Expert Rev. Mol. Med. 13: e29. doi: 10.1017/S1462399411001992
- Musselman CA, Lalonde ME, Côté J, et al. (2012) Perceiving the epigenetic landscape through histone readers. Nat. Struct. Mol. Biol. 19(12): 1218–1227. doi: 10.1038/nsmb.2436.
- Nebbioso A, Carafa V, Benedetti R, et al. (2012) Trials with 'epigenetic' drugs: an update. Mol. Oncol. 6(6):657-82. doi: 10.1016/j.molonc.2012.09.004.
- Nicodeme E, Jeffrey KL, Schaefer U, et al. (2010) Suppression of inflammation by a synthetic histone mimic. Nature. 468(7327):1119-23. doi: 10.1038/nature09589.
- Noseda M, Karsan A. (2006) Notch and minichromosome maintenance (MCM) proteins: integration of two ancestral pathways in cell cycle control. Cell Cycle. 5: 2704-9.
- Ott CJ, Kopp N, Bird L et al. (2012) BET bromodomain inhibition targets both c-Myc and IL7R in high-risk acute lymphoblastic leukemia. Blood. 120: 2843-52.

- Padur AA, Kumar N, Guru A, et al. (2016) Safety and Effectiveness of Total Thyroidectomy and Its Comparison with Subtotal Thyroidectomy and Other Thyroid Surgeries: A Systematic Review. J. Thyroid Res. 2016:7594615. doi: 10.1155/2016/7594615.
- Peifer M, Fernandez-Cuesta L, Sos ML, et al. (2012) Integrative genome analyses identify key somatic driver mutations of small-cell lung cancer. Nat. Genet. 44:1104-1110.
- Poot RA, Bozhenok L, van den Berg DL, et al. (2004) The Williams syndrome transcription factor interacts with PCNA to target chromatin remodelling by ISWI to replication foci. *Nat. Cell Biol.* 6:1236–44.
- Portela A, Esteller M. (2010) Epigenetic modifications and human disease. Nat Biotechnol.28:1057–1068.
- Prokopi M, Kousparou CA, Epenetos AA. (2015) The Secret Role of microRNAs in Cancer Stem Cell Development and Potential Therapy: A Notch-Pathway Approach. Front Oncol. 4: 389. doi:10.3389/fonc.2014.00389.
- Rahman S, Sowa ME, Ottinger M, et al. (2011) The Brd4 extraterminal domain confers transcription activation independent of pTEFb by recruiting multiple proteins, including NSD3. Mol. Cell. Biol. 31(13):2641-52. doi: 10.1128/MCB.01341-10.
- Ricarte-Filho JC, Ryder M, Chitale DA, et al. (2009) Mutational profile of advanced primary and metastatic radioactive iodine-refractory thyroid cancers reveals distinct pathogenetic roles for BRAF, PIK3CA, and AKT1. Cancer Res. 69:4885–4893.
- Russo D, Damante G, Puxeddu E, et al. (2011) Epigenetics of thyroid cancer and novel therapeutic targets. J. Mol. Endocrinol. 46(3):R73-81. doi: 10.1530/JME-10-0150.
- Safavi A, Vijayasekaran A, Guerrero MA. (2012) New Insight into the Treatment of Advanced Differentiated Thyroid Cancer. J. Thyroid Res. 2012:437569. doi: 10.1155/2012/437569.
- Schiano C, Vietri MT, Grimaldi V, et al. (2015) Epigenetic-related therapeutic challenges in cardiovascular disease. Trends Pharmacol. Sci. 36(4):226-35. doi: 10.1016/j.tips.2015.02.005.
- Schwartzentruber J, Korshunov A, Liu XY, et al. (2012) Driver mutations in histone H3.3 and chromatin remodelling genes in paediatric glioblastoma. Nature 482:226-231.
- Scollo C, Baudin E, Travagli JP, et al. (2003) Rationale for central and bilateral lymph node dissection in sporadic and hereditary medullary thyroid cancer. J. Clin. Endocrinol. Metab. 88:2070-2075.
- Segura MF, Fontanals-Cirera B, Gaziel-Sovran A et al. (2013) BRD4 sustains melanoma proliferation and represents a new target for epigenetic therapy. Cancer Res. 73: 6264-76.
- Seo S, Grzenda A, Lomberk GA, et al. (2013) Epigenetics: A Promising Paradigm for Better Understanding and Managing Pain. J. Pain. 14(6): 549–557. doi: 10.1016/j.jpain.2013.01.772.
- Sherman SI. (2010) Targeted therapy of thyroid cancer. Biochem. Pharmacol. 80(5):592-601. doi: 10.1016/j.bcp.2010.05.003.

- Shi J, Vakoc CR. (2014) The mechanisms behind the therapeutic activity of BET bromodomain inhibition. Mol Cell. 54: 728-36.
- Simó-Riudalbas L, Esteller M. (2015) Targeting the histone orthography of cancer: drugs for writers, erasers and readers. Br. J. Pharmacol. 172(11):2716-32. doi: 10.1111/bph.12844.
- Smallridge RC, Marlow LA, Copland JA. (2009) Anaplastic thyroid cancer: molecular pathogenesis and emerging therapies. Endocr Relat Cancer. 16: 17-44.
- Smith N, Nucera C. (2015) Personalized therapy in patients with anaplastic thyroid cancer: targeting genetic and epigenetic alterations. J. Clin. Endocrinol. Metab. 100(1):35-42. doi: 10.1210/jc.2014-2803.
- Sobrinho-Simões M, Eloy C, Magalhães J, et al. (2011) Follicular thyroid carcinoma. Mod. Pathol. 24, S10-8. doi:10.1038/modpathol.2010.133.
- Song R, Hennig GW, Wu Q, et al. (2011) Male germ cells express abundant endogenous siRNAs. Proc. Natl. Acad. Sci. USA. 108: 13159–13164.
- Sosonkina N, Starenki D, Park JI. (2014) The Role of STAT3 in Thyroid Cancer. Cancers (Basel). 6: 526–544.
- Spindel ON, World C, Berk BC. (2012) Thioredoxin Interacting Protein: Redox Dependent and Independent Regulatory Mechanisms. Antioxid Redox Signal. 16: 587–596. doi: 10.1089/ars.2011.4137.
- Takamizawa J, Konishi H, Yanagisawa K, et al. (2004) Reduced expression of the let-7 microRNAs in human lung cancers in association with shortened postoperative survival. Cancer Res. 64: 3753–3756.
- Tan J, Cang S,Ma Y, et al. (2010) Novel histone deacetylase inhibitors in clinical trials as anti-cancer agents. J. Hematol. Oncol. 3:5. doi: 10.1186/1756-8722-3-5.
- Tavares C, Melo M, Cameselle-Teijeiro JM, et al. (2016) ENDOCRINE TUMOURS: Genetic predictors of thyroid cancer outcome. Eur. J. Endocrinol. 174(4):R117-26. doi: 10.1530/EJE-15-0605.
- Taverna SD, Li H, Ruthenburg AJ, et al. (2007) How chromatin-binding modules interpret histone modifications: lessons from professional pocket pickers. Nat Struct Mol Biol. 14:1025–1040.
- Tollervey JR, Lunyak VV. (2012) Epigenetics: judge, jury and executioner of stem cell fate. Epigenetics. 7(8):823-40. doi: 10.4161/epi.21141.
- Trapnell C, Roberts A, Goff L et al. (2012) Differential gene and transcript expression analysis of RNA-seq experiments with TopHat and Cufflinks. Nat Protoc. 7: 562-78.
- Tsankova N, Renthal W, Kumar A, et al. (2007) Epigenetic regulation in psychiatric disorders. Nat Rev Neurosci. 8:355–367.
- Vezzi F, Del Fabbro C, Tomescu AI et al. (2012) rNA: a fast and accurate short reads numerical aligner. Bioinformatics. 28: 123-4.
- Vidler LR, Brown N, Knapp S, et al. (2012) Druggability analysis and structural classification of bromodomain acetyl-lysine binding sites. J. Med. Chem. 55(17):7346-59. doi: 10.1021/jm300346w.
- Vlachos IS, Kostoulas N, Vergoulis T et al. (2012) DIANA miRPath v.2.0: investigating the combinatorial effect of microRNAs in pathways. Nucleic Acids Res. 40: 498-504.

- Wang GG, Allis CD, Chi P. (2007) Chromatin remodeling and cancer, Part II: ATP-dependent chromatin remodeling. Trends Mol. Med. 13:373–80.
- Wee S, Dhanak D, Li H et al. (2014) Targeting epigenetic regulators for cancer therapy. Ann N Y Acad Sci. 1309: 30-36.
- Weichenhan D, Plass C. (2013) The evolving epigenoma. Hum. Mol. Genet. 22 (R1): R1-R6. doi: 10.1093/hmg/ddt348.
- Wu JI, Lessard J, Crabtree GR. (2009) Understanding the words of chromatin regulation. Cell.136:200–206.
- Wu SY, Chiang CM. (2007) The double bromodomain-containing chromatin adaptor Brd4 and transcriptional regulation. J. Biol. Chem. 282(18):13141-5.
- Xing M. (2005) BRAF mutation in thyroid cancer. Endocr. Relat. Cancer. 12(2):245-62.
- Xing M. (2013) Molecular pathogenesis and mechanisms of thyroid cancer. Nat. Rev. Cancer. 13:184–199.
- Xu X, Wu J, Li S et al. (2014) Down-regulation of microRNA-182-5p contributes to renal cell carcinoma proliferation via activating the AKT/FOXO3a signaling pathway. Mol Cancer. 13:109.
- Xu Z, Sharp PP, Yao Y et al. (2016) BET inhibition represses miR17-92 to drive BIM-initiated apoptosis of normal and transformed hematopoietic cells. Leukemia. Epub ahead of print.
- Yang Z, He N, Zhou Q. (2008) Brd4 recruits P-TEFb to chromosomes at late mitosis to promote G1 gene expression and cell cycle progression. Mol. Cell Biol. 28:967–976.
- Yoo CB, Jones PA. (2006) Epigenetic therapy of cancer: past, present and future. Nat Rev Drug Discov. 5:37–50.
- Yu XM, Lo CY, Lam AK, et al. (2008) Serum vascular endothelial growth factor C correlates with lymph node metastases and high-risk tumor profiles in papillary thyroid carcinoma. Ann. Surg. 247(3):483–489.
- Zaidi SK, Van Wijnen AJ, Lian JB, et al. (2013) Targeting deregulated epigenetic control in cancer. J. Cell Physiol. 228(11):2103-8. doi:10.1002/jcp.24387.
- Zaravinos A. (2015) The Regulatory Role of MicroRNAs in EMT and Cancer. J Oncol. 2015:865816. doi:10.1155/2015/865816.
- Zhang G, Pradhan S. (2014) Mammalian epigenetic mechanisms. IUBMB Life. 66(4):240-56. doi: 10.1002/iub.1264.
- Zhou J, Yu Q, Chng WJ. (2011) TXNIP (VDUP-1, TBP-2): a major redox regulator commonly suppressed in cancer by epigenetic mechanisms. Int J Biochem Cell Biol. 43:1668-73. doi: 10.1016/j.biocel.2011.09.005.
- Zolotov S. (2016) Genetic Testing in Differentiated Thyroid Carcinoma: Indications and Clinical Implications. Rambam Maimonides Med. J. 7(1). doi: 10.5041/RMMJ.10236.
- Zuber J, Rappaport AR, Luo W et al. (2011) An integrated approach to dissecting oncogene addiction implicates a Myb-coordinated self-renewal program as essential for leukemia maintenance. Genes Dev. 25: 1628-40.

Books:

- Eroschenko VP. Di Fiore's atlas of histology with functional correlations.
  2008; Lippincott Williams & Wilkins.
- Kaplan E, Angelos P, et al. Chapter 21: SURGERY OF THE THYROID.
  In: De Groot LJ, Beck-Peccoz P, Chrousos G, Dungan K, Grossman A, Hershman JM, Koch C, McLachlan R, New M, Rebar R, Singer F, Vinik A, Weickert MO, editors.
  2000-2015; Endotext. South Dartmouth (MA): MDText.com, Inc.
- Mescher AL. Junqueira's Basic Histology.
  2013; The McGraw-Hill Companies, Inc.
- Pacini F, DeGroot LJ. Thyroid Cancer.
  In: De Groot LJ, Beck-Peccoz P, Chrousos G, Dungan K, Grossman A, Hershman JM, Koch C, McLachlan R, New M, Rebar R, Singer F, Vinik A, Weickert MO, editors.
  2000-2013; Endotext. South Dartmouth (MA): MDText.com, Inc.
- Shaw AD, Riedel BJ, et al. Acute care of the cancer patient.
  2005; Boca Raton, FL: Taylor & Francis Group.